

Appendix A

Typical Transit through GIWW East Lock and Damage Caused by Barge Collisions to Approach



Barge and Tow Boat Approach to East Lock



Collision Damage to Approach (not on occasion of approach pictured on page A-1)

Appendix B

TABS-MDS Introduction

TABS-MDS (Multi-Dimensional, Sediment) is a finite element, hydrodynamic model. It is based on RMA10, a model written by Ian King of Resource Management Associates (King, 1993). It is capable of modeling turbulent, sub-critical flows using 1-D, 2-D, and/or 3-D elements. It is also capable of modeling constituent transport. This includes modeling salinity, temperature, and/or fine-grained sediment. The model is capable of coupling the spatial density variation induced by concentration gradients in the constituent field to the hydrodynamic calculations. This enables the model to simulate phenomena such as saline wedges in estuaries. The model has features that permit the simulation of intermittently wetted regions of the domain, such as coastal wetlands.

TABS-MDS Theoretical Development

3-D Equations

We have 6 unknowns (u,v,w,h,s,ρ). Therefore, we require 6 equations.

The Navier-Stokes Equations (i.e. conservation of fluid momentum)

$$\begin{aligned} \rho \frac{\partial u}{\partial t} + \rho u \frac{\partial u}{\partial x} + \rho v \frac{\partial u}{\partial y} + \rho w \frac{\partial u}{\partial z} - \frac{\partial}{\partial x} \left(\epsilon_{xx} \frac{\partial u}{\partial x} \right) - \frac{\partial}{\partial y} \left(\epsilon_{xy} \frac{\partial u}{\partial y} \right) - \frac{\partial}{\partial z} \left(\epsilon_{xz} \frac{\partial u}{\partial z} \right) \dots\dots \\ + \frac{\partial p}{\partial x} - \tau_x = 0 \end{aligned} \quad (1)$$

$$\begin{aligned} \rho \frac{\partial v}{\partial t} + \rho u \frac{\partial v}{\partial x} + \rho v \frac{\partial v}{\partial y} + \rho w \frac{\partial v}{\partial z} - \frac{\partial}{\partial x} \left(\epsilon_{yx} \frac{\partial v}{\partial x} \right) - \frac{\partial}{\partial y} \left(\epsilon_{yy} \frac{\partial v}{\partial y} \right) - \frac{\partial}{\partial z} \left(\epsilon_{yz} \frac{\partial v}{\partial z} \right) \dots\dots \\ + \frac{\partial p}{\partial y} - \tau_y = 0 \end{aligned} \quad (2)$$

$$\begin{aligned} \rho \frac{\partial w}{\partial t} + \rho u \frac{\partial w}{\partial x} + \rho v \frac{\partial w}{\partial y} + \rho w \frac{\partial w}{\partial z} - \frac{\partial}{\partial x} \left(\epsilon_{zx} \frac{\partial w}{\partial x} \right) - \frac{\partial}{\partial y} \left(\epsilon_{zy} \frac{\partial w}{\partial y} \right) - \frac{\partial}{\partial z} \left(\epsilon_{zz} \frac{\partial w}{\partial z} \right) \dots\dots \\ + \frac{\partial p}{\partial z} + \rho g - \tau_z = 0 \end{aligned} \quad (3)$$

The Volume Continuity Equation

$$\frac{\partial u}{\partial x} + \frac{\partial v}{\partial y} + \frac{\partial w}{\partial z} = 0 \dots\dots\dots (4)$$

The Advection-Diffusion Equation

$$\frac{\partial s}{\partial t} + u \frac{\partial s}{\partial x} + v \frac{\partial s}{\partial y} + w \frac{\partial s}{\partial z} - \frac{\partial}{\partial x} \left(D_x \frac{\partial s}{\partial x} \right) - \frac{\partial}{\partial y} \left(D_y \frac{\partial s}{\partial y} \right) - \frac{\partial}{\partial z} \left(D_z \frac{\partial s}{\partial z} \right) \dots\dots\dots (5)$$

$-\theta_s = 0$

The Equation of State

$$\rho = F(s, t) \dots\dots\dots (6)$$

where:

τ = applied forces (e.g. wind stress, bed shear stress, Coriolis force)

θ_s = salinity source/sink term

Now we reduce the number of unknowns requiring a simultaneous solution from 6 to 3.

Assuming that the influence of vertical momentum on the system is small and may be neglected, equation 3 reduces to the following equation:

$$\frac{\partial p}{\partial z} + \rho g = 0 \dots\dots\dots (7)$$

Equation 7 is a statement that the vertical pressure distribution is hydrostatic.

Equation 4 may then be integrated in the vertical direction to yield the following equation:

$$\int_a^{a+h} \left(\frac{\partial u}{\partial x} + \frac{\partial v}{\partial y} \right) d\eta = - \int_a^{a+h} \frac{\partial w}{\partial z} d\eta = -w_s + w_b \dots\dots\dots (8)$$

where:

w_s = the vertical velocity at the water surface

w_b = the vertical velocity at the bed

The surface velocity can be expressed as follows:

$$w_s = u_s \frac{\partial(z_b + h)}{\partial x} + v_s \frac{\partial(z_b + h)}{\partial y} + \frac{\partial(z_b + h)}{\partial t} \dots\dots\dots (9)$$

Similarly, the bed velocity can be expressed as:

$$w_b = u_b \frac{\partial z_b}{\partial x} + v_b \frac{\partial z_b}{\partial y} + \frac{\partial z_b}{\partial t} \dots\dots\dots (10)$$

where:

u_s, v_s = the surface horizontal velocity components

u_b, v_b = the near bed horizontal velocity components

z_b = the bed elevation

Note that by replacing equations 3 and 4 with 6 and 8, we recast the equations such that w is present only in the horizontal momentum equations and the advection diffusion equation. It can now be solved in a separate decoupled calculation using the original form of the continuity equation (equation 4). This is done by taking the derivative of equation 4 with respect to z and solving for w , applying w_s and w_b as boundary conditions.

We can further eliminate ρ from the list of unknowns requiring a simultaneous solution by solving the equation of state (equation 6) in a decoupled step.

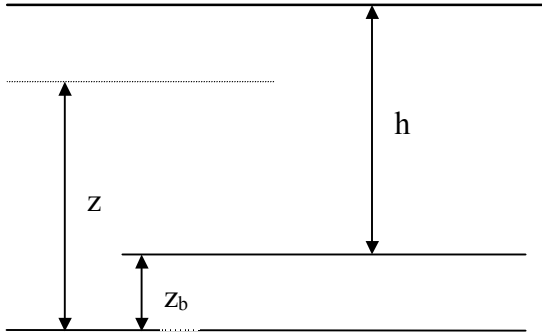
Thus, we are left with 4 equations (1,2,8 and 5) and 4 unknowns (u,v,h and s) to be solved simultaneously. In practice, however, the solution is broken up into 2 steps: First the velocities and depth are solved simultaneously, and then the constituent concentration is solved. This method improves solution efficiency dramatically over the simultaneous solution of all 4 equations and unknowns.

Hence, the solution of a system of 4 equations and 4 unknowns becomes the solution of a system of 3 equations (1,2, and 8) and 3 unknowns (u,v , and h), followed by the solution of 1 equation (5) and 1 unknown (s).

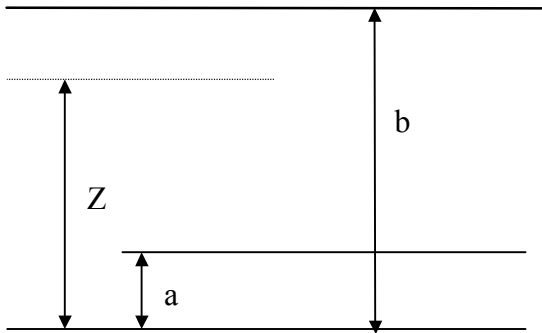
Geometric transform

In order to use a fixed geometry to model a system with a time varying vertical dimension (depth) it is convenient to use a geometric transformation to map the system to a fixed geometry.

Time varying system



Fixed grid system



The transformation is based on the following relation:

$$\frac{h}{(z - z_b)} = \frac{(b - a)}{(Z - a)} \dots\dots\dots (11)$$

$$z = \frac{(Z - a)}{(b - a)} h + z_b \dots\dots\dots (12)$$

Hence:

$$U(x, y, z) = u(X, Y, \left(\left(\frac{Z - a}{b - a} \right) h + z_b \right)) \dots\dots\dots (13)$$

After completing the transformation of the terms and simplifying, we arrive at the following transformed equations:

The Momentum Equations

$$\left\{ \begin{aligned} & \rho \left[h \frac{\partial u}{\partial t} + hu \frac{\partial u}{\partial x} + hv \frac{\partial u}{\partial y} + \frac{\partial u}{\partial z} (b - a) \left(w - uT_x - vT_y - \frac{(z - a)}{(b - a)} \frac{\partial h}{\partial t} - \frac{\partial z_b}{\partial t} \right) \right] \\ & - h \frac{\partial}{\partial x} \left(\epsilon_{xx} \frac{\partial u}{\partial x} \right) - h \frac{\partial}{\partial y} \left(\epsilon_{xy} \frac{\partial u}{\partial y} \right) - (b - a) \frac{\partial}{\partial z} \left(\epsilon_{xz} \left(\frac{(b - a)}{h} \right) \frac{\partial u}{\partial z} \right) \\ & + \rho gh \frac{\partial z_b}{\partial x} + \rho gh \frac{\partial h}{\partial x} + h \frac{\partial p}{\partial x} + \rho gh \frac{\partial h_D}{\partial x} - h\tau_x \end{aligned} \right\} \frac{1}{(b - a)} = 0 \quad (14)$$

$$\left\{ \begin{aligned} & \rho \left[h \frac{\partial v}{\partial t} + hu \frac{\partial v}{\partial x} + hv \frac{\partial v}{\partial y} + \frac{\partial v}{\partial z} (b - a) \left(w - uT_x - vT_y - \frac{(z - a)}{(b - a)} \frac{\partial h}{\partial t} - \frac{\partial z_b}{\partial t} \right) \right] \\ & - h \frac{\partial}{\partial x} \left(\epsilon_{yx} \frac{\partial v}{\partial x} \right) - h \frac{\partial}{\partial y} \left(\epsilon_{yy} \frac{\partial v}{\partial y} \right) - (b - a) \frac{\partial}{\partial z} \left(\epsilon_{yz} \left(\frac{(b - a)}{h} \right) \frac{\partial v}{\partial z} \right) \\ & + \rho gh \frac{\partial z_b}{\partial y} + \rho gh \frac{\partial h}{\partial y} + h \frac{\partial p}{\partial y} + \rho gh \frac{\partial h_D}{\partial y} - h\tau_y \end{aligned} \right\} \frac{1}{(b - a)} = 0 \quad (15)$$

Volume Continuity

$$\int_a^b \left[\frac{h}{(b-a)} \left(\frac{\partial u}{\partial x} + \frac{\partial v}{\partial y} \right) - \frac{\partial u}{\partial z} T_x - \frac{\partial v}{\partial z} T_y \right] dz$$

$$+ u_s \frac{\partial(z_b + h)}{\partial x} + v_s \frac{\partial(z_b + h)}{\partial y} + \frac{\partial(z_b + h)}{\partial t} - u_b \frac{\partial z_b}{\partial x} - v_b \frac{\partial z_b}{\partial y} - \frac{\partial z_b}{\partial t} = 0 \dots\dots (16)$$

Advection-Diffusion Equation

$$\left\{ \begin{aligned} & h \frac{\partial \mathcal{S}}{\partial t} + hu \frac{\partial \mathcal{S}}{\partial x} + hv \frac{\partial \mathcal{S}}{\partial y} + \frac{\partial \mathcal{S}}{\partial z} (b-a) \left(w - uT_x - vT_y - \frac{(z-a)}{(b-a)} \frac{\partial h}{\partial t} - \frac{\partial z_b}{\partial t} \right) \\ & - h \frac{\partial}{\partial x} \left(D_x \frac{\partial \mathcal{S}}{\partial x} \right) - h \frac{\partial}{\partial y} \left(D_y \frac{\partial \mathcal{S}}{\partial y} \right) - (b-a) \frac{\partial}{\partial z} \left(D_z \left(\frac{(b-a)}{h} \right) \frac{\partial \mathcal{S}}{\partial z} \right) - h\theta_s \end{aligned} \right\} \frac{1}{(b-a)} = 0 \quad (17)$$

where:

$$T_x = \frac{\partial z_b}{\partial x} + \frac{(z-a)}{(b-a)} \frac{\partial h}{\partial x} - \frac{h}{(b-a)} \frac{\partial a}{\partial x} + \frac{(z-a)}{(b-a)^2} h \frac{\partial a}{\partial x} \dots\dots\dots (18)$$

$$T_y = \frac{\partial z_b}{\partial y} + \frac{(z-a)}{(b-a)} \frac{\partial h}{\partial y} - \frac{h}{(b-a)} \frac{\partial a}{\partial y} + \frac{(z-a)}{(b-a)^2} h \frac{\partial a}{\partial y} \dots\dots\dots (19)$$

$$h_D = -\frac{(b-z)}{(b-a)} h \dots\dots\dots (20)$$

2-D Vertically Averaged Equations

If u, v , and s are assumed constant with respect to elevation (z), the 3-D equations can be integrated over depth to yield 2-D vertically averaged equations. For example, the X-momentum equation reduces to the following:

$$\left\{ \begin{array}{l} \rho(b-a) \left[h \frac{\partial u}{\partial t} + hu \frac{\partial u}{\partial x} + hv \frac{\partial u}{\partial y} \right] \\ - h(b-a) \frac{\partial}{\partial x} \left(\varepsilon_{xx} \frac{\partial u}{\partial x} \right) - h(b-a) \frac{\partial}{\partial y} \left(\varepsilon_{xy} \frac{\partial u}{\partial y} \right) \\ + \rho gh(b-a) \left(\frac{\partial z_b}{\partial x} + \frac{\partial h}{\partial x} \right) + (b-a) \frac{gh^2}{2} \frac{\partial \rho}{\partial x} - h(b-a) \tau_x \end{array} \right\} \frac{1}{(b-a)} = 0 \dots\dots\dots (21)$$

Similarly, the continuity equation reduces to:

$$h \left(\frac{\partial u}{\partial x} + \frac{\partial v}{\partial y} \right) + u \frac{\partial h}{\partial x} + v \frac{\partial h}{\partial y} + \frac{\partial h}{\partial t} = 0 \dots\dots\dots (22)$$

And the advection-diffusion equation reduces to:

$$\left\{ \begin{array}{l} h(b-a) \frac{\partial s}{\partial t} + h(b-a)u \frac{\partial s}{\partial x} + h(b-a)v \frac{\partial s}{\partial y} \\ - h(b-a) \frac{\partial}{\partial x} \left(D_x \frac{\partial s}{\partial x} \right) - h(b-a) \frac{\partial}{\partial y} \left(D_y \frac{\partial s}{\partial y} \right) - h(b-a)\theta_s \end{array} \right\} \frac{1}{(b-a)} = 0 \dots\dots\dots (23)$$

2-D Laterally Averaged Equations

Lateral averaging eliminates the momentum equation in the direction normal to the dominant flow direction. The equations are integrated across the width of the channel. This operation requires that the channel width c is specified. For the purposes of TABS-MDS, the channel width in laterally averaged elements is constrained such that it is constant with respect to depth, but can vary with respect to x and y (i.e. along the channel length). For example, the X-momentum equation reduces to the following.

$$\left\{ \begin{aligned} & \rho \left[h \frac{\partial u}{\partial t} + hu \frac{\partial u}{\partial x} + \frac{\partial u}{\partial z} (b-a) \left(w - uT_x - \frac{(z-a)}{(b-a)} \frac{\partial h}{\partial t} - \frac{\partial z_b}{\partial t} \right) \right] \\ & - h \frac{\partial}{\partial x} \left(\epsilon_{xx} \frac{\partial u}{\partial x} \right) - (b-a) \frac{\partial}{\partial z} \left(\epsilon_{xz} \left(\frac{(b-a)}{h} \right) \frac{\partial u}{\partial z} \right) \\ & + \rho gh \frac{\partial z_b}{\partial x} + \rho gh \frac{\partial h}{\partial x} + h \frac{\partial p}{\partial x} + \rho gh \frac{\partial h_D}{\partial x} - h\tau_x \end{aligned} \right\} \frac{c}{(b-a)} = 0 \dots\dots\dots (24)$$

Similarly, the continuity equation reduces to:

$$\begin{aligned} & \int_a^b \left[\frac{h}{(b-a)} \left(c \frac{\partial u}{\partial x} + u \frac{\partial c}{\partial x} \right) - c \frac{\partial u}{\partial z} T_x \right] dz \\ & + cu_s \frac{\partial (z_b + h)}{\partial x} + \frac{\partial (z_b + h)}{\partial t} - cu_b \frac{\partial a}{\partial x} - \frac{\partial z_b}{\partial t} = 0 \dots\dots\dots (25) \end{aligned}$$

And the advection-diffusion equation reduces to:

$$\left\{ \begin{aligned} & h \frac{\partial s}{\partial t} + hu \frac{\partial s}{\partial x} + \frac{\partial s}{\partial z} (b-a) \left(w - uT_x - \frac{(z-a)}{(b-a)} \frac{\partial h}{\partial t} - \frac{\partial z_b}{\partial t} \right) \\ & - h \frac{\partial}{\partial x} \left(D_x \frac{\partial s}{\partial x} \right) - (b-a) \frac{\partial}{\partial z} \left(D_z \left(\frac{(b-a)}{h} \right) \frac{\partial s}{\partial z} \right) - h\theta_s \end{aligned} \right\} \frac{c}{(b-a)} = 0 \dots\dots\dots (26)$$

1-D Equations

Under this approximation both vertical and lateral integration are applied. Hence, the form of the cross-section must be defined. In TABS-MDS, the cross section is assumed trapezoidal, with allowance made for off-channel storage.

For example, the X-momentum equation reduces to the following:

$$\left\{ \begin{aligned} &\rho \left[A \frac{\partial u}{\partial t} + Au \frac{\partial u}{\partial x} \right] \\ &- A \frac{\partial}{\partial x} \left(\epsilon_{xx} \frac{\partial u}{\partial x} \right) \\ &+ \rho g A \frac{\partial z_b}{\partial x} + \rho g A \frac{\partial h}{\partial x} + \frac{g A h}{2} \frac{\partial \rho}{\partial x} - A \tau_x \end{aligned} \right\} = 0 \dots\dots\dots (27)$$

Similarly, the continuity equation reduces to:

$$A \left(\frac{\partial u}{\partial x} \right) + u \frac{\partial A}{\partial x} + \frac{\partial (A + A_{oc})}{\partial t} = 0 \dots\dots\dots (28)$$

And the advection diffusion equation reduces to:

$$\left\{ (A + A_{oc}) \frac{\partial s}{\partial t} + A \frac{\partial s}{\partial x} - A \frac{\partial}{\partial x} \left(D_x \frac{\partial s}{\partial x} \right) - A \theta_s \right\} = 0 \dots\dots\dots (29)$$

where:

A = The main channel cross-sectional area

A_{oc}= The off-channel storage cross-sectional area

Finite Element Formulation

In order to generate the finite element equations, we must integrate each of the equations over the element volume (for 3-D), area (for 2-D), or length (for 1-D), remembering to include the weight function in the integration (which, for the Galerkin method, is the same as the basis function).

In addition, we must recast the higher-order terms using integration by parts. This causes the boundary terms to drop out of the equations. For example,

Take the following pressure term, multiplied through by a weight function N.

$$N \frac{\rho g h}{(b-a)} \frac{\partial h}{\partial x} \dots\dots\dots (30)$$

This can be rewritten as:

$$N \frac{\rho g}{2(b-a)} \frac{\partial h^2}{\partial x} \dots\dots\dots (31)$$

Then , it can be integrated by parts:

$$\begin{aligned} N \frac{\rho g}{2(b-a)} \frac{\partial h^2}{\partial x} &= \frac{\partial}{\partial x} \left(N \frac{\rho g h^2}{2(b-a)} \right) - \frac{\partial N}{\partial x} \left(\frac{\rho g h^2}{2(b-a)} \right) \dots\dots\dots (32) \\ &- N \frac{g h^2}{2(b-a)} \frac{\partial \rho}{\partial x} - N \frac{\rho g h^2}{2(b-a)^2} \frac{\partial a}{\partial x} \end{aligned}$$

Note that the first term on the right hand side of the equation can be evaluated as an area integral via the Gauss Divergence Theorem. Hence, it becomes a boundary term.

Time Derivative Solution Method

The time derivative is approximated with a simple, fully-implicit finite difference formulation. I.e.,

$$\frac{\partial \beta_t}{\partial t} = \frac{(\beta_t - \beta_{t-\Delta t})}{\Delta t} \dots\dots\dots (33)$$

where:

β_t = any of the unknown variables at time t.

Δt = the time step

Newton-Rhapson Implementation

Once the finite element equations are built, they are solved using the Newton-Rhapson iterative method. In order to do this, partial derivatives with respect to each of the unknown variables must be derived for each system equation. These derivatives compose the stiffness matrix, and are used to drive the residual (i.e. the integral of each equation across an element) to 0.

$$\begin{bmatrix} X_u Y_u Z_u \\ X_v Y_v Z_v \\ X_h Y_h Z_h \end{bmatrix} \begin{bmatrix} u \\ v \\ h \end{bmatrix} = \begin{bmatrix} X \\ Y \\ Z \end{bmatrix} \dots\dots\dots (34)$$

Expressions for Applied Loads and Turbulent Mixing

Bed Shear Stress

The bed shear stress is given by a modified form of Manning's Equation, as given by Christensen (1970). Any of 3 expressions can be used, depending on the instantaneous value of the depth/roughness height ratio ($\frac{d}{k}$). The expressions are as follows (given for the X-direction only):

$$\text{for } \frac{d}{k} < 4.32 \quad \tau_x = \frac{\rho g}{L^2} \frac{|v|v_x}{d^{2/3}} \quad \text{where } L = \frac{6.46\sqrt{g}}{k^{1/3}} \dots\dots\dots (35)$$

$$\text{for } 4.32 < \frac{d}{k} < 276 \quad \tau_x = \frac{\rho g}{M^2} \frac{|v|v_x}{d^{1/3}} \quad \text{where } M = \frac{8.25\sqrt{g}}{k^{1/6}} \dots\dots\dots (36)$$

$$\text{for } \frac{d}{k} > 276 \quad \tau_x = \frac{\rho g}{N^2} \frac{|v|v_x}{d^{1/6}} \quad \text{where } N = \frac{13.18\sqrt{g}}{k^{1/12}} \dots\dots\dots (37)$$

where:

τ_x = the bed shear in the X-direction

k = the roughness height

d = the local depth

v = the local velocity

g = the gravitational constant

ρ = the density of water

k is found as a function of Manning's n from the following expression:

$$k = \left(\frac{8.25 \sqrt{g \, n}}{1.486} \right)^6 \dots\dots\dots (38)$$

The Wind Stress

The wind stress is given by the following expression (given for the X-direction only):

$$\tau_{wx} = \rho_a C_w V_w^2 \cos \theta_w \dots\dots\dots (39)$$

where:

τ_{wx} = the wind stress in the X-direction

ρ_a = the density of air

V_w = the wind velocity

θ_w = the direction from which the wind is blowing, measured counterclockwise from the positive X- axis.

C_w = the wind stress coefficient

For deep water, the wind stress coefficient is given by Wu (1980).

$$C_w = \frac{0.8 + 0.065 \times V_w}{1000} \dots\dots\dots (40)$$

For shallow water, the wind stress is given by Teeter et. al., (2001)

$$C_w = \left(\frac{0.4}{16.11 - 0.5 \ln(d) - 2.48 \ln(V_w)} \right)^2 \times \left(1 - \frac{1.118}{\sqrt{V_{wl}}} e^{-6(d_l-2)} \right) \dots\dots\dots (41)$$

where:

d = the local water depth (in meters)

d_1 = the maximum of the local water depth (in meters) and 2 meters

V_{w1} = the maximum of the wind velocity (in m/s) and 5.063 m/s

Horizontal Turbulent Mixing and Diffusion

Horizontal Turbulent mixing can be specified directly, or it can be controlled by the method of Smagorinsky (1963). A description of this method follows.

The Smagorinsky method of describing horizontal eddy viscosities and diffusion coefficients is a “tensorially invariant generalization of the mixing length type representation” (Speziale, 1998). The Smagorinsky description of the turbulent mixing terms in the Navier-Stokes Equations are given as follows. For the x-momentum equation

$$\rho h \frac{\partial}{\partial x} \left(2S \frac{\partial u}{\partial x} \right) + \rho h \frac{\partial}{\partial y} \left(S \left(\frac{\partial u}{\partial y} + \frac{\partial v}{\partial x} \right) \right) \dots\dots\dots (42)$$

For the y momentum equation

$$\rho h \frac{\partial}{\partial y} \left(2S \frac{\partial v}{\partial y} \right) + \rho h \frac{\partial}{\partial x} \left(S \left(\frac{\partial u}{\partial y} + \frac{\partial v}{\partial x} \right) \right) \dots\dots\dots (43)$$

where:

$$\dots\dots\dots S = kA \left[\left(\frac{\partial u}{\partial x} \right)^2 + \left(\frac{\partial v}{\partial y} \right)^2 + \frac{1}{2} \left(\frac{\partial u}{\partial y} + \frac{\partial v}{\partial x} \right)^2 \right]^{\frac{1}{2}} \quad (44)$$

k = Smagorinsky coefficient, usually given a value ranging from approximately 0.005 for rivers to 0.05 for estuaries and lakes (Speziale, 1998; Thomas et al, 1995)

A = the surface area of the element

The Smagorinsky description of the turbulent diffusion terms in the advection-diffusion equation is given as follows:

$$h \frac{\partial}{\partial x} \left(2S \frac{\partial C}{\partial x} \right) + h \frac{\partial}{\partial y} \left(2S \frac{\partial C}{\partial y} \right) \dots\dots\dots (45)$$

In order to promote numerical stability, TABS-MDS provides a means of establishing minimum values of turbulent mixing and turbulent diffusion. These values are used in place of the Smagorinsky term (S) when they are found to exceed the value of that term. The minimum turbulent mixing value is given by the following equation:

$$S_{Emin} = TBMINF \times \rho \alpha \sqrt{A} \dots\dots\dots (46)$$

The minimum turbulent diffusion value is given by the following equation:

$$S_{Dmin} = TBMINFS \times \alpha \sqrt{A} \dots\dots\dots (47)$$

where

TBMINF = minimum turbulent mixing factor (default = 1.0)

TBMINFS = minimum diffusion factor (default = 1.0)

α = a coefficient, given as 5.00×10^{-3} ft/sec or 1.52×10^{-3} m/s, depending on the unit system being used in the simulation. This value is an arbitrary estimate of the minimum turbulent mixing needed to ensure model stability. It equals the value of eddy viscosity/diffusion which corresponds to a Peclet number of 40 and a velocity magnitude of 0.2 ft/sec.

Also, if $|V| < TBMINF \times V_{min}$, S_{Emin} is applied, regardless of the turbulent mixing as given by the Smagorinsky calculation. This is done to inhibit numerical instability in areas with both extremely small velocities and high velocity gradients.

Vertical Turbulent Mixing and Diffusion

Vertical turbulent mixing and diffusion are given by the method of Mellor-Yamada (1982) with a modification according to Hendersen-Sellers (1984).

The Mellor-Yamada expressions for vertical eddy viscosity and diffusion are given as follows:

$$E_{xz} = E_{yz} = \rho S_m l_m q \dots\dots\dots (48)$$

$$D_z = S_h l_m q \dots\dots\dots (49)$$

where:

$$l_m = 0.4(z-a) \left| 1 - \frac{(z-a)}{h} \right|^{\frac{1}{2}} \dots\dots\dots (50)$$

$$q = \left\{ b_1 l_m^2 S_m \left[\left| \frac{\partial u}{\partial z} \right|^2 + \left| \frac{\partial v}{\partial z} \right|^2 \right] \right\}^{\frac{1}{2}} \dots\dots\dots (51)$$

$$S_m = 0.393$$

$$S_h = 0.494$$

$$b_1 = 16.6$$

The Henderson-Sellers adjustment is a factor that accounts for the dampening affect on turbulence induced by stable stratification. The factor is expressed in terms of the Richardson Number:

$$R_i = \frac{-g(\partial\rho/\partial z)}{\rho \left[\left(\frac{\partial u}{\partial z} \right)^2 + \left(\frac{\partial v}{\partial z} \right)^2 \right]} \dots\dots\dots (52)$$

For vertical diffusion of momentum (i.e. vertical eddy viscosity) the expression is given as follows:

$$E_z = \frac{E_{zo}}{(1 + 0.74R_i)} \dots\dots\dots (53)$$

Where E_z is the vertical eddy viscosity, and E_{zo} is the vertical eddy viscosity assuming no stratification influence on the turbulence (i.e. the value taken from Mellor-Yamada).

For vertical diffusion of salinity (i.e. vertical diffusion coefficient) the expression is given as follows:

$$D_z = \frac{D_{zo}}{(1 + 37R_i^2)} \dots\dots\dots (54)$$

Where D_z is the vertical diffusion coefficient, and D_{zo} is the vertical diffusion coefficient assuming no stratification influence on the turbulence (i.e. the value taken from Mellor-Yamada).

References

Christensen, B. A. (1970) *Manning's n For Cast-In-Place Concrete Pipe; Discussions by Bent A. Christensen, and R. Sakthivadivel, S. Seetharaman and M.V. Somasundaram*, Journal of the Hydraulics Division, Proceedings of the American Society of Civil Engineers, Vol. 96, No. HY3.

Henderson-Sellers, B. (1984) *Engineering Limnology*, Pitman Advanced Publishing, Boston, pp 81-91.

King, I.P. (1988) *A Finite Element Model for Three Dimensional Hydrodynamic Systems*, Report prepared by Resource Management Associates, Lafayette California, for U.S. Army Corps of Engineers, Waterways Experiment Station, Vicksburg, Mississippi.

Mellor, G.L. and Yamada, T. (1982) *Development of a Turbulence Closure Model for Geophysical Fluid Problems*, Reviews of Geophysics and Space Physics, Vol20, No.4, pp 851-875.

Smagorinsky, J. (1963) *General Circulation Experiments with the Primitive Equations, I. The Basic Experiment*, Monthly Weather Review, 91, 99-164.

Speziale, Charles G. (1998) *Turbulence Modeling for Time-Dependent RANS and VLES: A Review*, AIAA Journal, Vol 36, No 2, pp 173-184.

Teeter, A. M., Johnson, B. H., Berger, C., Stelling, G., Scheffner, N. W., Garcia, M. H., Parchure, T. M.,(2001) *Hydrodynamic and Sediment Transport Modeling With Emphasis on Shallow-water, Vegetated Areas (Lakes, Reservoirs, Estuaries, and Lagoons)*. Hydrobiologia 444: 1-23.

Thomas, T.G., Williams, J.R.R. (1995) *Large Eddy Simulation of a Symmetric Trapezoidal Channel at a Reynolds Number of 430,000*, Journal of Hydraulic Research, Vol 33, No 6, pp 825-830.

Appendix C

Description of Statistics

Statistical analysis of the model and field data is given with 4 statistics: mean error (ME), mean absolute error (MAE), root mean square error (RMS), and index of agreement (d). The index of agreement is a descriptive measure of predictive success. It gives a value between 0 and 1, with 1 indicating perfect agreement. Since it is a relative measure of modeling success, and it is bounded (between 0 and 1) it is also useful for making comparisons between models (Willmott, 1982)¹.

Letting O and P be the observed and predicted values of a quantity N, the following expressions result:

$$ME = \frac{1}{N} \sum_{n=1}^N (O_n - P_n) \dots\dots\dots (1)$$

$$MAE = \frac{1}{N} \sum_{n=1}^N |O_n - P_n| \dots\dots\dots (2)$$

$$RMS = \sqrt{\frac{1}{N} \sum_{n=1}^N (O_n - P_n)^2} \dots\dots\dots (3)$$

$$d = 1 - \left[\frac{\sum_{n=1}^N (P_n - O_n)^2}{\sum_{n=1}^N (|P_n - \bar{O}| + |O_n - \bar{O}|)^2} \right] \dots\dots\dots (4)$$

¹ Willmott, C. J. (1982) "Some Comments on the Evaluation of Model Performance" Bulletin of the American Meteorological Society, Volume 63, Number 11, pp 1309-1310.

Appendix D

Field Data Collection Memorandum for Record

CEWES-CE-TH

MEMORANDUM FOR Commander, U.S. Army Engineer District, Galveston,
ATTN: CESWG-EC -EH (Mr. Mike Bragg),
Jadwin Building, 2000 Ft. Point Road, Galveston, TX 77550

SUBJECT: Field Data Collection at the Colorado River and Gulf Intercoastal Waterway,
Matagorda, TX

1. Enclosed please find the Memorandum for Record that describes the assistance provided your office by the U.S. Army Engineer Waterways Experiment Station Coastal and Hydraulics Laboratory. The field data collection began on 21 May 2001 and was completed on 26 October 2001. The data processing of the tides, velocities and laboratory work on the analysis of the water samples was completed in November 2001.
2. The information provided in this memorandum completes the work required for this project. If you have questions concerning the information provided, please contact Mr. Tim Fagerburg at 601-634-2257 or Mr. Howard Benson at 601-634-3589.

Encl

JAMES. R. HOUSTON, PhD
Director, Coastal and Hydraulic Laboratory

MEMORANDUM FOR RECORD

SUBJECT: Field Data Collection at the Colorado River and Gulf Intercoastal Waterway, Matagorda, TX

Introduction

1. In response to a request of the U.S. Army Engineer District, Matagorda (SWG), the U.S. Army Engineer Waterways Experiment Station (WES) discussed plans with the District for the data collection at the Colorado River and the Gulf Intercoastal Waterway (GIWW), Matagorda, TX. Messrs. Ed Reindl and Mike Bragg requested that the Hydraulic Analysis Group of WES provide personnel and equipment to investigate the hydrodynamics, bathymetry and salinity concentrations in the area of the GIWW, Colorado River, East Matagorda Bay, and Upper Matagorda Bay. It was requested that WES provide support for and complete this effort prior to 30 December 2001.
2. The purpose of the data collection was to provide detailed tidal hydrodynamic and bathymetric information that can be used to address concerns of shoaling in the GIWW/Colorado River that creates an adverse impact on commercial navigation in the area. The data collected will also be used to verify numerical model simulations of the salinity movement in the project area.
3. The data collection program was planned and performed by WES. The equipment provided by WES included an Acoustic Doppler Current Profiler (ADCP), Acoustic Doppler Velocity Meters, pressure measurement tide gauges, salinity concentration sensors, water sampling pumps and meteorological station. A Contractor performed the bathymetric survey and prepared digital maps of the most recent bathymetry of the study area.

FIELD DATA COLLECTION

Long-term Instrumentation

4. Twelve long-term data collection locations within the study area were established to provide adequate coverage for determination of tidal velocity magnitudes and directions, ranges of water-level elevations, and changes in salinity concentration and the variability of bottom sediment characteristics. At each of these data collection locations, shown in Figures 1 and 2, instruments were installed for the purpose of collecting water levels and salinity variations over a five to six month period.
5. The data collection program was initiated with instruments being installed in May 2001. At all data collection locations (Stations 1-12), a pressure sensing water level recorder and salinity recorder were installed. The water level recorders were *WaterLOG®* DH-21 submersible pressure transducer and data logger. This instrument has unique dry air system that provides automatic compensation for changes in atmospheric pressure. The instrument is fully programmable to set the sampling rate, starting time, and output units. The accuracy of the pressure sensor is ± 0.01 feet. The salinity recorders used in the data collection effort were Hydrolab DataSonde® 3 Water Quality Probes. This instrument provides the capability of measuring in-situ temperature, conductivity and salinity during long-term unattended monitoring applications. The instruments are fully programmable for selecting the sampling interval. Calibration is accomplished simply by immersing the sensor in a standard salinity solution of known concentration, waiting for stable readings to appear, and setting the instrument to the new calibration value. A meteorological station was installed near Station 7 to collect wind speed, wind direction, ambient air temperature and barometric pressures. These meteorological parameters were monitored in 15-minute increments for the duration of the data collection program. The meteorological station was a Campbell Scientific W2000® programmable weather data acquisition station. The system can be programmed to sample the input signals

each second over a set period of time to determine the mean wind speed, mean direction, maximum wind gust speed, and maximum wind gust direction.

6. At two of the data collection locations (Stations 10 and 12), Acoustic Doppler Velocity (ADV) meters were installed in addition to the water level and salinity recorders. These velocity meters were used to determine the tidal flow magnitudes and directions in the East Matagorda Bay and upper Matagorda Bay areas. The ADV's used were Nortek Aquadopp® current meters. These instruments are a programmable current meter for measurements with time scales ranging from 1 second to 1 year. The current meter has no moving parts, requires no recalibration, and uses proven Doppler technology to provide 3-dimensional vector velocity measurements. This Doppler sensor includes a built-in solid-state recorder, pressure sensor, compass- and tilt sensor, batteries and an internal temperature sensor. The pressure sensor is a silicone piezoresistive pressure sensor that has an accuracy of ± 0.003 feet.

Bathymetric Survey

7. A bathymetric survey was performed to determine the existing water depths in the project study area. Figure 3 depicts the area of coverage for the bathymetric survey. Detailed maps of depths were provided the numerical modelers for use in the development of the model.

Field Procedures At Installation and During the Monitoring Program

8. The water level recorders were differential pressure sensor devices that record the depth of water over the sensor. The recorded pressures are atmospherically corrected using a dry air system in the electronics cable that extends above the water surface to the data recorder housing. The pressure sensors were deployed at a depth well below the predicted low tide level for the data collection period and were programmed to record the water level readings at 15-minute intervals. Instrument service periods were performed every 3 weeks. Specific procedures

were routinely followed prior to retrieving each water level sensor and immediately following redeployment of the sensor. Immediately before and after the water level sensors were serviced, a physical measurement of the depth of submergence was obtained and recorded for verification of the depth readings logged by the sensor. These procedures were followed for data quality assurance purposes. In addition, prior to the beginning of the deployment period each sensor was re-zeroed at the existing atmospheric pressure. If the instrument pressure could not be reset to zero before deployment then the instrument was pulled from service.

9. The salinity recording sensors were deployed at or near the level of the water level sensor. The sensors were set-up to record salinity concentrations and temperatures at 15-minute intervals. Also, no depth recording capabilities were available with these instruments. Specific procedures were routinely followed prior to retrieving and immediately following redeployment of the each salinity sensor. Immediately before and after the salinity sensors were serviced, a physical measurement of the depth of submergence was obtained and recorded for verification of the depth readings logged by the sensor. A water sample was also obtained at the depth of the salinity sensor. These water samples were returned to ERDC and analyzed in the laboratory for salinity concentration. The salinity concentration values from the laboratory analysis would later be used in the data processing efforts to indicate salinity-reading offsets at the end of each deployment period. Prior to cleaning the sensor, it was immersed in a standard salinity solution of known concentration, in parts per thousand (ppt), to determine the offset in the sensors reading due to aquatic fouling. These readings were allowed to stabilize for temperature compensation and the value of the salinity reading recorded. After the instrument was cleaned of any dirt and aquatic growth it was again immersed in the standard salinity solution, readings allowed to stabilize and the sensor reading recorded. This procedure was performed for field calibration of the sensor. The procedures described above were followed for

data quality assurance purposes. If the instrument salinity reading could not be reset to match the calibration standard value before deployment then the instrument was pulled from service.

10. Service trips to download data, clean and recalibrate instruments were performed in 3-week intervals. All work performed during the service trips on the instruments were recorded in a field-log book. These field records provided a quality control and assurance check for each of the instruments used in the project study effort.

Intensive Velocity and Salinity Data Collection

11. In addition to the long-term data collection effort, an intensive velocity data collection effort was performed to obtain detailed hydrodynamic information over a single spring tide event. A total of 8 velocity transects (Figures 4-6) were monitored during a 25-hour period. Immediately following each ADCP data collection transect, water samples were obtained at predetermined locations and depths for identification of salinity concentration changes with tidal flows.
12. Acoustic equipment such as the ADCP is used for fast and accurate profiling in the field of velocity magnitude and direction. The equipment employed for this investigation was 1200 kHz frequency RD Instruments Broad-Band ADCP. The instrument was mounted over the side of the boat with the acoustic transducers submerged and data were collected while the vessel was underway.
13. A general description of the ADCP operation is provided here. The acoustic transducers of the ADCP transmit sound bursts into the water column. These sound bursts are then scattered back to the instrument by particulate matter suspended in the flowing water. The ADCP transducers listen for the returning signal and assign depth and velocity to the received signal based on the time of travel and the change in frequency caused by the moving particles, respectively. The change in frequency is referred to as a Doppler shift. The ADCP is also

capable of measuring vessel direction, velocity magnitude and direction, water temperature, and bottom depth. Communication with the instrument for setup and data recording is performed with a portable computer using manufacturer-supplied software, hardware, and communication cable. The ADCP is for deployment on the side of a vessel that is operated at a very slow speed (less than 2.5 knots).

14. The general location of the ADCP transects for the Intensive Data Collection effort are shown in Figures 4-6 and are described below. Transect R1 was located north of the intersection of the GIWW and the Colorado River. Transect R2 was located south of the intersection of the GIWW and the Colorado River in the freshwater diversion channel into Matagorda Bay. Two transect lines extended the width of the GIWW channel and were designated as Transects R3 and R4. The near shore areas of these transects along both sides of the channel were found to be very shallow and therefore data collection at these transects were limited to the deeper water of the navigable channel as identified by the navigation markers for the channel. Transect R5 was located in the bypass channel that connects the GIWW to the old Colorado River. Transects R6 and R7 were located in the old Colorado River channel. The near shore areas of these transects along both sides of the old channel were very shallow and therefore bank-to-bank velocity profile coverage could not be performed.

Data Presentation

Water Level.

15. As previously discussed, twelve locations were established in the study area for obtaining long-term records of water level (tide) changes and salinity concentrations. The long-term data collection period extended from 21 May 2001 until 26 October 2001. The majority of the instruments performed satisfactorily during the 6-month deployment period. However during the long-term deployment, two of the water-level recorders (Station 3 and Station 10) were destroyed after the mounting unit were pulled or knocked from the piling and the instrument became submerged. The recorder housings are water-resistant but not waterproof. This caused the recorder housing to flood with water and shorted out all the electronics. As a result, no data could be retrieved from the instruments once this occurred. Due to budget constraints of the project, no replacement instruments were available for continuing the recording of water level at these locations. One other water level recorder experienced problems during the deployment period. The water level recorder for Station 7 in the GIWW (Corp of Engineers Boat House) developed internal recording problems during the September deployment and data recording failed. No replacement instrument was available to continue recording of water level at this location. A time history log of each water level instrument during the deployment period is provided in Table 1. Figures 7-18 are the time history plots of the water-level changes in Colorado River Project study area.

Salinity

16. Time history plots of salinity data collected during the deployment period 21 March 2001 through 26 October, 2001 are shown in Figures 19 - 37. The observed maximum salinities for each data collection location are quite varied depending on the instrument location. The time history records of the salinities indicate the occurrence of at least two significant events which caused a distinct lowering of the salinity concentrations recorded at the instrument locations.

These events occurred during the data collection period and are evident around the periods 07/10/01 and 09/03/01. The dramatic lowering of the salinity concentrations that occurred around 09/03/01 was evident at all salinity sensor locations including the sensors located in East Matagorda and Matagorda Bay. It is assumed that a substantial rainfall event may have occurred in the general area of the project introducing freshwater runoff into the rivers and bays. Salinity concentrations recorded at Station 4, located near the mouth of the Old Colorado River, were consistently higher, as shown in Figure 22, than those recorded at the other locations due to the proximity to the Gulf of Mexico.

17. Biological fouling of the salinity sensors is the major factor affecting the accuracy of the instruments recordings. Fouling due to biological growth is usually more prevalent in the higher salinity concentration areas, during the spring and summer months, when the water temperature in the shallow areas increased. The effect of biological growth on the salinity sensor is to alter the calibration of the conductivity electrodes. The covering of the salinity sensors with this growth results in a pronounced drift \pm from the initial reading when the instrument was redeployed after servicing. The scheduled time interval between service trips was rarely longer than 3 weeks. The regularity of these intervals, to clean the sensors and download the data, proved to be very effective in minimizing the effects of biological fouling of the salinity sensors. The quality control check on the se maintenance periods is provided in the comparison of the water sample salinity concentrations to the sensor salinity readings prior to retrieval and immediately following deployment of the sensor at the time of the service trip. The sensors deployed at Stations 3, 4, 10, 11, and 12 were more prone to various degrees of significant biological fouling due to the higher salinity concentrations, shallow depths and warm water temperatures. Stations 3 and 11 experienced the most biological fouling and operational problems.

18. As stated earlier, water samples were also collected at a minimum of three depths at each ADCP transect during the intensive velocity and salinity survey period.

Samples were pumped from a predetermined depth into 100-ml plastic bottles for storage and transport. These samples were transported to WES for analysis following the completion of the field effort. These samples were later analyzed in the laboratory to identify changes in salinity during various periods of the ebb and flood tide. The results of the laboratory salinity analysis are shown in Table 2-22 and are plotted in Figures 31-37. Also shown in these figures are the water-level changes during the intensive data collection period. The salinity concentration changes within the study area indicated very small differences over the 25-hour data collection period. The concentrations of the samples ranged from 12 ppt to 33 ppt. The most significant salinity concentration changes occurred in the near surface depth (3 ft below the surface) at Transects R1 and R2, in the Colorado River and Diversion Channel, respectively. During the ebb tide cycle, a significant freshening of the upper water surface occurred at both transects due to freshwater flow in the Colorado River.

Meteorological Data

19. The data from the meteorological data acquisition system were processed to provide the time history plots of the various parameters. Figures 38 – 41 are the plots of the recorded wind direction, wind speed, air temperature, and the atmospheric pressure during the 6-month data collection effort. In addition, other meteorological data were obtained from an existing National Oceanographic and Aerospace Administration (NOAA) located in Sabine Texas. This NOAA meteorological location is identified as Station 42019 - Freeport, TX., 60-nautical miles (NM) south of Freeport, TX. It is owned and maintained by the National Data Buoy Center and is located at coordinates 27°55'12"N 95°21'36"W. The recorded data from this location includes wind speed, wind direction, wind gusts, wave, height, atmospheric pressure, water temperature and air temperature. The data is available and can be downloaded at the website address <http://seaboard.ndbc.noaa.gov>.

Velocity Data

20. As stated previously, an ADV was deployed at Stations 10 and 12 to monitor the velocity magnitudes in Matagorda Bay and East Matagorda Bay, respectively. These data are presented in Figures 42 and 43. The velocity magnitudes were generally less than or equal to 1.0 ft per second.
21. The field data collection effort was completed on 26 October 2001. The data reduction was completed in December 2001.

Tim Fagerburg
Research Hydraulic Engineer
Hydraulic Analysis Group

Table 1 Colorado River Project Field Data Instrumentation Log											
Station No.	Instrument	May	June	July	August	September	October	November	December		
1 Upper Colorado River	Tide										
	Salinity										
2 Old Colorador River at Bypass	Tide										
	Salinity										
Salinity Sensor found not operating; could not solve problem; no replacement available											
3 Old Colorador River	Tide										
	Salinity										
Piling where instruments mounted knocked over in July; found by construction crew and placed on barge; retrieved the sensors; the tide gage destroyed when submerged; data lost; salinity sensor still operating and reinstalled at new location.											
4 Old Colorador River Above Entrance	Tide										
	Salinity										
5 West Colorado Lock	Tide										
	Salinity										
6 GIWWWest	Tide										
	Salinity										
7 Colorado Lock's East	Tide										
	Salinity										
Tide level recorder malfunctioned; no replacement available											
8 GIWW East	Tide										
	Salinity										
9 Matagorda Bay Diversion Channel	Tide										
	Salinity										
(XXX = No data available for the period of deployment)											

Table 1 (Concluded) Colorado River Project Field Data Instrumentation Log											
Station No.	Instrument	May	June	July	August	September	October	November	December		
10 Matagorda Bay West	Tide	—	—	—	—	XXXXXXX	XXXXXXX				
	Salinity	—	—	—	—	—	—				
	Current	—	—	—	—	—	—				
Instrument mount for tide and salinity meter were torn from the piling sometime in August; lay on the bottom of the bay for 1 month; Tide gage destroyed; Data lost; No replacement available; Salinity sensor reinstalled											
11 East Matagorda Bay	Tide	—	—	—	—	—	—				
	Salinity	—	—	—	—	—	—				
Late start for installation due to having to fabricate mounting apparatus and install the sensor											
12 East Matagorda Bay (East)	Tide	—	—	—	—	—	—				
	Salinity	—	—	—	—	—	—				
	Current	—	—	—	—	—	—				
Late start for installation due to having to fabricate mounting apparatus and install the sensor (XXX = No data available for the period of deployment)											

Table 2					
Range 1 Surface Salinity Concentration during 25 hour Survey					
Range		Date/ Time	Depth, ft		Salinity, ppt
1		7/20/01 7:08	3		22.1
1		7/20/01 8:30	3		23.19
1		7/20/01 9:14	3		20.33
1		7/20/01 10:01	3		20.95
1		7/20/01 11:02	3		21.31
1		7/20/01 12:07	3		20.33
1		7/20/01 13:04	3		21.9
1		7/20/01 14:05	3		22.03
1		7/20/01 15:06	3		18.99
1		7/20/01 16:06	3		18.72
1		7/20/01 17:09	3		16.76
1		7/20/01 18:02	3		15.46
1		7/20/01 19:11	3		14.94
1		7/20/01 20:14	3		14.12
1		7/20/01 22:10	3		13.44
1		7/20/01 23:13	3		12.98
1		7/21/01 0:13	3		12.54
1		7/21/01 1:07	3		12.49
1		7/21/01 2:03	3		12.63
1		7/21/01 3:11	3		12.29
1		7/21/01 4:07	3		12.15
1		7/21/01 5:09	3		12.37
1		7/21/01 6:03	3		13.15
1		7/21/01 7:04	3		14.75

Table 3					
Range 1 Mid-depth Salinity Concentration during 25 hour Survey					
Range		Date/ Time	Depth, ft		Salinity, ppt
1		7/20/01 7:12	9.2		22.59
1		7/20/01 8:28	7.2		23.65
1		7/20/01 9:13	7.7		25.38
1		7/20/01 10:02	7.7		25.07
1		7/20/01 11:05	8.7		24.94
1		7/20/01 12:06	7.2		24.69
1		7/20/01 13:04	7.8		25.37
1		7/20/01 14:06	7.5		26.45
1		7/20/01 15:06	7.4		25.51
1		7/20/01 16:06	8.3		25.94
1		7/20/01 17:09	8.1		26.31
1		7/20/01 18:02	8.2		27.08
1		7/20/01 19:10	7.5		25.75
1		7/20/01 20:13	7.8		25.73
1		7/20/01 22:09	8		26.02
1		7/20/01 23:12	7.5		27.24
1		7/21/01 0:14	7.7		27.29
1		7/21/01 1:06	7.7		25.28
1		7/21/01 2:02	7.5		25.33
1		7/21/01 3:11	7		24.97
1		7/21/01 4:05	6.8		24.15
1		7/21/01 5:08	8.2		26.42
1		7/21/01 6:02	7.4		26.57
1		7/21/01 7:03	7.7		27.05

Table 4					
Range 1 Bottom Salinity Concentration during 25 hour Survey					
Range		Date/ Time	Depth, ft		Salinity, ppt
1		7/20/01 7:06	14.5		29.11
1		7/20/01 8:26	11.5		26.86
1		7/20/01 9:12	12.5		28.44
1		7/20/01 10:01	12.5		28.54
1		7/20/01 11:04	14.4		28.93
1		7/20/01 12:05	11.5		24.53
1		7/20/01 13:03	12.6		28.48
1		7/20/01 14:05	12		27.34
1		7/20/01 15:05	11.9		28.6
1		7/20/01 16:05	13.6		25.72
1		7/20/01 17:08	13.2		24.01
1		7/20/01 18:01	13.5		24.64
1		7/20/01 19:09	12		28.13
1		7/20/01 20:11	12.7		28.34
1		7/20/01 22:07	13		26.7
1		7/20/01 23:10	12		27.95
1		7/21/01 0:11	12.5		23.17
1		7/21/01 1:05	12.5		26.4
1		7/21/01 2:00	12.5		24.55
1		7/21/01 3:09	10.9		26.95
1		7/21/01 4:04	10.6		26.95
1		7/21/01 5:06	13.5		26.26
1		7/21/01 6:01	11.9		25.29
1		7/21/01 7:02	12.5		27.05

Table 5					
Range 2 Surface Salinity Concentration during 25 hour Survey					
Range		Date/ Time	Depth, ft		Salinity, ppt
2		7/20/01 7:31	3		26.2
2		7/20/01 8:44	3		24
2		7/20/01 9:28	3		24.9
2		7/20/01 10:14	3		24.78
2		7/20/01 11:15	3		25.09
2		7/20/01 12:20	3		25.93
2		7/20/01 13:18	3		26.75
2		7/20/01 14:18	3		27.21
2		7/20/01 15:18	3		27.26
2		7/20/01 16:19	3		27.42
2		7/20/01 17:25	3		27.23
2		7/20/01 18:13	3		27.3
2		7/20/01 19:27	3		27.12
2		7/20/01 20:31	3		27.25
2		7/20/01 22:26	3		27.13
2		7/20/01 23:31	3		18.89
2		7/21/01 0:24	3		17.04
2		7/21/01 1:24	3		16.07
2		7/21/01 2:16	3		16.03
2		7/21/01 3:29	3		15.44
2		7/21/01 4:21	3		17
2		7/21/01 5:24	3		17.55
2		7/21/01 6:16	3		18.96
2		7/21/01 7:16	3		20.35

Table 6					
Range 2 Mid-depth Salinity Concentration during 25 hour Survey					
Range		Date/ Time	Depth, ft		Salinity, ppt
2		7/20/01 7:30	7.7		27.27
2		7/20/01 8:43	7		27.2
2		7/20/01 9:29	7.1		26.99
2		7/20/01 10:15	7.4		27.1
2		7/20/01 11:18	7.6		27.34
2		7/20/01 12:20	7.2		26.93
2		7/20/01 13:18	7.2		27.17
2		7/20/01 14:19	7.3		27.24
2		7/20/01 15:18	7		27.2
2		7/20/01 16:18	6.8		27.25
2		7/20/01 17:26	7.1		27.27
2		7/20/01 18:13	7		27.37
2		7/20/01 19:26	7.5		27.34
2		7/20/01 20:30	6.9		27.34
2		7/20/01 22:25	6.7		27.23
2		7/20/01 23:32	6.7		27.33
2		7/21/01 0:26	7		27.35
2		7/21/01 1:22	7		27.33
2		7/21/01 2:15	6.5		27.33
2		7/21/01 3:28	6.6		27.3
2		7/21/01 4:20	7.7		27.26
2		7/21/01 5:23	7.2		27.59
2		7/21/01 6:15	7.2		27.53
2		7/21/01 7:17	7.3		27.58

Table 7					
Range 2 Bottom Salinity Concentration during 25-hour survey					
Range		Date/ Time	Depth, ft		Salinity, ppt
2		7/20/01 7:29	12.5		27.71
2		7/20/01 8:41	11		27.81
2		7/20/01 9:27	11.2		27.83
2		7/20/01 10:14	11.9		25.25
2		7/20/01 11:16	12.3		25.28
2		7/20/01 12:19	11.4		26.59
2		7/20/01 13:17	11.4		27.24
2		7/20/01 14:17	11.7		27.29
2		7/20/01 15:17	11.1		27.17
2		7/20/01 16:17	10.6		27.2
2		7/20/01 17:24	11.2		27.25
2		7/20/01 18:12	11.1		27.2
2		7/20/01 19:25	11.9		27.2
2		7/20/01 20:29	10.8		27.39
2		7/20/01 22:23	9.5		27.31
2		7/20/01 23:30	10.5		27.32
2		7/21/01 0:24	11		22.24
2		7/21/01 1:21	11		27.44
2		7/21/01 2:13	10		26.1
2		7/21/01 3:26	10.2		27.52
2		7/21/01 4:18	10.5		27.2
2		7/21/01 5:21	11.4		27.56
2		7/21/01 6:14	11.1		27.31
2		7/21/01 7:15	11.7		27.63

Table 8					
Range 3 Surface Salinity Concentration during 25-hour Survey					
Range		Date/Time	Depth, ft		Salinity, ppt
3		7/20/01 8:07	3		24.17
3		7/20/01 8:55	3		23.25
3		7/20/01 9:44	3		23.68
3		7/20/01 10:32	3		23.83
3		7/20/01 11:42	3		24
3		7/20/01 12:36	3		24.15
3		7/20/01 13:43	3		24.4
3		7/20/01 14:36	3		24.54
3		7/20/01 15:43	3		24.47
3		7/20/01 16:34	3		24.52
3		7/20/01 17:45	3		24.53
3		7/20/01 18:25	3		24.69
3		7/20/01 19:45	3		24.64
3		7/20/01 22:41	3		24.47
3		7/20/01 23:58	3		22.03
3		7/21/01 0:42	3		21.15
3		7/21/01 1:49	3		19.98
3		7/21/01 2:29	3		20.7
3		7/21/01 3:52	3		21.82
3		7/21/01 4:41	3		21.88
3		7/21/01 5:44	3		22.22
3		7/21/01 6:30	3		22.41
3		7/21/01 7:38	3		22.4

Table 9**Range 3 Mid-depth Salinity Concentration during 25-hour Survey**

Range		Date/Time	Depth, ft		Salinity, ppt
3		7/20/01 8:06	8.7		25.6
3		7/20/01 8:54	9		25.71
3		7/20/01 9:44	8.4		25.33
3		7/20/01 10:33	8.3		24.81
3		7/20/01 11:41	8.6		24.87
3		7/20/01 12:37	8.3		24.83
3		7/20/01 13:43	8.5		24.91
3		7/20/01 14:36	8.7		24.7
3		7/20/01 15:43	8.8		24.75
3		7/20/01 16:35	8		24.72
3		7/20/01 17:47	8.4		24.59
3		7/20/01 18:26	7.8		24.7
3		7/20/01 19:44	7.5		24.65
3		7/20/01 22:40	7.7		24.52
3		7/20/01 23:57	7.5		24.11
3		7/21/01 0:40	7.6		24.03
3		7/21/01 1:46	7.7		24.52
3		7/21/01 2:30	8		25.61
3		7/21/01 3:51	7		24.47
3		7/21/01 4:40	8.2		25.46
3		7/21/01 5:43	8.3		25.32
3		7/21/01 6:29	8.7		24.85
3		7/21/01 7:38	6.4		24.11

Table 10**Range 3 Bottom Salinity Concentration during 25-hour Survey**

Range		Date/Time	Depth, ft		Salinity, ppt
3		7/20/01 8:04	14.2		26.47
3		7/20/01 8:53	15		27.5
3		7/20/01 9:43	12.8		26.06
3		7/20/01 10:32	13.6		25.96
3		7/20/01 11:40	14.2		25.76
3		7/20/01 12:35	13.7		25.39
3		7/20/01 13:42	14		25.07
3		7/20/01 14:35	14.5		25.15
3		7/20/01 15:42	13.7		25.24
3		7/20/01 16:35	13.1		25
3		7/20/01 17:46	13.8		24.85
3		7/20/01 18:25	12.7		24.75
3		7/20/01 19:43	12.7		24.68
3		7/20/01 22:39	12.5		26.05
3		7/20/01 23:55	12		24.26
3		7/21/01 0:39	12.2		24.13
3		7/21/01 1:46	12.5		25.35
3		7/21/01 2:28	13		25.88
3		7/21/01 3:49	11.1		25.73
3		7/21/01 4:38	13.4		25.88
3		7/21/01 5:42	13.6		26
3		7/21/01 6:28	14.4		25.07
3		7/21/01 7:37	9.8		25.49

Table 11					
Range 4 Surface Salinity Concentration during 25-hour Survey					
Range		Date/Time	Depth, ft		Salinity, ppt
4		7/20/01 7:03	3		28.48
4		7/20/01 8:18	3		28.46
4		7/20/01 9:05	3		29.69
4		7/20/01 10:20	3		28.24
4		7/20/01 11:08	3		28.6
4		7/20/01 12:16	3		27.5
4		7/20/01 13:07	3		26.9
4		7/20/01 14:28	3		26.6
4		7/20/01 15:06	3		27.11
4		7/20/01 16:17	3		27.51
4		7/20/01 17:08	3		27.4
4		7/20/01 18:25	3		28.75
4		7/20/01 19:06	3		29.3
4		7/20/01 20:28	3		29.06
4		7/20/01 21:12	3		28.75
4		7/20/01 22:26	3		27.35
4		7/20/01 23:12	3		27.3
4		7/21/01 0:20	3		27.58
4		7/21/01 1:12	3		27.73
4		7/21/01 2:23	3		27.61
4		7/21/01 3:08	3		27.59
4		7/21/01 4:21	3		27.69
4		7/21/01 5:15	3		27.34
4		7/21/01 6:21	3		27.76
4		7/21/01 7:07	3		28.1

Table 12**Range 4 Mid-depth Salinity Concentration during 25-hour Survey**

Range	Date/Time	Depth, ft	Salinity, ppt
4	7/20/01 7:02	8	28.57
4	7/20/01 8:17	9	28.56
4	7/20/01 9:04	9	29.92
4	7/20/01 10:19	8.5	29.8
4	7/20/01 11:07	9	30.5
4	7/20/01 12:15	9	29.3
4	7/20/01 13:06	9	29.12
4	7/20/01 14:27	9	27.6
4	7/20/01 15:05	9	28.45
4	7/20/01 16:16	9	28.23
4	7/20/01 17:07	9	28.52
4	7/20/01 18:24	9	29
4	7/20/01 19:05	9	29.3
4	7/20/01 20:27	9	29.1
4	7/20/01 21:11	9	28.92
4	7/20/01 22:25	9	27.51
4	7/20/01 23:10	9	27.38
4	7/21/01 0:19	9	27.6
4	7/21/01 1:11	9	27.79
4	7/21/01 2:22	9	27.61
4	7/21/01 3:07	9	27.69
4	7/21/01 4:20	9	27.68
4	7/21/01 5:14	9	27.43
4	7/21/01 6:20	9	27.83
4	7/21/01 7:06	9	28.1

Table 13					
Range 4 Bottom Salinity Concentration during 25-hour Survey					
Range		Date/Time	Depth, ft		Salinity, ppt
4		7/20/01 7:01	13		28.67
4		7/20/01 8:16	15		28.51
4		7/20/01 9:03	15		29.96
4		7/20/01 10:18	14		30.35
4		7/20/01 11:06	15		30.94
4		7/20/01 12:14	15		30.67
4		7/20/01 13:05	15		30.47
4		7/20/01 14:26	15		28.6
4		7/20/01 15:04	15		29.08
4		7/20/01 16:15	15		29.64
4		7/20/01 17:06	15		29.54
4		7/20/01 18:23	15		29.1
4		7/20/01 19:04	15		29.32
4		7/20/01 20:26	15		29.1
4		7/20/01 21:10	15		28.98
4		7/20/01 22:24	15		27.9
4		7/20/01 23:09	15		27.36
4		7/21/01 0:18	15		27.59
4		7/21/01 1:10	15		27.92
4		7/21/01 2:21	15		27.69
4		7/21/01 3:06	15		27.66
4		7/21/01 4:19	15		27.69
4		7/21/01 5:05	15		28.12
4		7/21/01 5:13	15		27.67
4		7/21/01 6:19	15		27.86

Table 14**Range 5 Surface Salinity Concentration during 25-hour Survey**

Range		Date/Time	Depth, ft		Salinity, ppt
5		7/20/01 7:17	3		29.36
5		7/20/01 8:06	3		31.16
5		7/20/01 9:18	3		31.73
5		7/20/01 10:03	3		32
5		7/20/01 11:23	3		32.43
5		7/20/01 12:04	3		32.55
5		7/20/01 13:30	3		26.82
5		7/20/01 14:13	3		26.36
5		7/20/01 15:21	3		26.67
5		7/20/01 16:04	3		26.28
5		7/20/01 17:23	3		25.83
5		7/20/01 18:04	3		26.42
5		7/20/01 19:24	3		26.89
5		7/20/01 20:06	3		27.52
5		7/20/01 21:30	3		27.86
5		7/20/01 22:05	3		27.62
5		7/20/01 23:24	3		27.3
5		7/21/01 0:05	3		27.17
5		7/21/01 1:33	3		27.44
5		7/21/01 2:05	3		27.42
5		7/21/01 3:23	3		27.27
5		7/21/01 4:06	3		27.26
5		7/21/01 5:30	3		28.06
5		7/21/01 6:07	3		28.1
5		7/21/01 7:20	3		28.04

Table 15					
Range 5 Mid-depth Salinity Concentration during 25-hour Survey					
Range		Date/Time	Depth, ft		Salinity, ppt
5		7/20/01 7:16	9.5		29.39
5		7/20/01 8:05	9.5		31.17
5		7/20/01 9:17	9.5		31.76
5		7/20/01 10:02	9.5		32.02
5		7/20/01 11:22	9.5		32.46
5		7/20/01 12:03	9.5		32.6
5		7/20/01 13:29	9.5		32.67
5		7/20/01 14:12	9.5		31.9
5		7/20/01 15:20	9		28.64
5		7/20/01 16:03	9		26.58
5		7/20/01 17:22	9		26.46
5		7/20/01 18:03	9		27.1
5		7/20/01 19:23	9		27.68
5		7/20/01 20:05	9		28.18
5		7/20/01 21:29	9		28.36
5		7/20/01 22:04	9		28.16
5		7/20/01 23:23	9		27.39
5		7/21/01 0:04	9		27.16
5		7/21/01 1:32	9		27.47
5		7/21/01 2:04	9		27.48
5		7/21/01 3:22	9		27.3
5		7/21/01 4:05	9		27.27
5		7/21/01 5:29	9		28.08
5		7/21/01 6:06	9		28.1
5		7/21/01 7:19	9		28.06

Table 16					
Range 5 Bottom Salinity Concentration during 25-hour Survey					
Range		Date/Time	Depth, ft		Salinity, ppt
5		7/20/01 7:15	16		29.37
5		7/20/01 8:04	16		31.15
5		7/20/01 9:16	16		31.75
5		7/20/01 10:01	16		32.03
5		7/20/01 11:21	16		32.44
5		7/20/01 12:02	16		32.6
5		7/20/01 13:28	16		32.7
5		7/20/01 14:11	16		32.74
5		7/20/01 15:19	15		32.67
5		7/20/01 16:02	15		29.06
5		7/20/01 17:21	15		26.5
5		7/20/01 18:02	15		27.26
5		7/20/01 19:22	15		27.8
5		7/20/01 20:04	15		28.6
5		7/20/01 21:28	15		28.64
5		7/20/01 22:03	15		28.42
5		7/20/01 23:22	15		27.38
5		7/21/01 0:03	15		27.17
5		7/21/01 1:31	15		27.5
5		7/21/01 2:03	15		27.48
5		7/21/01 3:21	15		27.29
5		7/21/01 4:04	15		27.26
5		7/21/01 5:28	15		28.06
5		7/21/01 6:05	15		28.11
5		7/21/01 7:18	15		28.05

Table 17					
Range 6 Surface Salinity Concentration during 25-hour Survey					
Range		Date/Time	Depth, ft		Salinity, ppt
6		7/20/2001 7:09	3		32.51
6		7/20/01 8:03	3		32.9
6		7/20/01 9:01	3		33.18
6		7/20/01 10:04	3		33.31
6		7/20/01 11:02	3		33
6		7/20/01 12:23	3		33.05
6		7/20/01 13:01	3		33.04
6		7/20/01 14:22	3		33.06
6		7/20/01 15:06	3		33.04
6		7/20/01 16:24	3		33.09
6		7/20/01 17:03	3		31.1
6		7/20/01 18:22	3		27.67
6		7/20/01 19:03	3		26.2
6		7/20/01 20:23	3		27.19
6		7/20/01 21:02	3		27.32
6		7/20/01 22:25	3		28
6		7/20/01 23:07	3		28.07
6		7/21/01 0:28	3		28.15
6		7/21/01 1:03	3		28.12
6		7/21/01 2:23	3		28.24
6		7/21/01 3:07	3		28.13
6		7/21/01 4:27	3		28.07
6		7/21/01 5:05	3		28.03
6		7/21/01 6:23	3		30.9
6		7/21/01 7:05	3		32.14
6		7/21/01 8:09	3		33.25

Table 18**Range 6 Mid-depth Salinity Concentration during 25-hour Survey**

6		7/20/01 8:10	8		33.29
6		7/20/01 10:06	10		33.52
6		7/20/01 11:08	8		32.95
6		7/20/01 12:25	8.2		32.95
6		7/20/01 13:02	8.2		32.96
6		7/20/01 14:23	8.2		32.99
6		7/20/01 15:07	8.2		32.97
6		7/20/01 16:25	8		33.04
6		7/20/01 17:05	7.8		32.22
6		7/20/01 18:23	7.8		27.67
6		7/20/01 19:04	7.5		26.17
6		7/20/01 20:25	7.5		27.27
6		7/20/01 21:03	7.2		27.36
6		7/20/01 22:26	7.5		27.96
6		7/20/01 23:08	7.8		28.07
6		7/21/01 0:29	7.8		28.14
6		7/21/01 1:05	8.5		28.13
6		7/21/01 2:24	8.2		28.14
6		7/21/01 3:08	7.8		28.15
6		7/21/01 4:28	8.2		28.05
6		7/21/01 5:06	7.5		28.02
6		7/21/01 6:24	7.5		31.13
6		7/21/01 7:08	8.2		32.13
6		7/21/01 7:15	8.8		32.49
6		7/21/01 8:05	10		33.1
6		7/21/01 9:03	8.4		33.1

Table 19					
Range 6 Bottom Salinity Concentration during 25-hour Survey					
Range		Date/Time	Depth, ft		Salinity, ppt
6		7/20/01 7:09	14.5		32.49
6		7/20/01 8:21	17.3		32.99
6		7/20/01 9:01	13.4		33.15
6		7/20/01 10:05	17		33.52
6		7/20/01 11:02	13		32.96
6		7/20/01 12:24	13.5		32.94
6		7/20/01 13:01	13.5		32.95
6		7/20/01 14:22	13.5		32.94
6		7/20/01 15:06	13.5		32.94
6		7/20/01 16:24	13		33.07
6		7/20/01 17:03	12.5		32.6
6		7/20/01 18:22	12.5		27.81
6		7/20/01 19:03	12		26.16
6		7/20/01 20:23	12		27.26
6		7/20/01 21:02	11.5		27.28
6		7/20/01 22:25	12		27.96
6		7/20/01 23:07	12.5		28.09
6		7/21/01 0:28	12.5		28.13
6		7/21/01 1:03	13		28.11
6		7/21/01 2:23	13.5		28.14
6		7/21/01 3:07	12.5		28.15
6		7/21/01 4:27	13.5		28.05
6		7/21/01 5:05	13.5		28.01
6		7/21/01 6:23	13.5		31.2
6		7/21/01 7:05	13.5		32.13
6		7/21/01 8:03	17		33.18
6		7/21/01 8:09	13		33.26

Table 20					
Range 7 Surface Salinity Concentration during 25-hour Survey					
Range		Date/Time	Depth, ft		Salinity, ppt
7		7/20/01 7:32	3		32.86
7		7/20/01 9:18	3		33.23
7		7/20/01 10:20	3		33
7		7/20/01 11:24	3		33.54
7		7/20/01 13:19	3		33.58
7		7/20/01 2:04 PM	3		33.66
7		7/20/01 3:26 PM	3		33.48
7		7/20/01 16:05	3		33.41
7		7/20/01 17:22	3		32.98
7		7/20/01 18:03	3		33.07
7		7/20/01 19:20	3		30.05
7		7/20/01 20:04	3		27.29
7		7/20/01 21:27	3		26.78
7		7/20/01 22:04	3		27.26
7		7/20/01 23:31	3		28.04
7		7/21/01 0:09	3		27.99
7		7/21/01 1:31	3		27.99
7		7/21/01 2:07	3		27.99
7		7/21/01 3:30	3		29.26
7		7/21/01 4:07	3		30.24
7		7/21/01 5:24	3		33.08
7		7/21/01 6:06	3		33.83
7		7/21/01 7:21	3		34.03
7		7/21/01 7:53	3		34.27
7		7/21/01 8:21	3		33.02
7		7/21/01 12:04	3		33.56

Table 21					
Range 7 Mid-depth Salinity Concentration during 25-hour Survey					
Range		Date/Time	Depth, ft		Salinity, ppt
7		7/20/01 7:36	10.4		33.09
7		7/20/01 9:20	10.2		33.34
7		7/20/01 10:22	8.5		33.03
7		7/20/01 11:25	10		33.6
7		7/20/01 12:06	9		33.59
7		7/20/01 13:21	10		33.63
7		7/20/01 14:05	9.2		33.59
7		7/20/01 15:27	8.2		33.51
7		7/20/01 16:07	9.2		33.37
7		7/20/01 17:23	9		32.98
7		7/20/01 18:04	8.2		33.05
7		7/20/01 19:21	9.2		30.12
7		7/20/01 20:05	9		27.15
7		7/20/01 20:06	7.2		27.37
7		7/20/01 21:29	9		26.72
7		7/20/01 23:32	9.5		28
7		7/21/01 0:10	9.5		27.94
7		7/21/01 1:33	10		27.9
7		7/21/01 2:08	10		27.98
7		7/21/01 3:32	10		30.24
7		7/21/01 4:08	9.8		32.64
7		7/21/01 5:25	10.2		33.71
7		7/21/01 6:08	8.5		33.7
7		7/21/01 7:22	9.8		34.24
7		7/21/01 7:54	9.5		34.32
7		7/21/01 8:24	8.4		33

Table 22					
Range 7 Bottom Salinity Concentration during 25-hour Survey					
Range		Date/Time	Depth, ft		Salinity, ppt
7		7/20/01 7:32	20.8		33.09
7		7/20/01 9:19	17.5		33.41
7		7/20/01 10:21	14		33.05
7		7/20/01 11:24	17		33.64
7		7/20/01 12:05	16.5		33.6
7		7/20/01 13:19	17		33.64
7		7/20/01 14:04	15.5		33.6
7		7/20/01 15:26	13.5		33.46
7		7/20/01 16:05	15.5		33.42
7		7/20/01 17:22	15		32.97
7		7/20/01 18:03	13.5		33.05
7		7/20/01 19:20	15.5		30.33
7		7/20/01 20:04	11.5		27.5
7		7/20/01 20:04	15		27.2
7		7/20/01 21:27	15		26.79
7		7/20/01 23:31	16		28.06
7		7/21/01 0:09	16		27.97
7		7/21/01 1:31	17		27.97
7		7/21/01 2:07	17		27.97
7		7/21/01 3:30	17		33.31
7		7/21/01 4:07	16.5		33.17
7		7/21/01 5:24	17.5		33.76
7		7/21/01 6:06	14		33.91
7		7/21/01 7:21	16.5		34.22
7		7/21/01 7:53	16		34.27

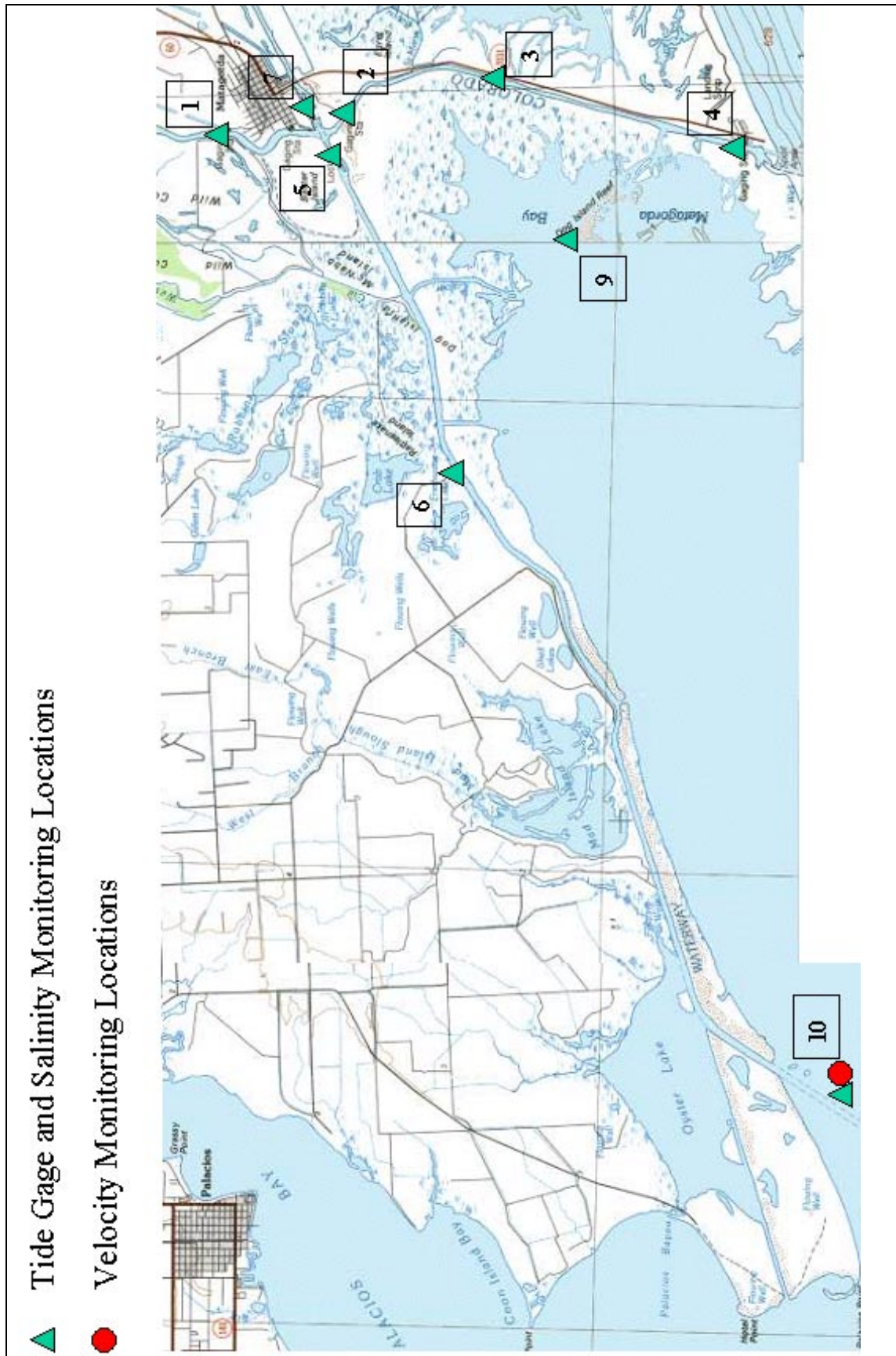


Figure 1. Instrument locations in the Colorado River, diversion channel and west GIWW

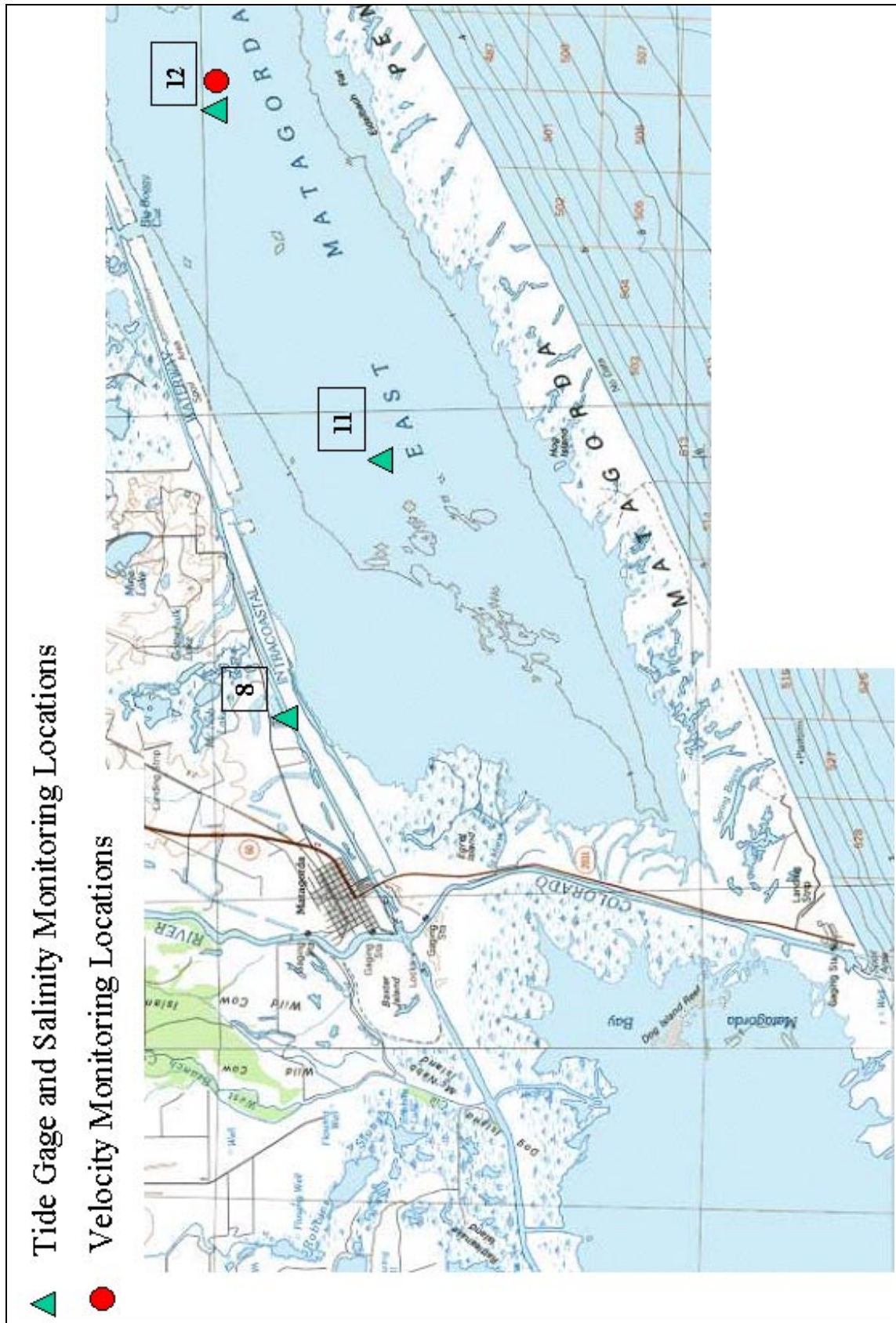


Figure 2. Instrument locations in East Matagorda Bay and the east GIWW

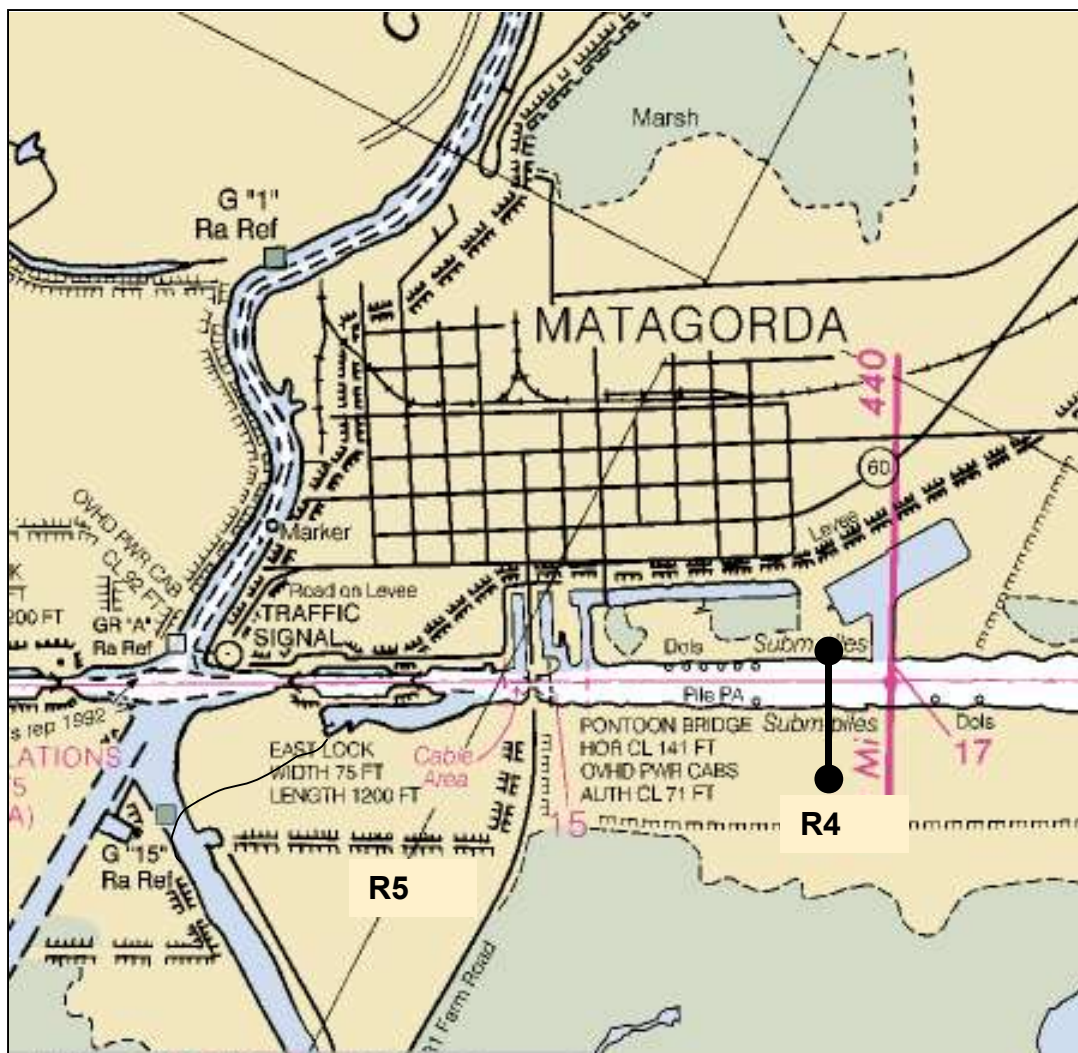


Figure 4. 25 hr velocity data collection locations for Boat No. 1

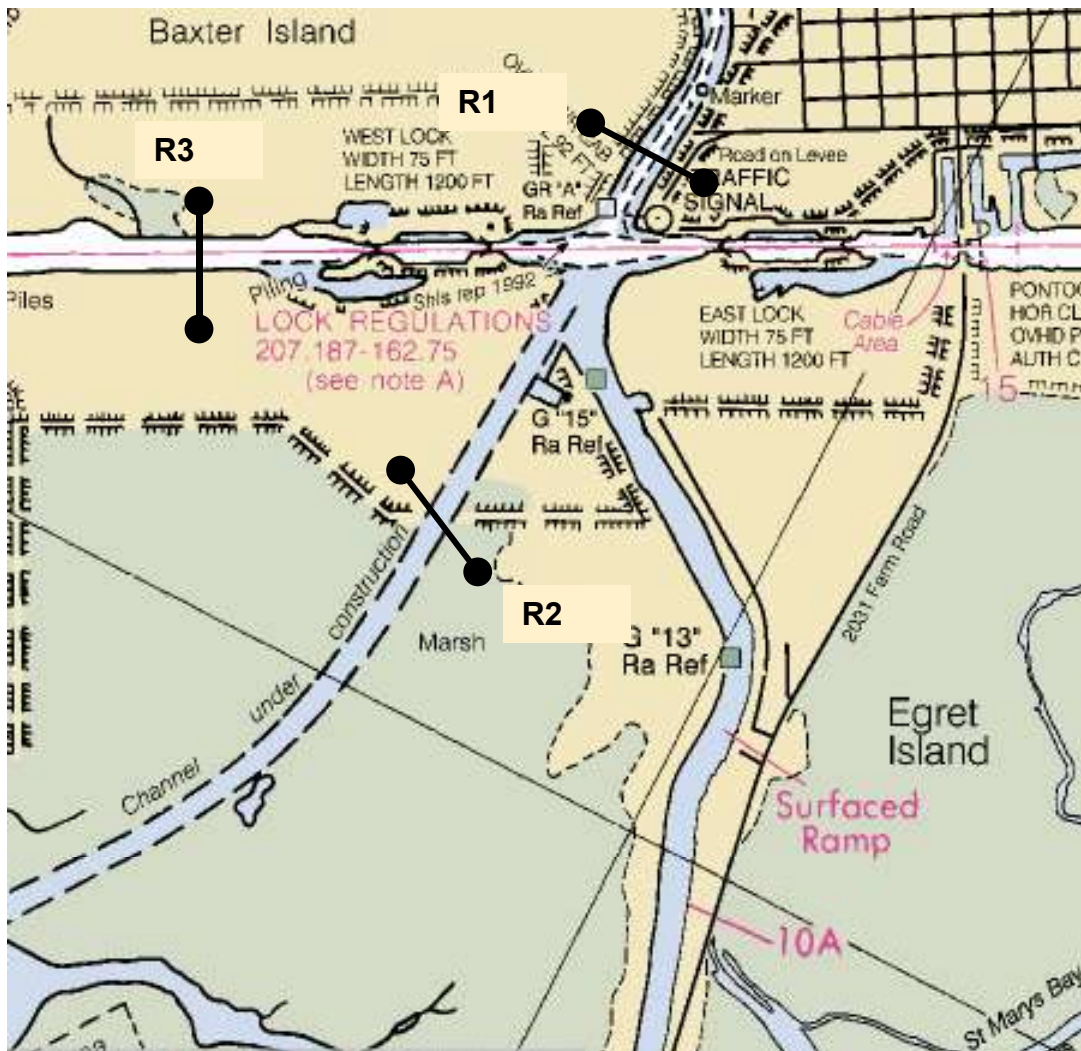


Figure 5. 25 hr velocity data collection transect locations for Boat No. 3

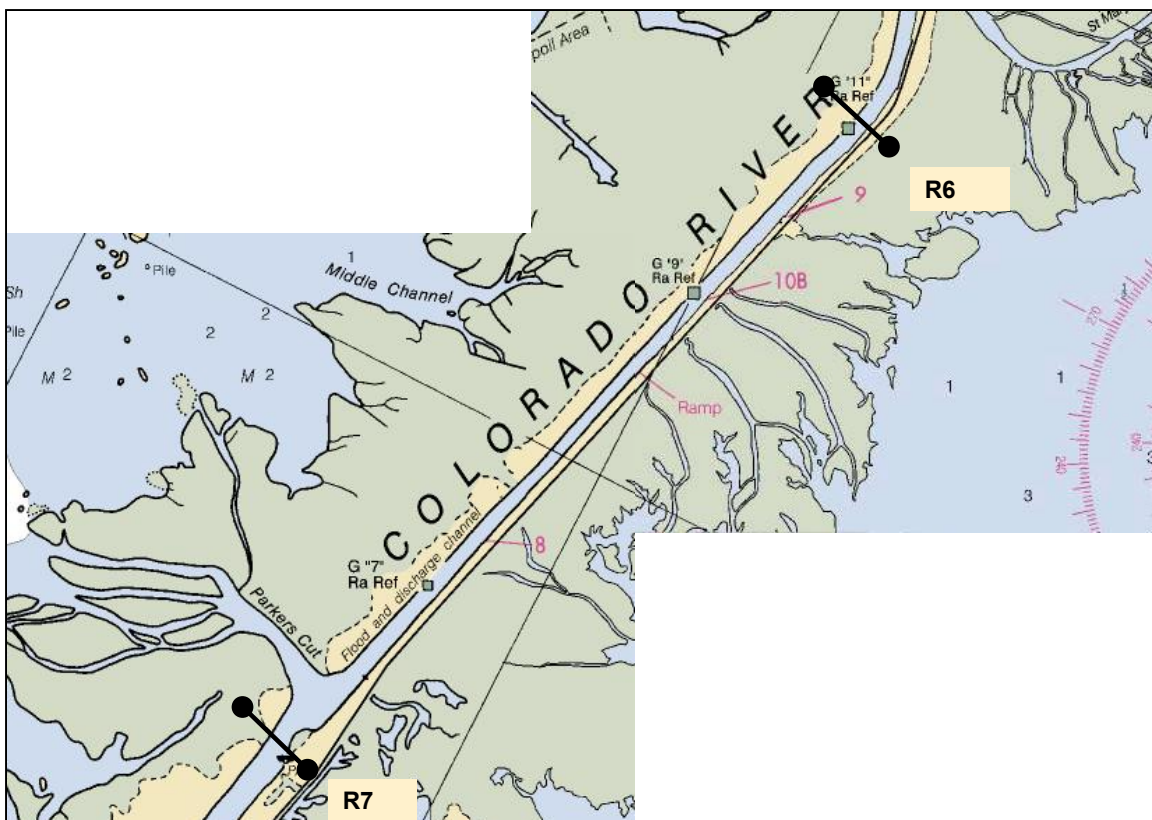


Figure 6. 25 hr velocity data collection transect locations for Boat No. 2

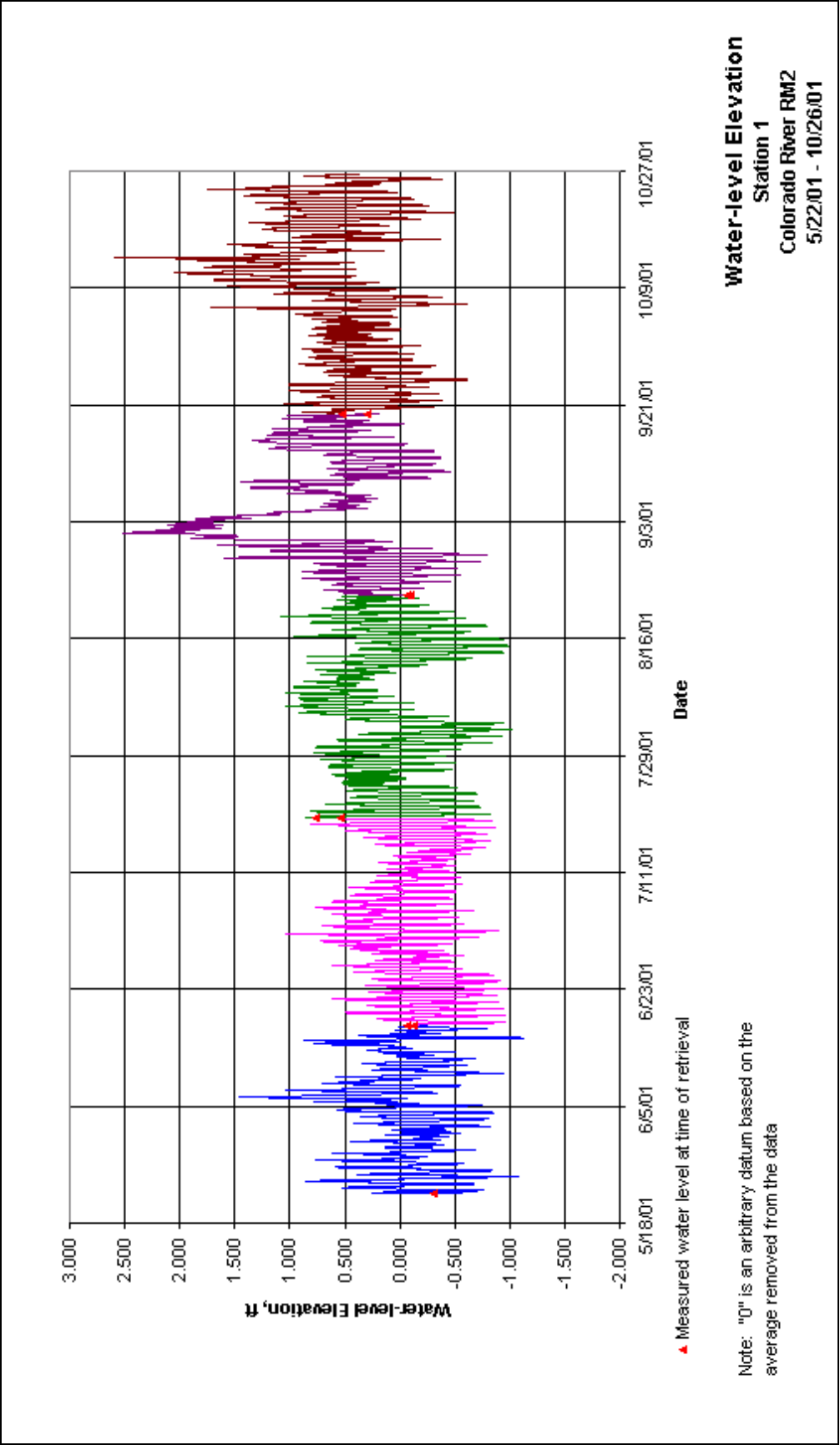


Figure 7. Time-history of water-level elevations for Station 1 during the period 5/22/01 – 10/26/01

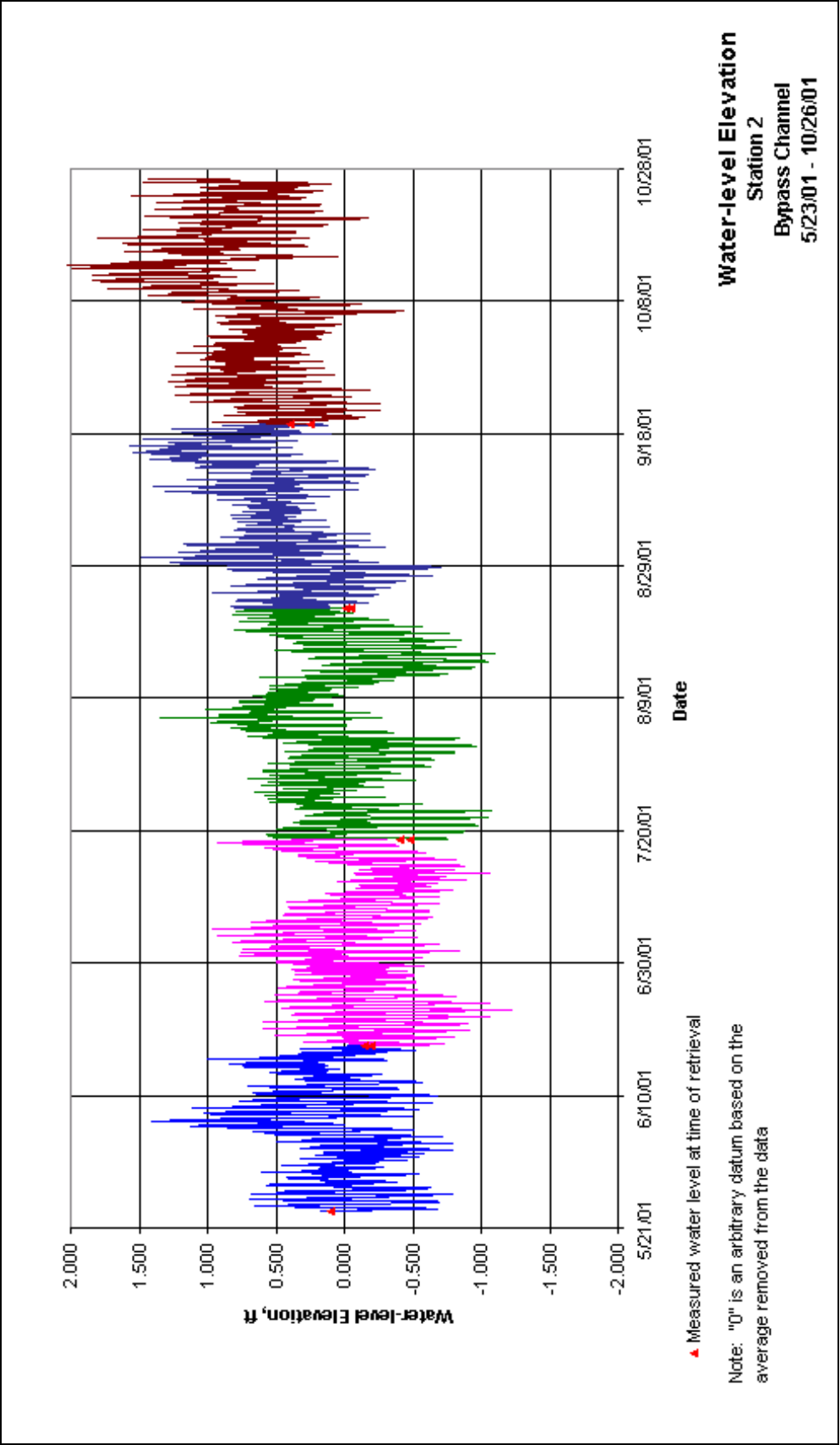


Figure8. Time-history of water-level elevations for Station 2 during the period 5/22/01 – 10/26/01

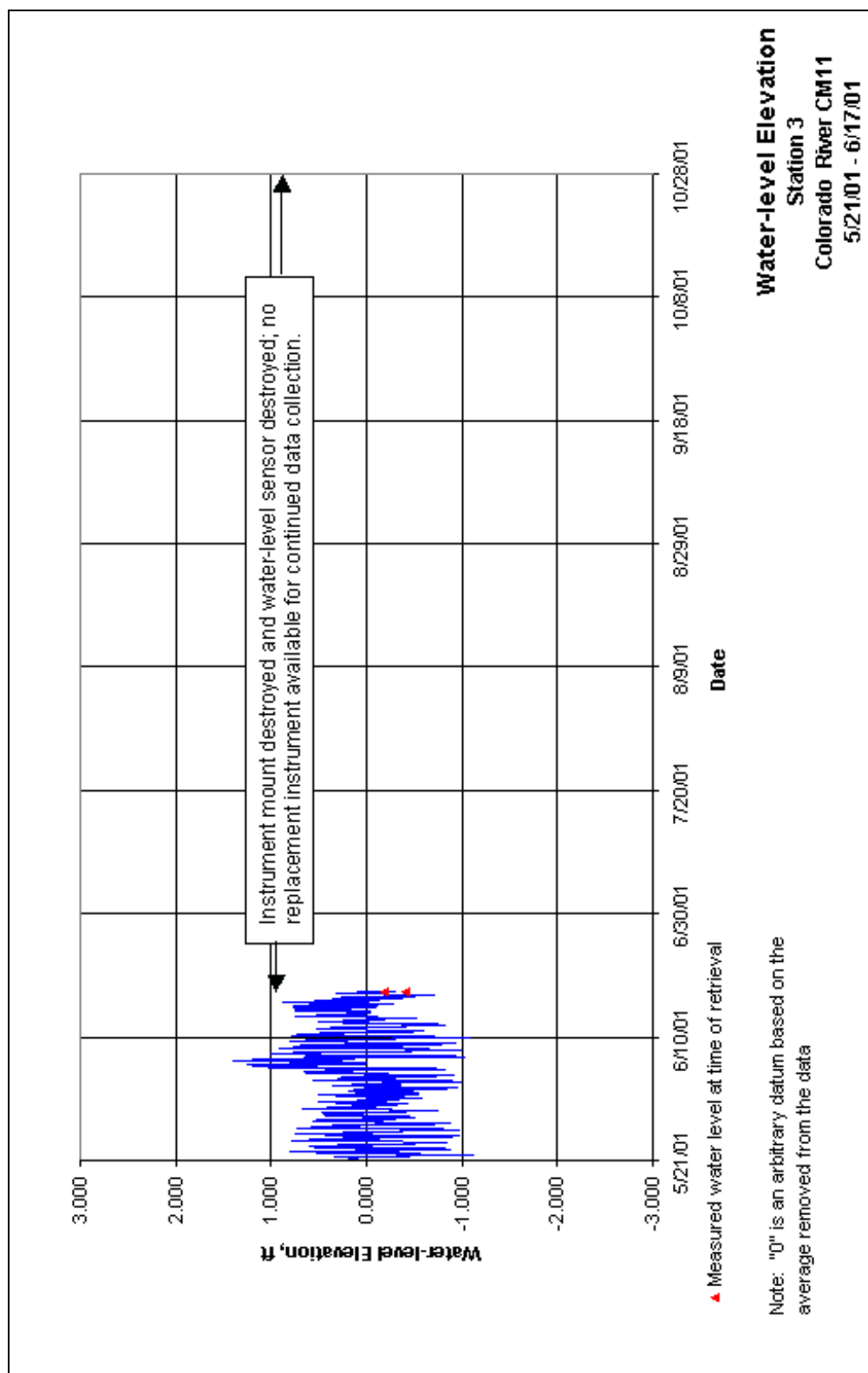


Figure 9. Time-history plot of water level elevations for Station 3 during the period 5/21/01 – 6/17/01

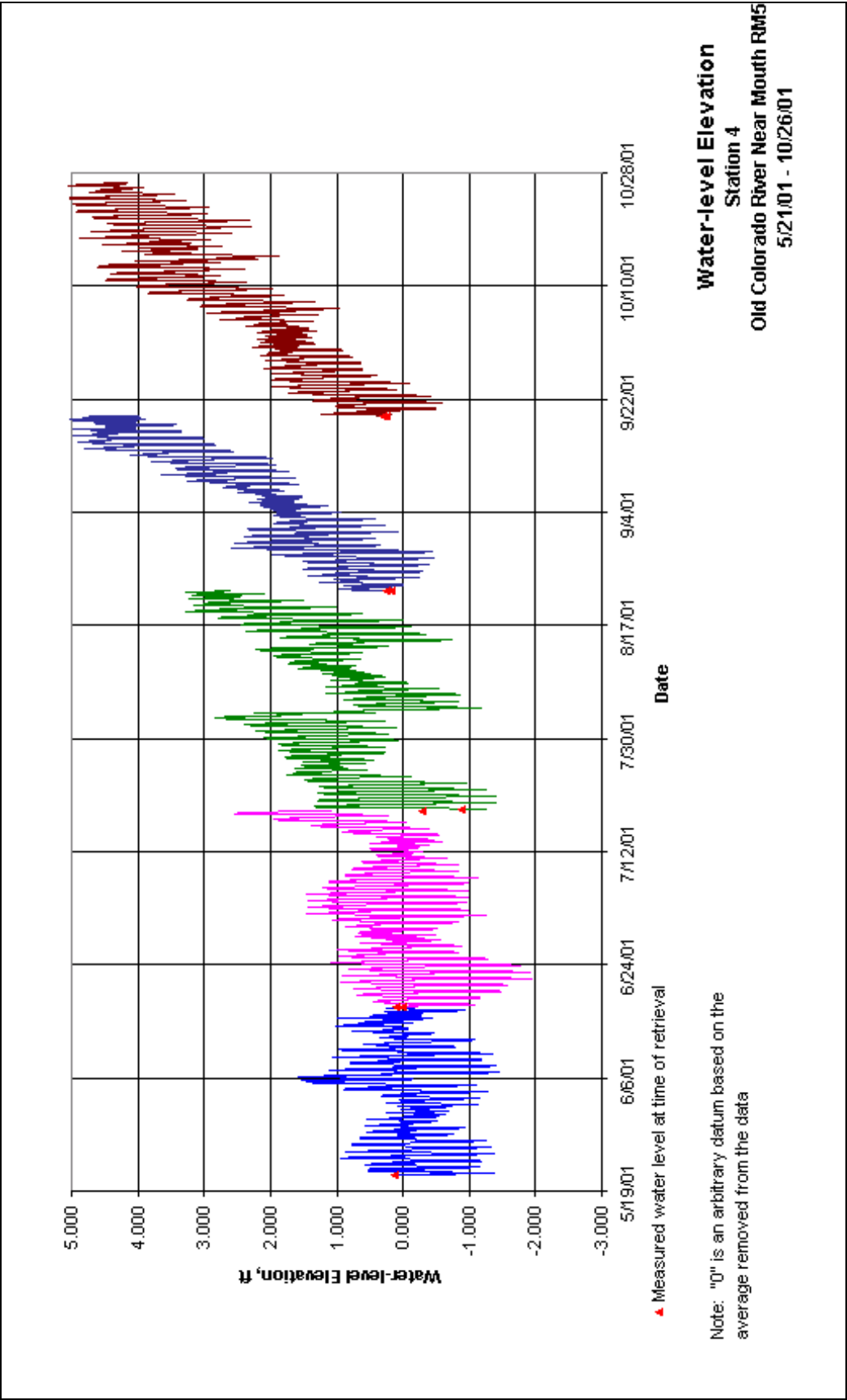


Figure 10. Time-history plot of water level elevations for Station 4 during the period 5/19/01 – 10/26/01

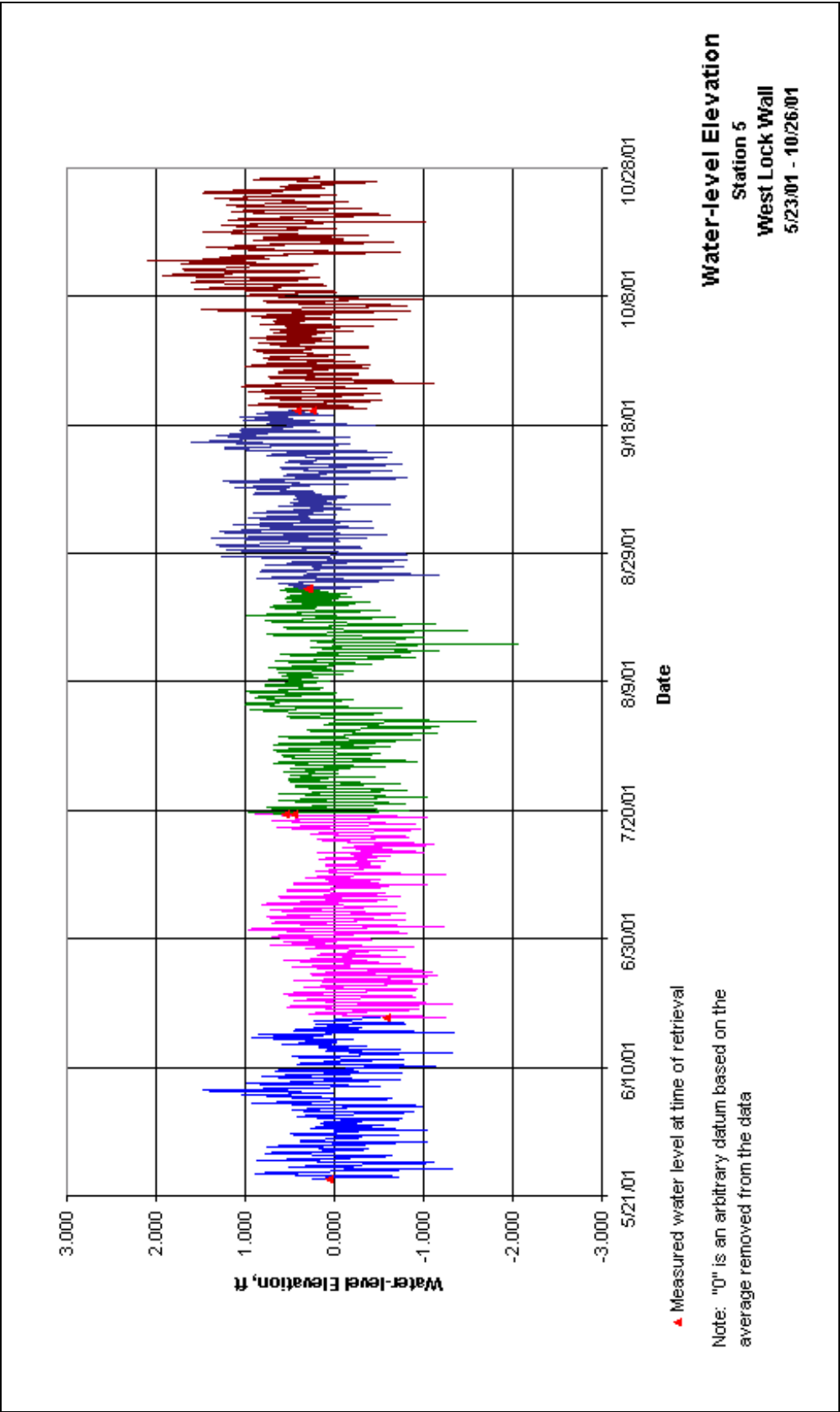


Figure 11. Time-history plot of water level elevations for Station 5 during the period 5/23/01 – 10/26/01

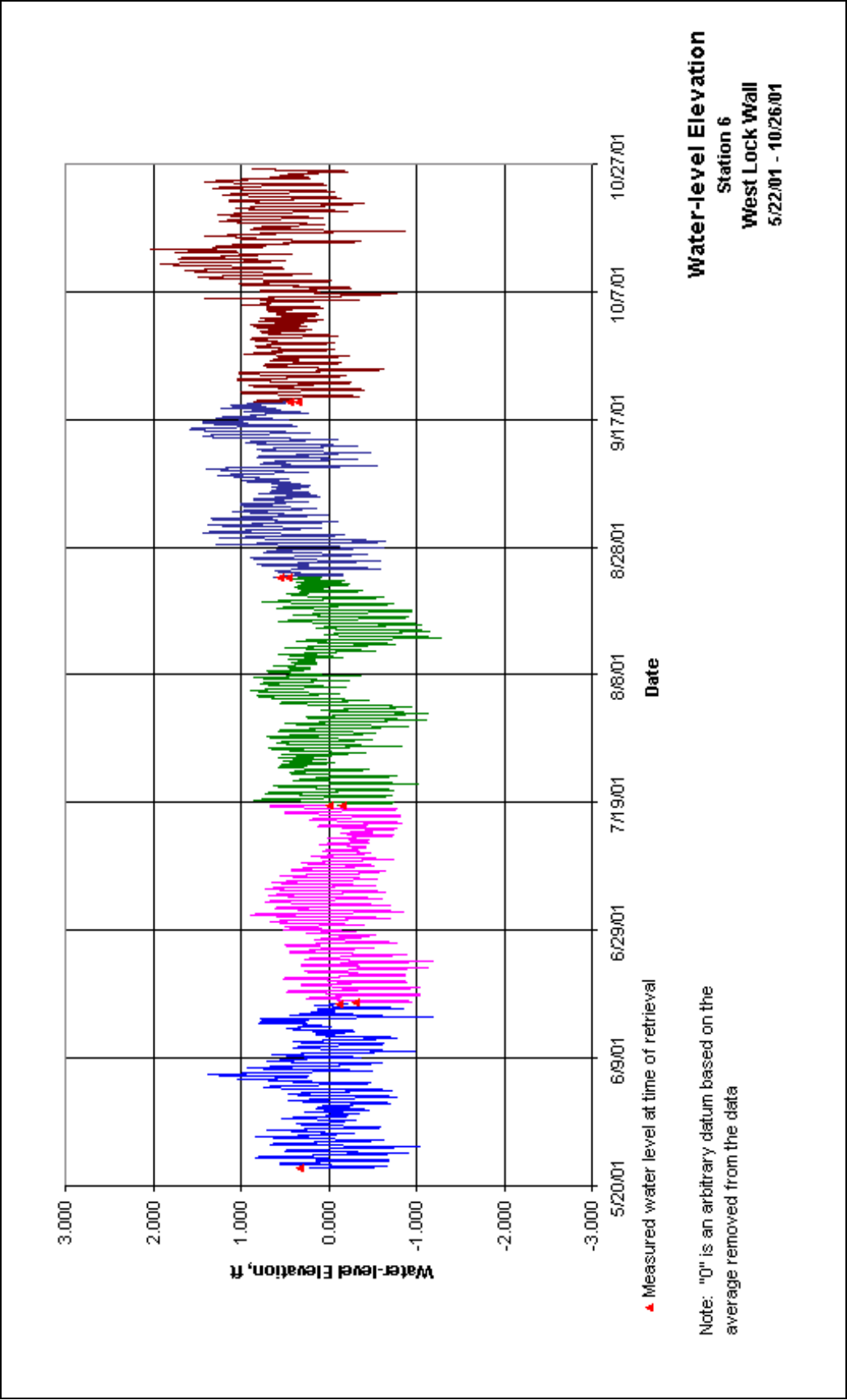


Figure 12. Time-history plot of water level elevations for Station 6 during the period 5/22/01 – 10/26/01

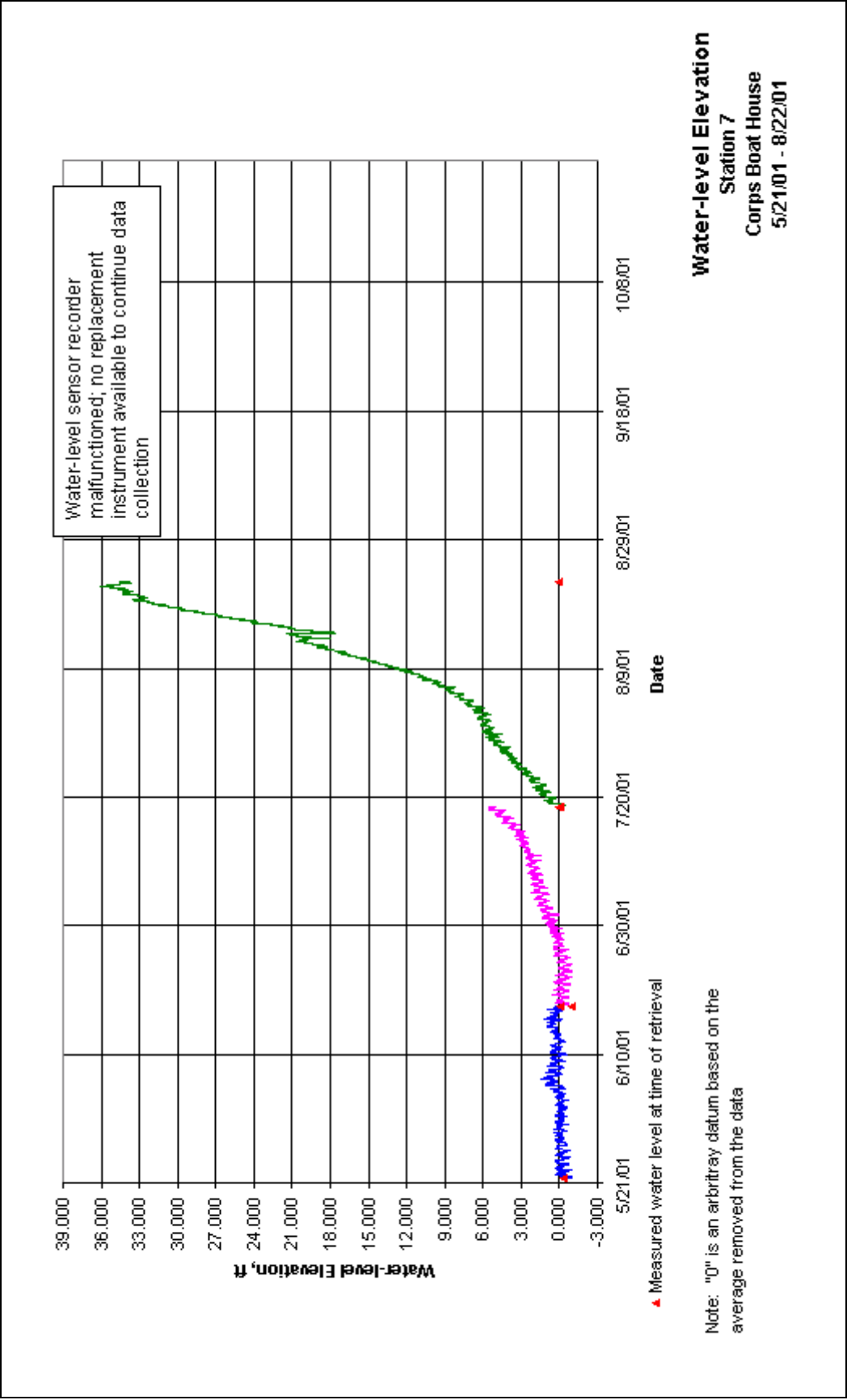


Figure 13. Time-history plot of water level elevations for Station 7 during the period 5/21/01 – 08/22/01

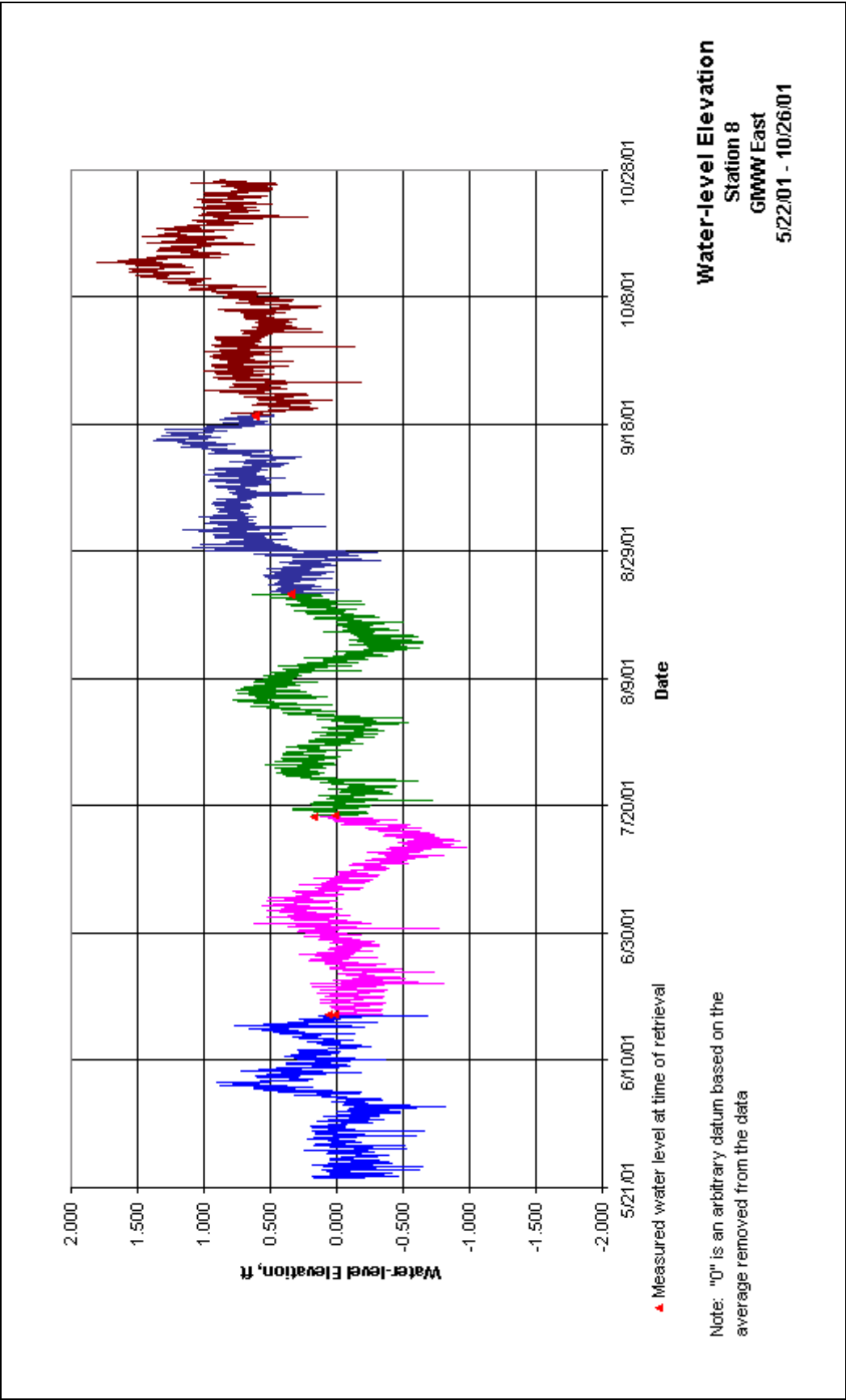


Figure 14. Time-history plot of water level elevations for Station 8 during the period 5/22/01 – 10/26/01

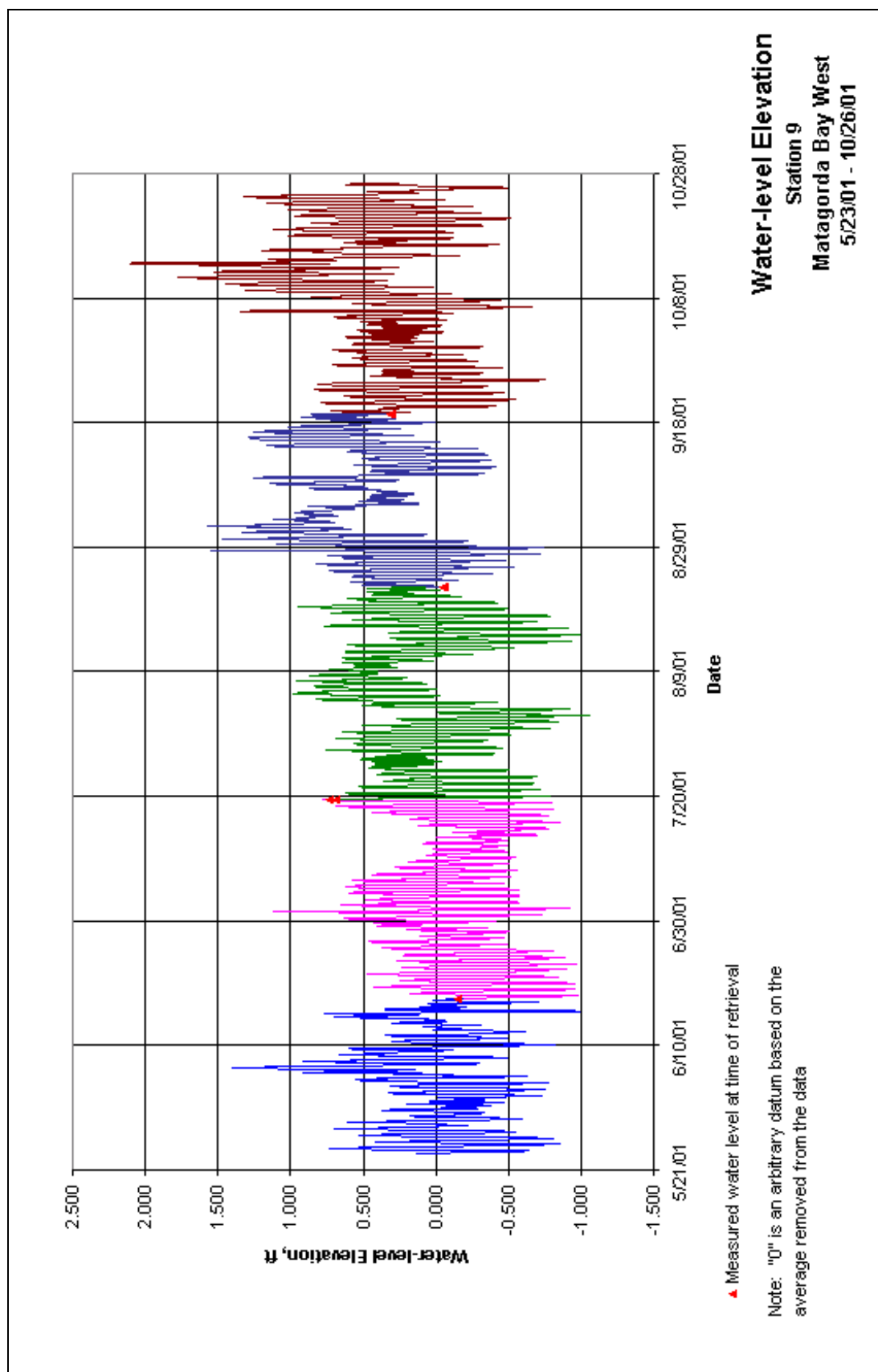


Figure 15. Time-history plot of water level elevations for Station 9 during the period 5/23/01 – 10/26/01

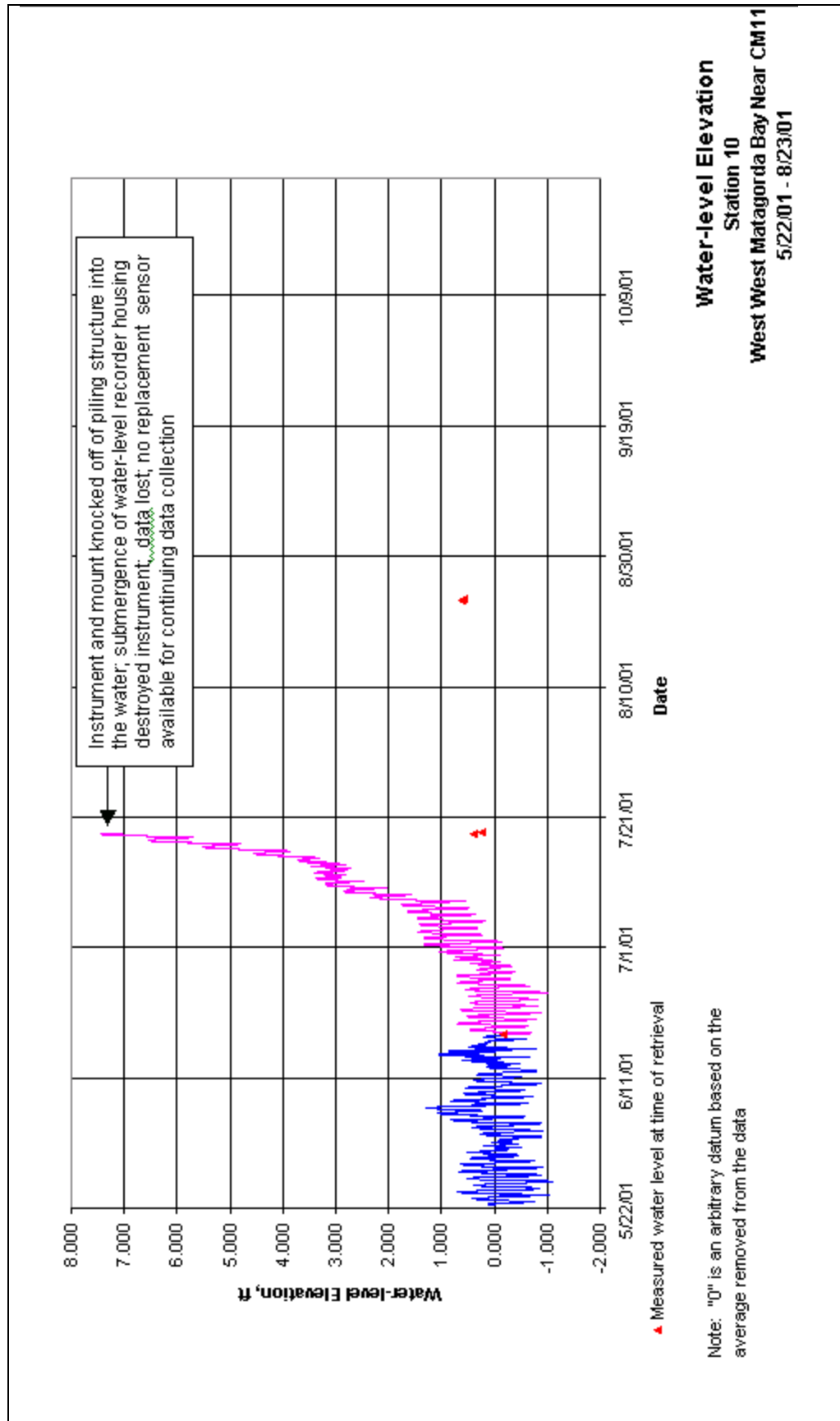


Figure 16. Time-history plot of water level elevations for Station 10 during the period 5/23/01 – 08/23/01

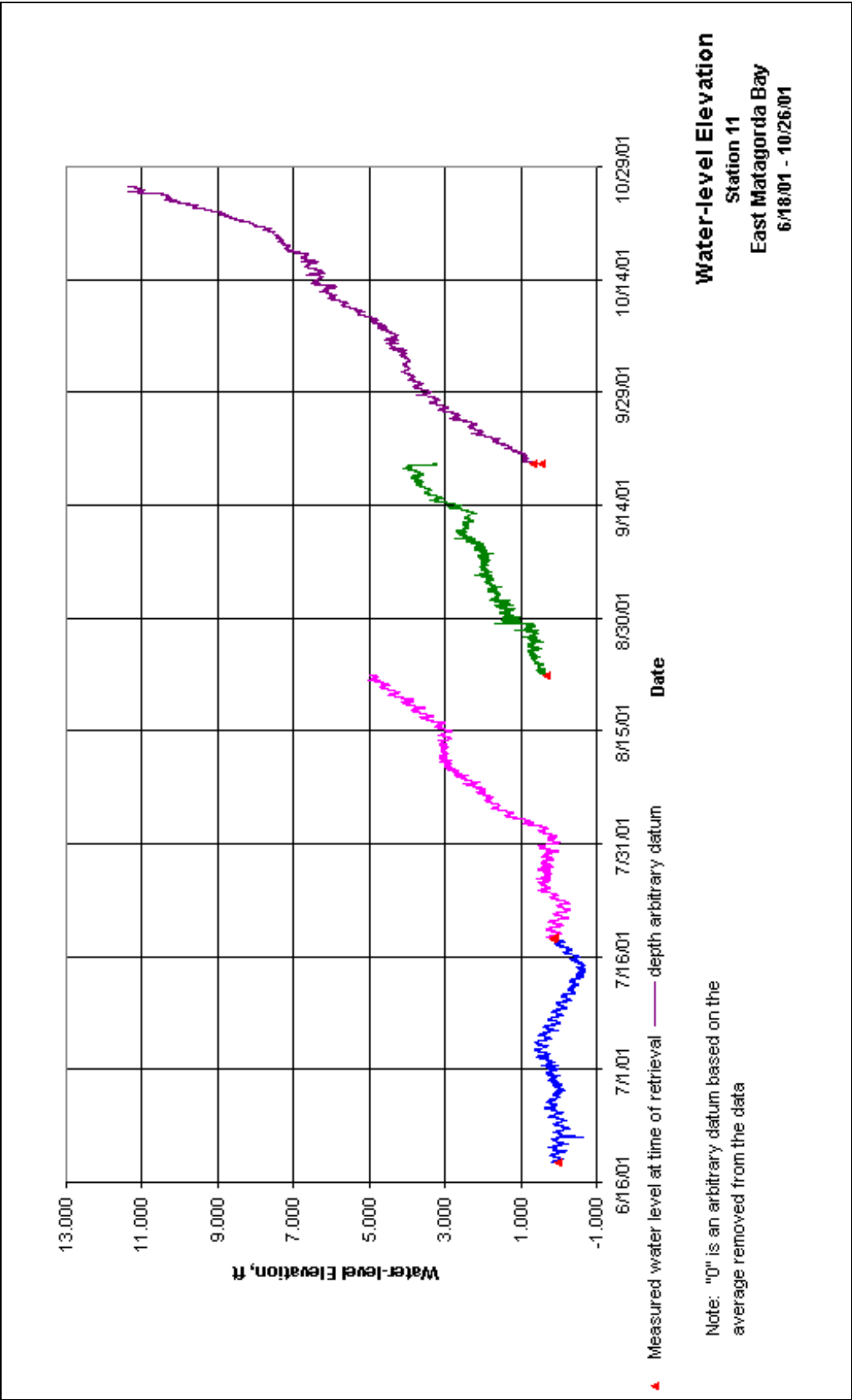


Figure 17. Time-history plot of water level elevations for Station 11 during the period 6/18/01 – 10/26/01

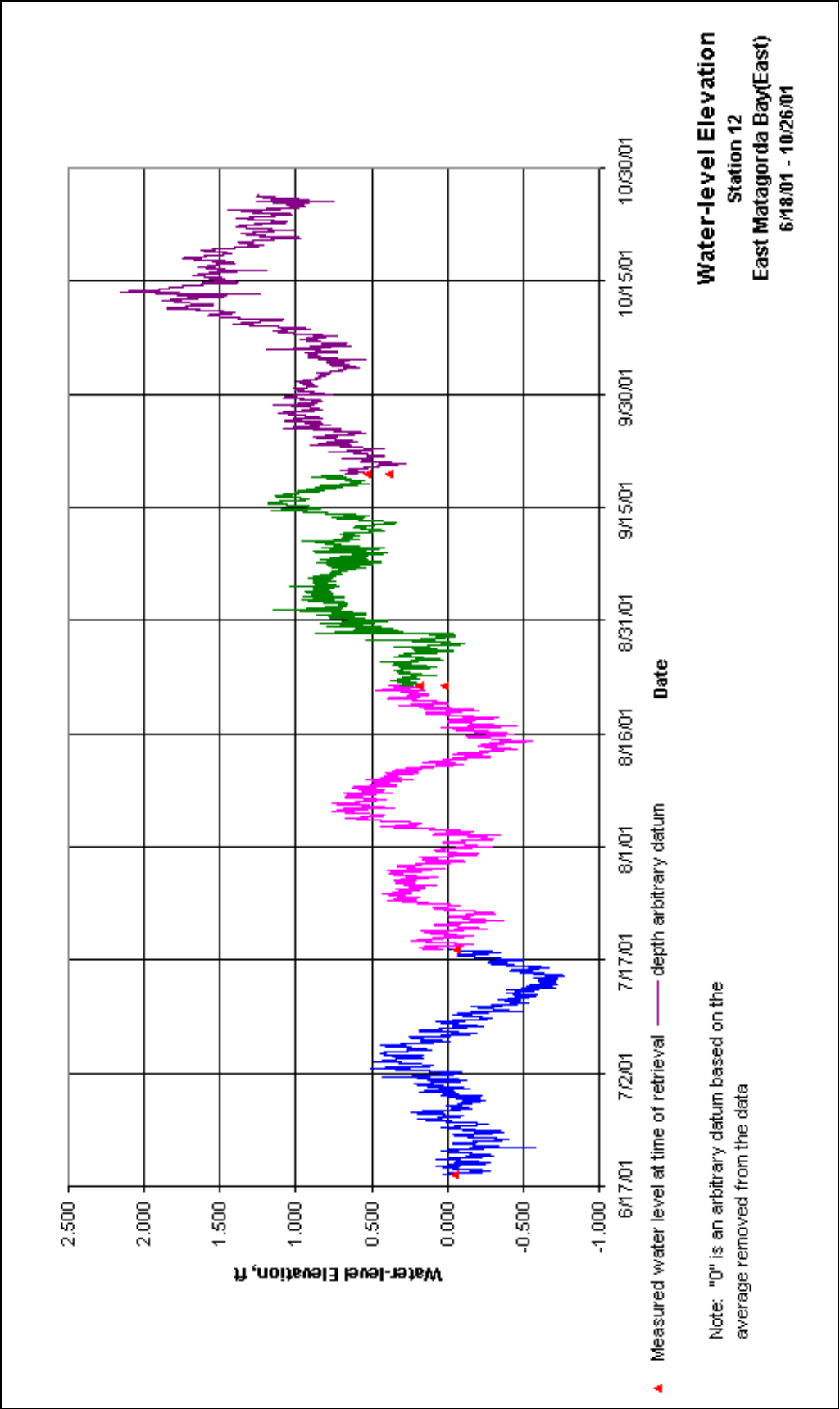


Figure 18. Time-history plot of water level elevations for Station 12 during the period 6/18/01 – 10/26/01

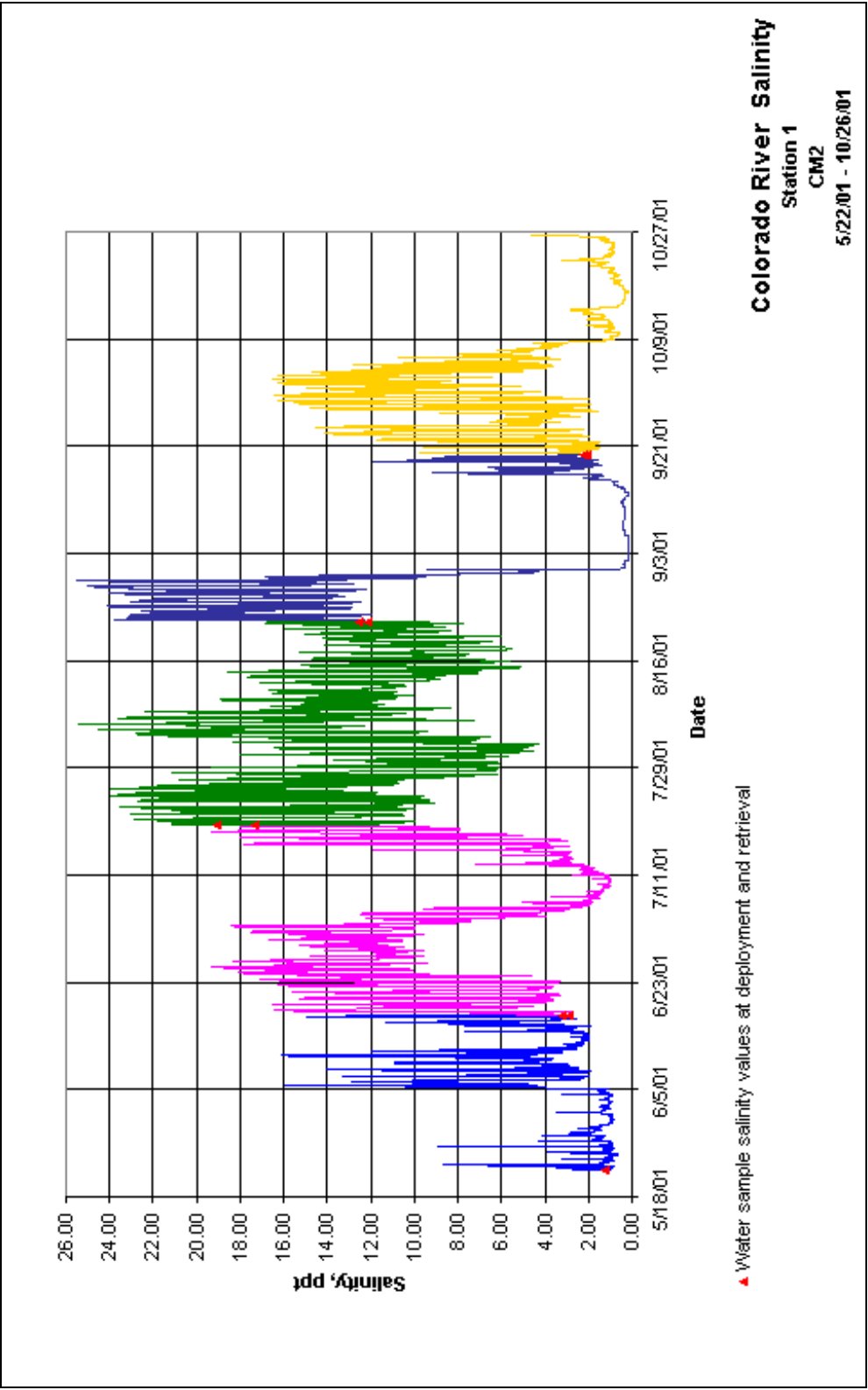


Figure 19. Time-history of salinity for Station 1 during the period 5/22/01 – 10/26/01

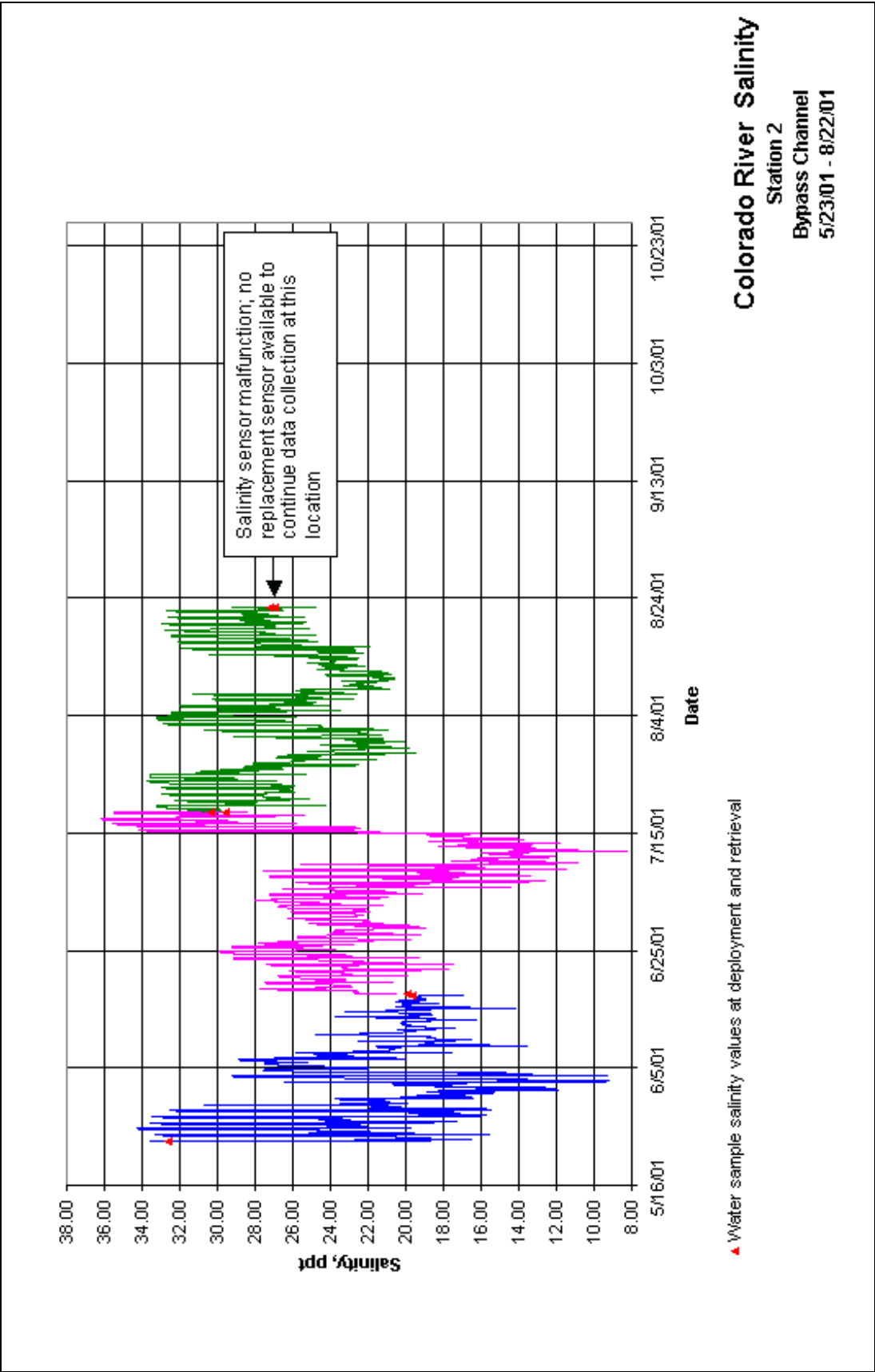


Figure 20. Time-history of salinity for Station 2 during the period 5/23/01 – 08/22/01

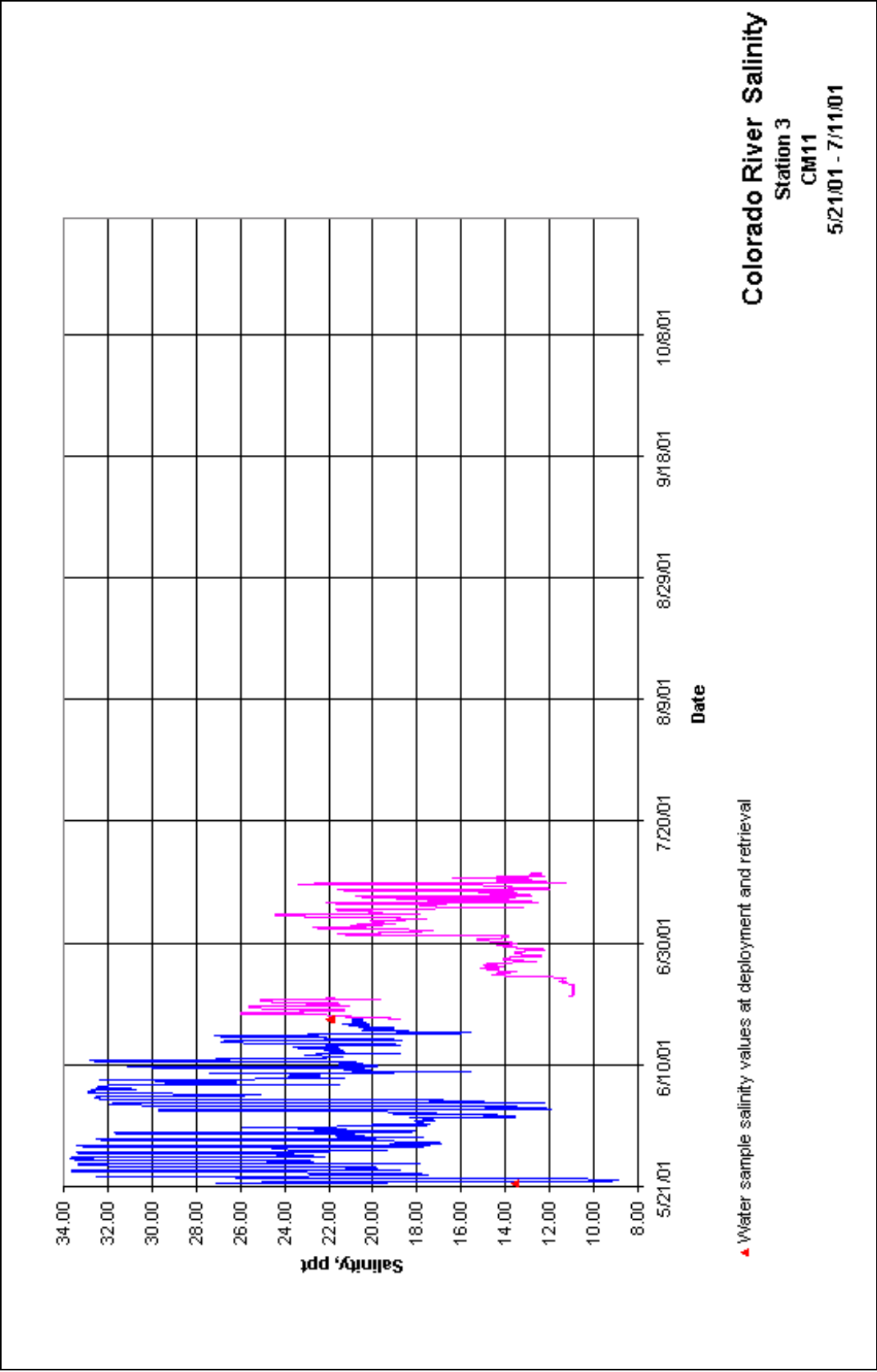


Figure 21. Time-history of salinity for Station 3 during the period 5/22/01 – 07/11/01

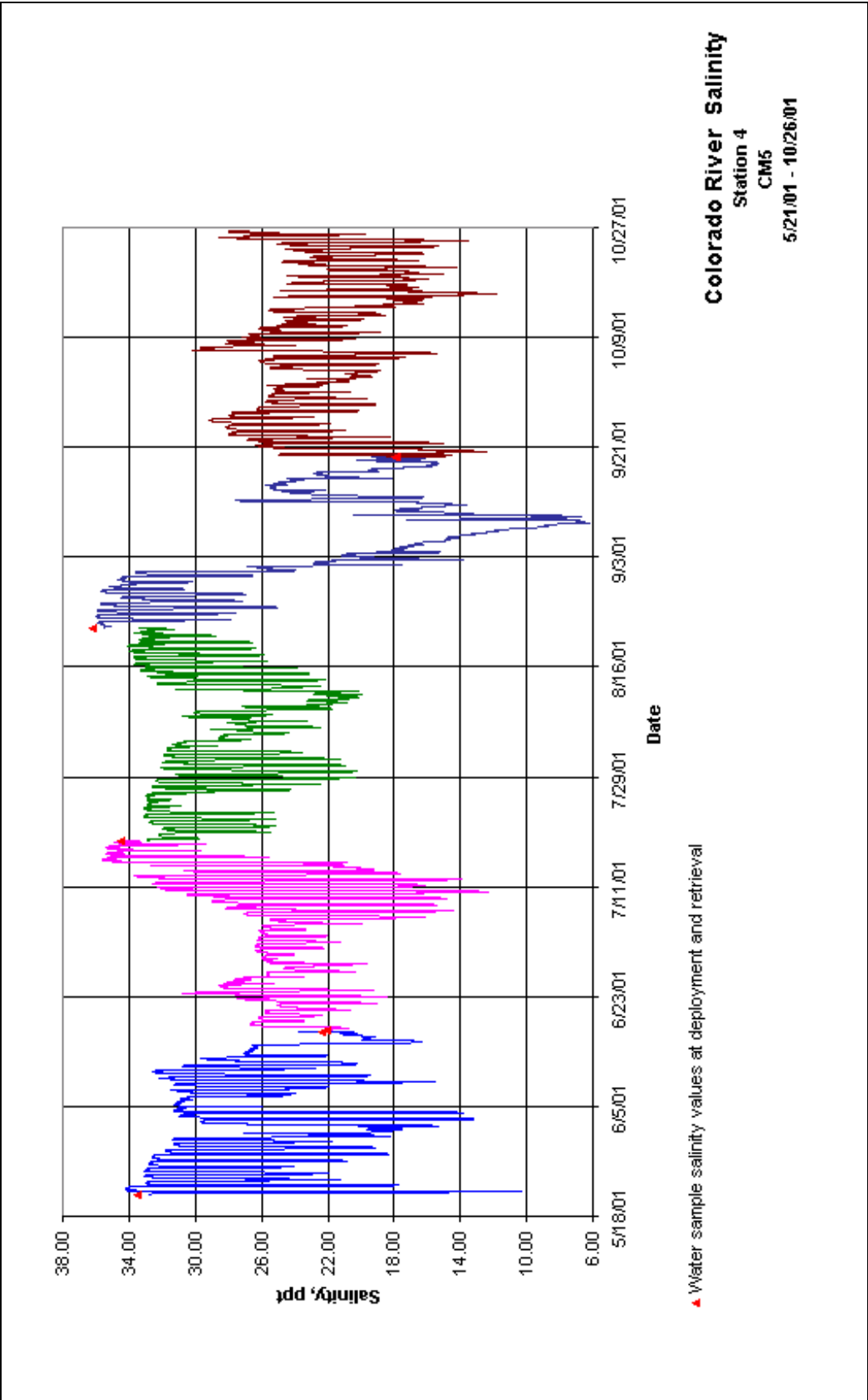


Figure 22. Time-history of salinity for Station 4 during the period 5/21/01 – 10/26/01

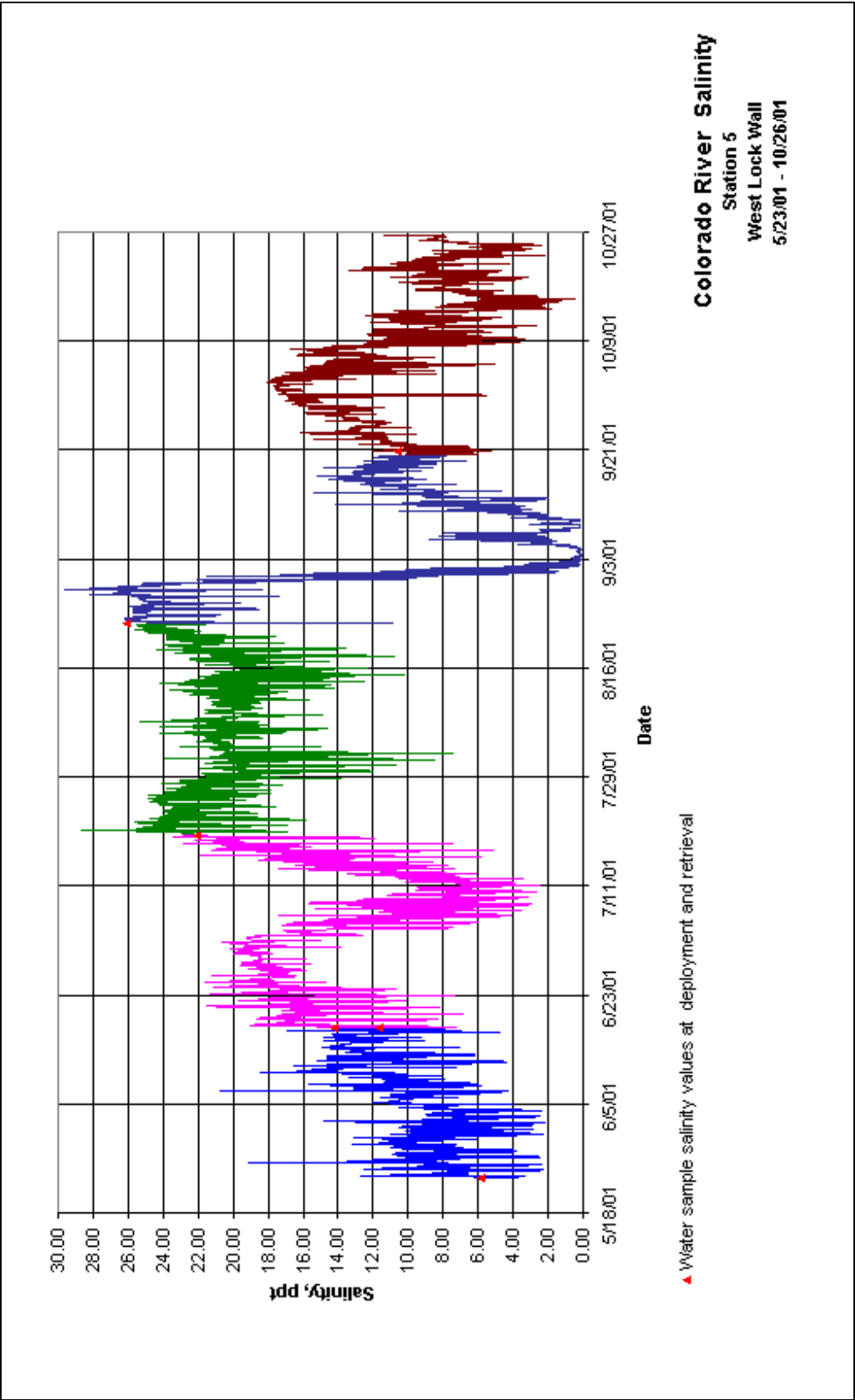


Figure 23. Time-history of salinity for Station 5 during the period 5/23/01 – 10/26/01

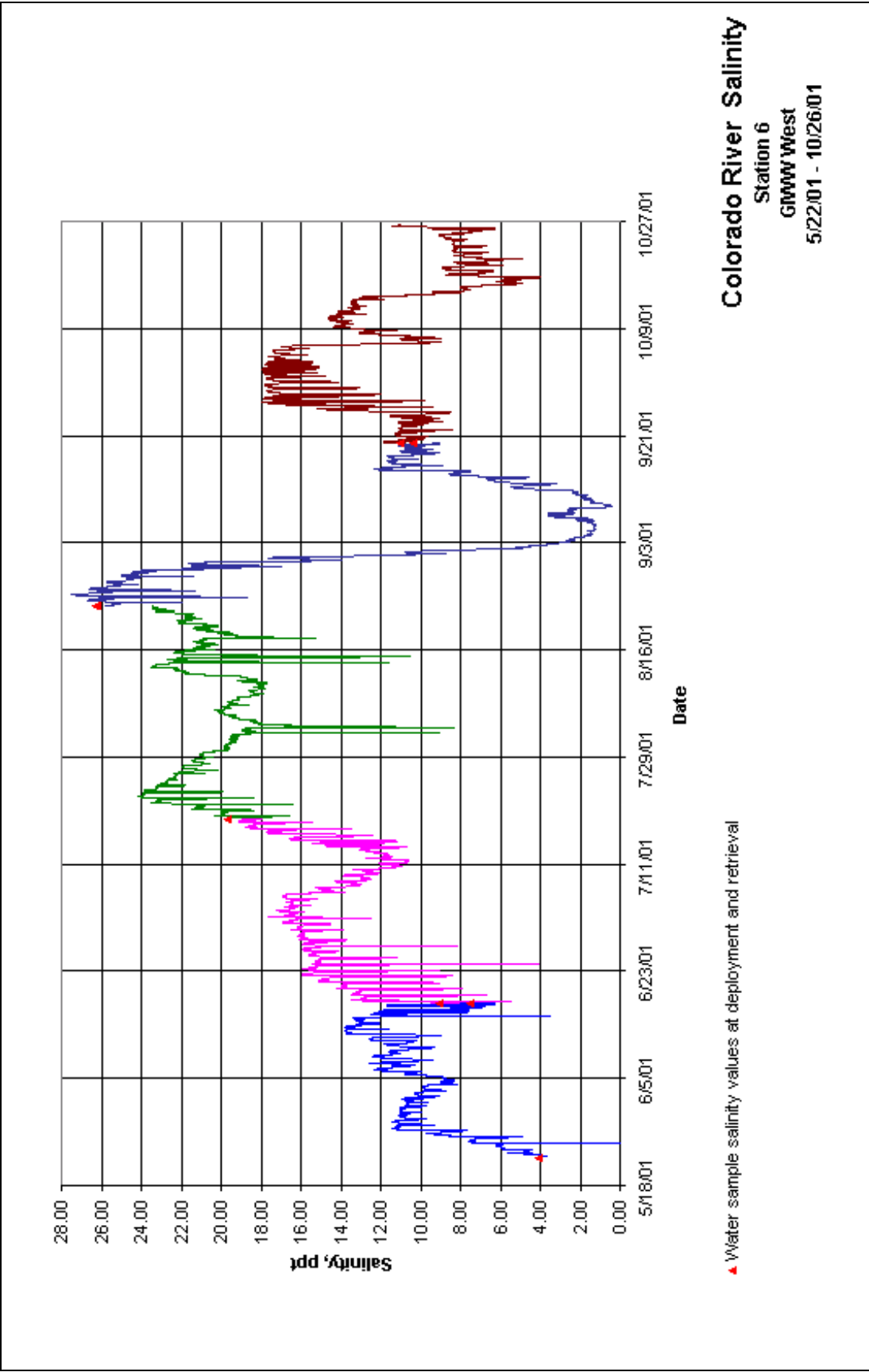


Figure 24. Time-history of salinity for Station 6 during the period 5/22/01 – 10/26/01

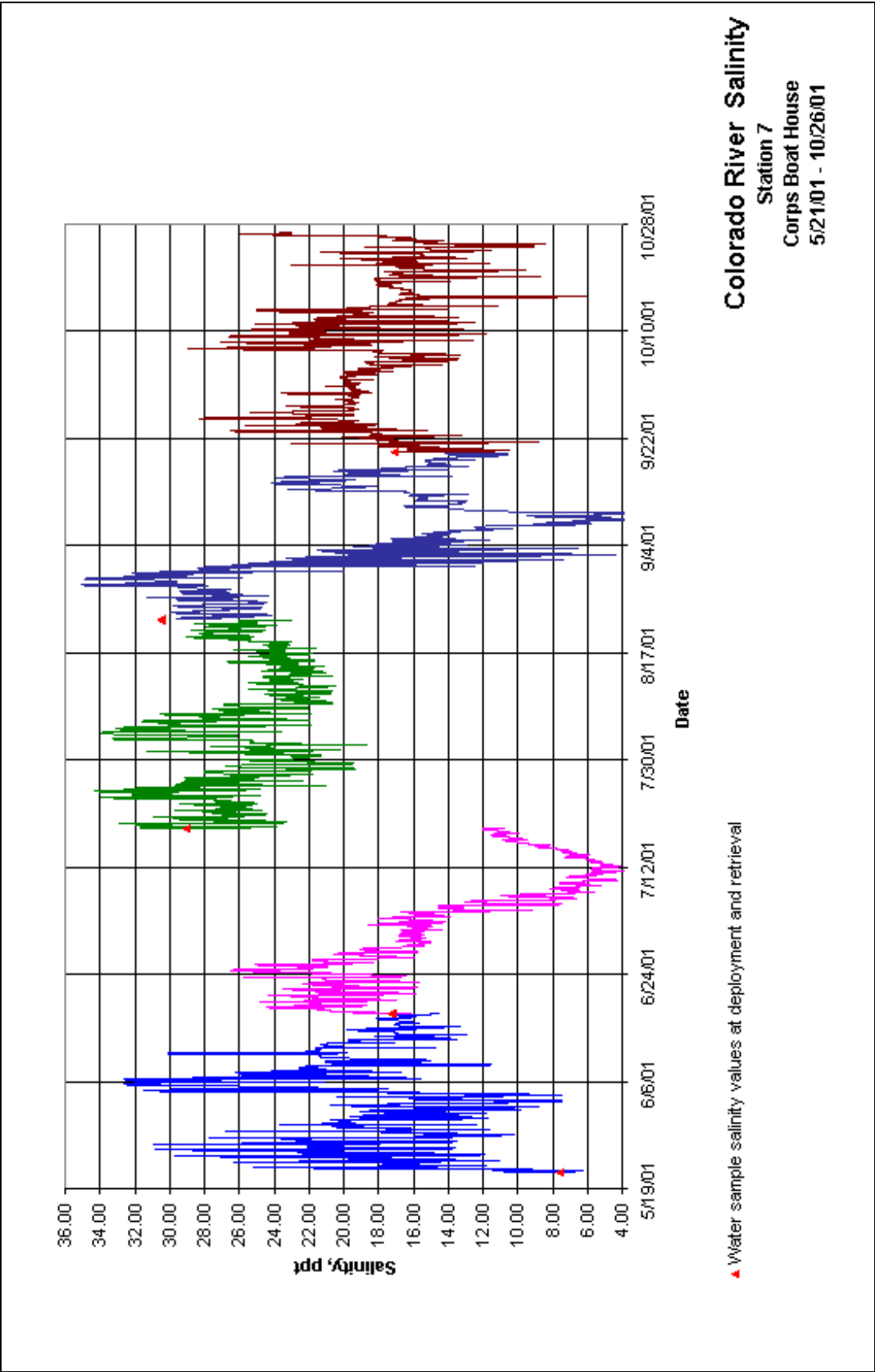


Figure 25. Time-history of salinity for Station 7 during the period 5/21/01 – 10/26/01

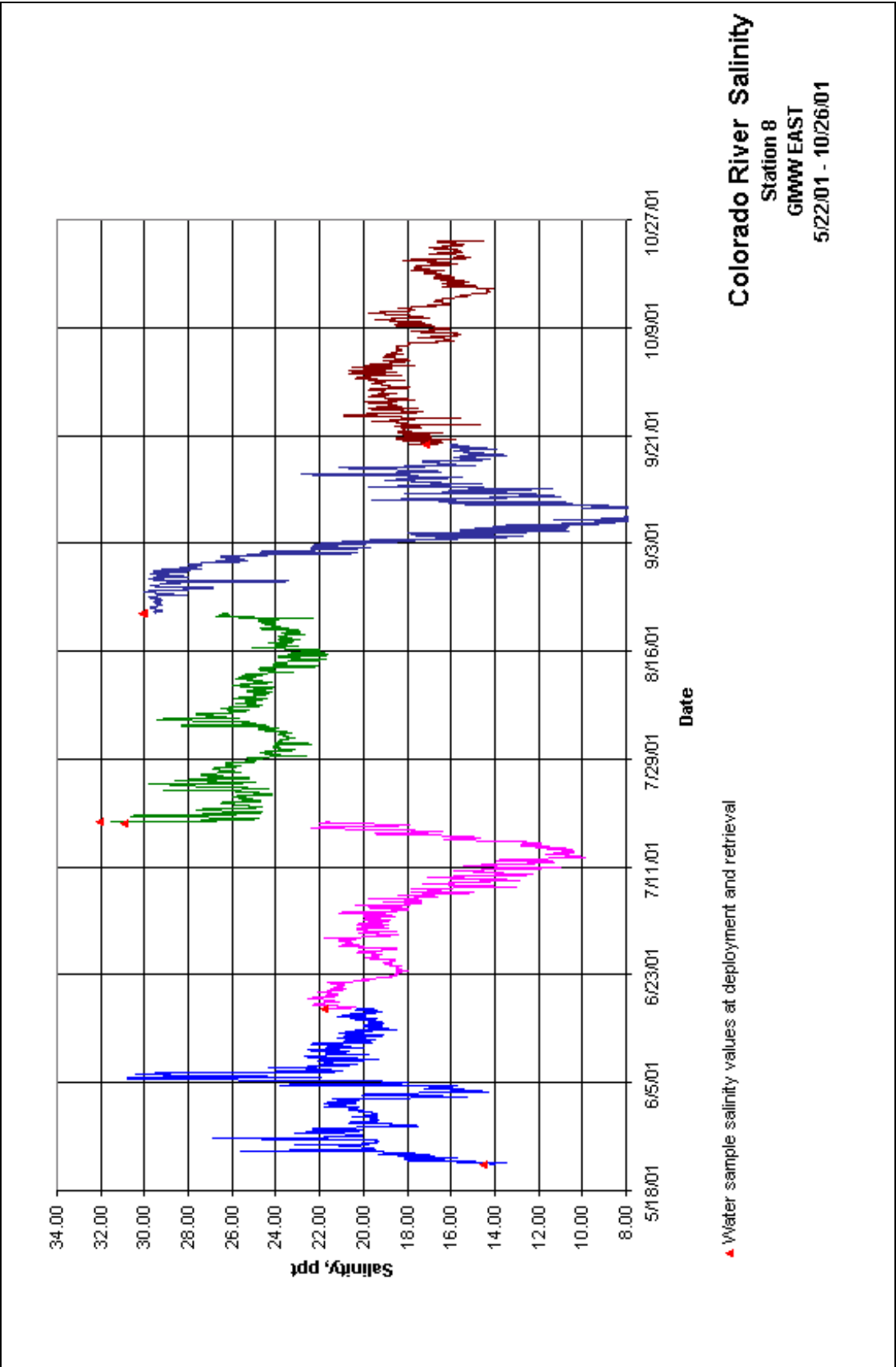


Figure 26. Time-history of salinity for Station 8 during the period 5/22/01 – 10/26/01

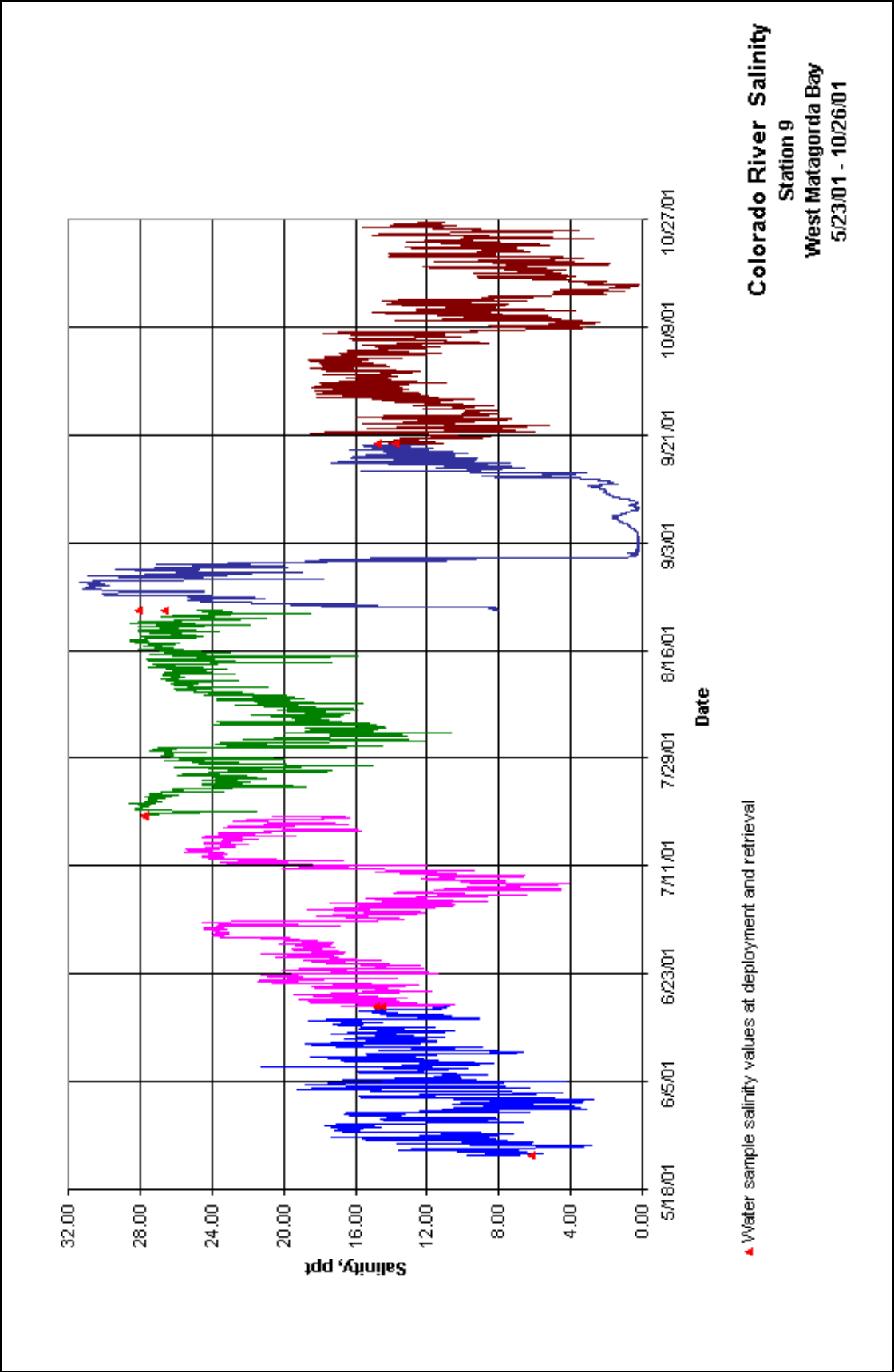


Figure 27. Time-history of salinity for Station 9 during the period 5/23/01 – 10/26/01

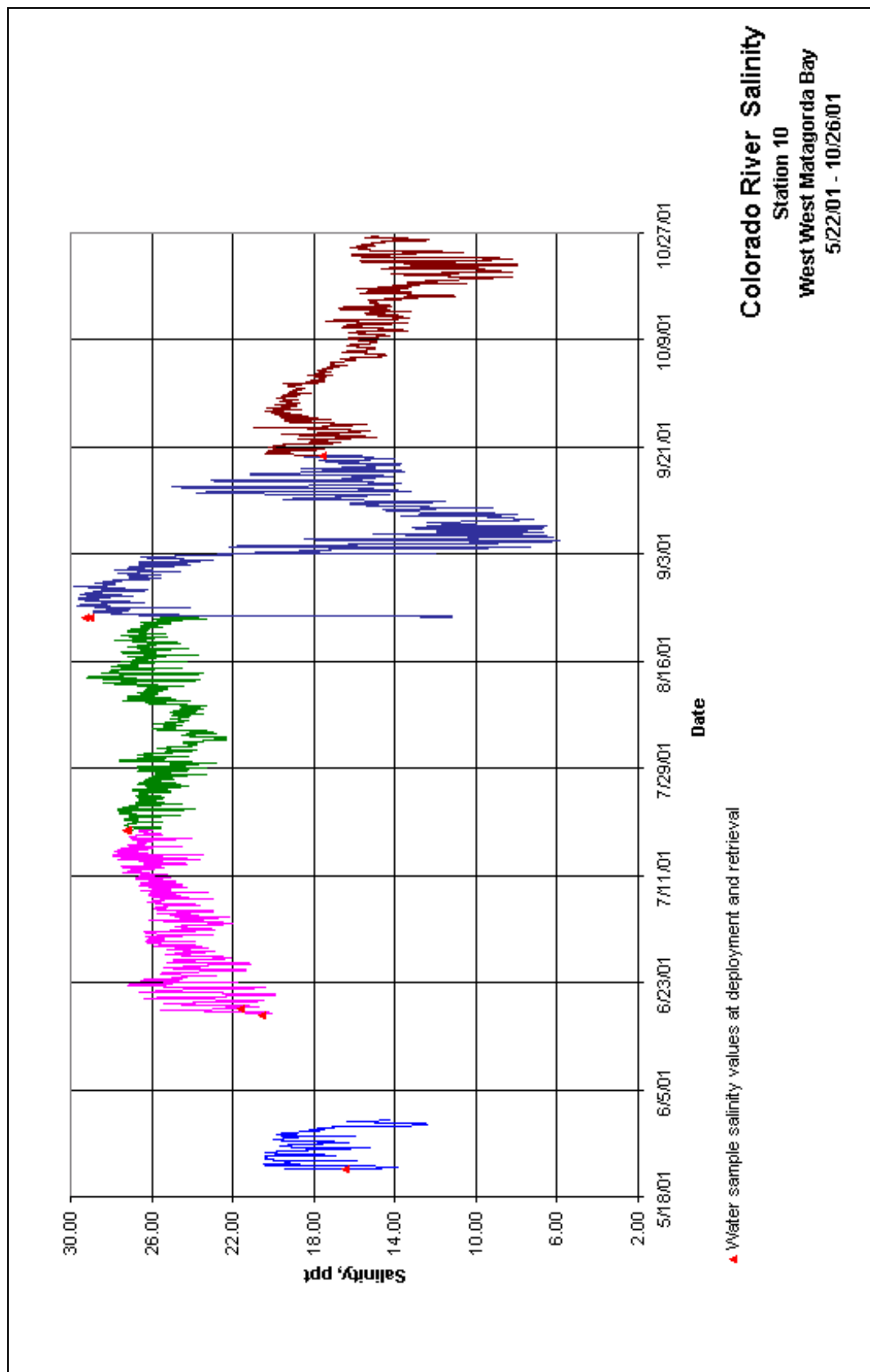


Figure 28. Time-history of salinity for Station 10 during the period 5/22/01 – 10/26/01

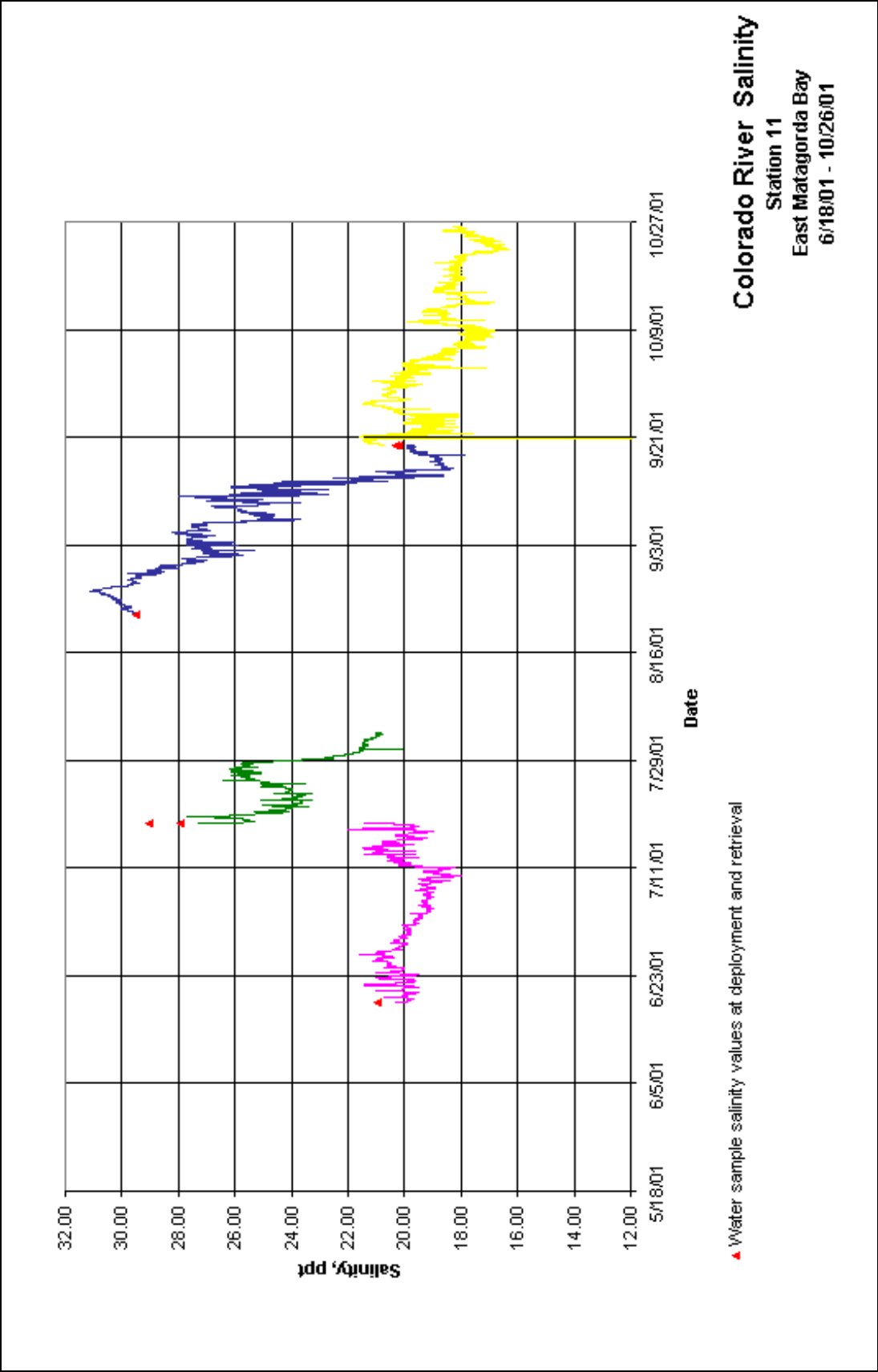


Figure 29. Time-history of salinity for Station 11 during the period 6/18/01 – 10/26/01

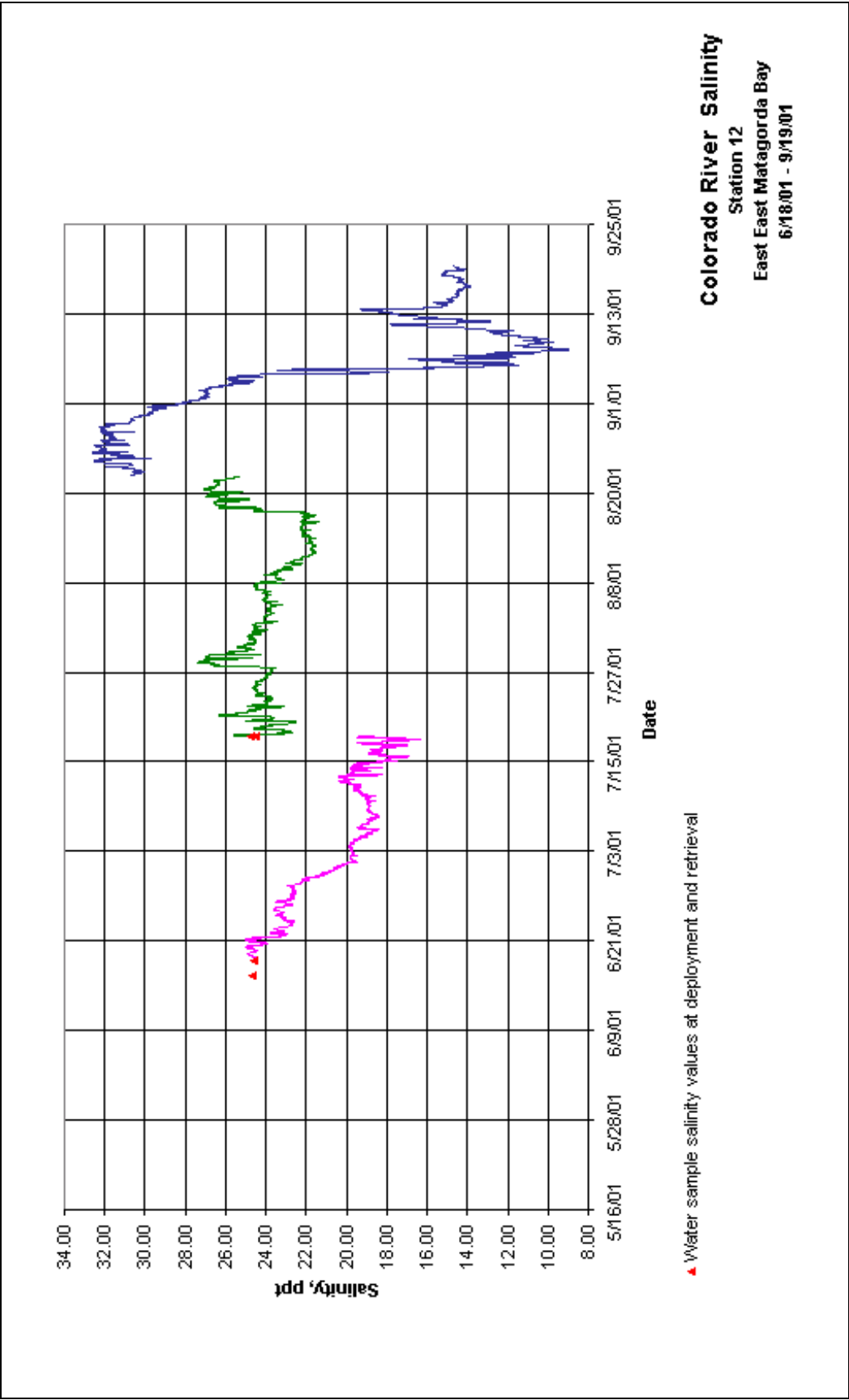


Figure 30. Time-history of salinity for Station 12 during the period 6/18/01 – 09/19/01

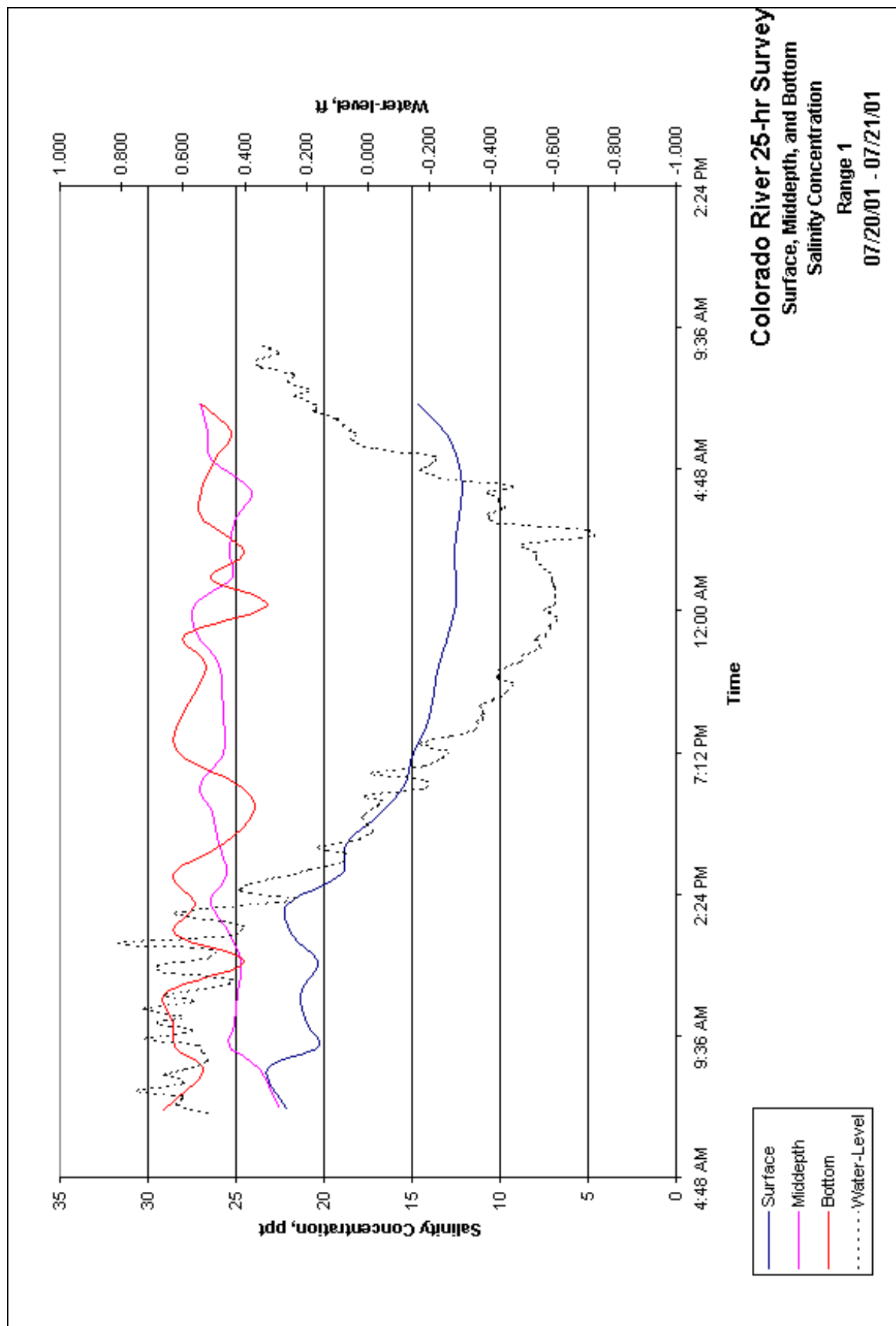


Figure 31. Range 1 salinity concentration variations with depth during a tidal cycle

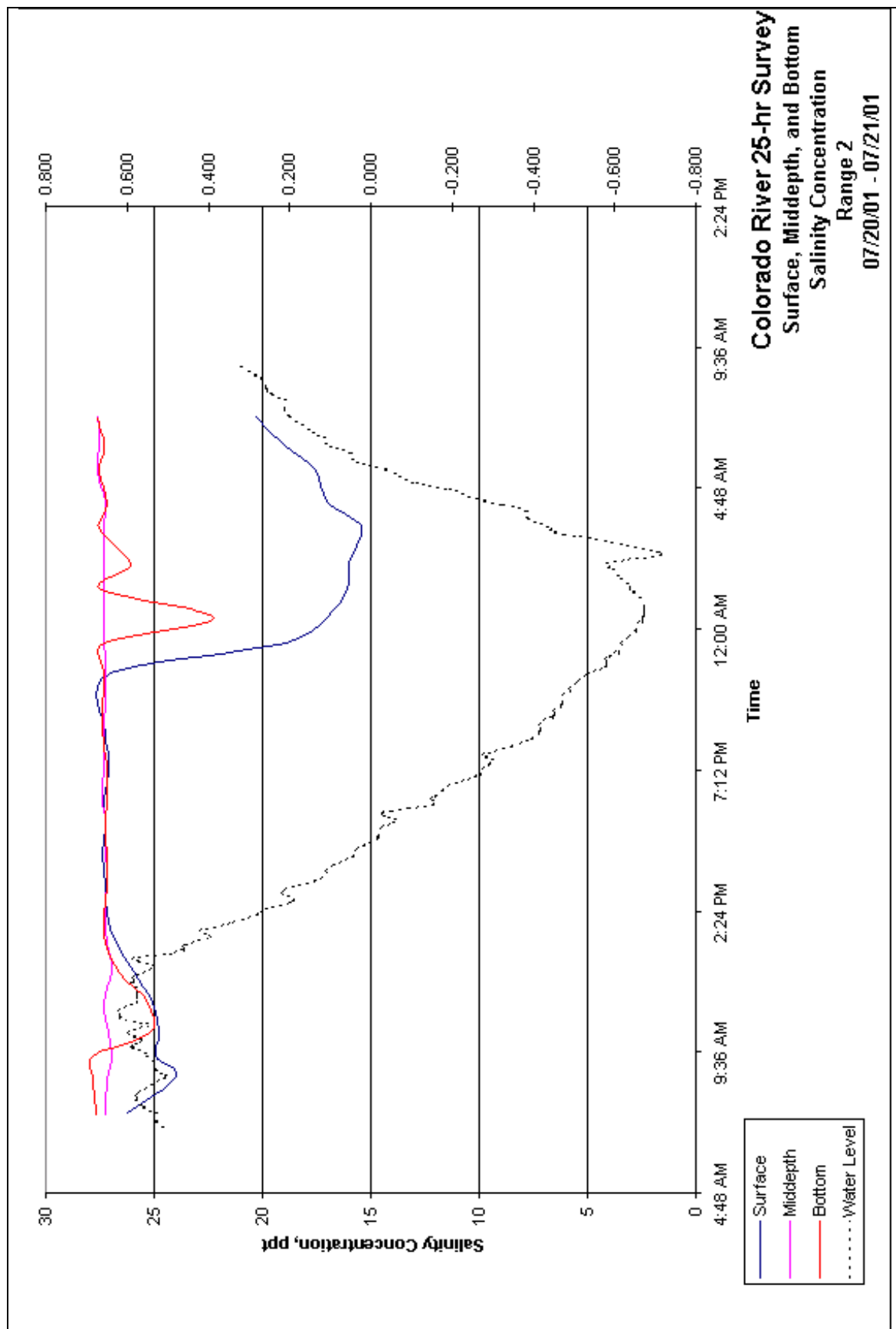


Figure 32. Range 2 salinity concentration variations with depth during a tidal cycle

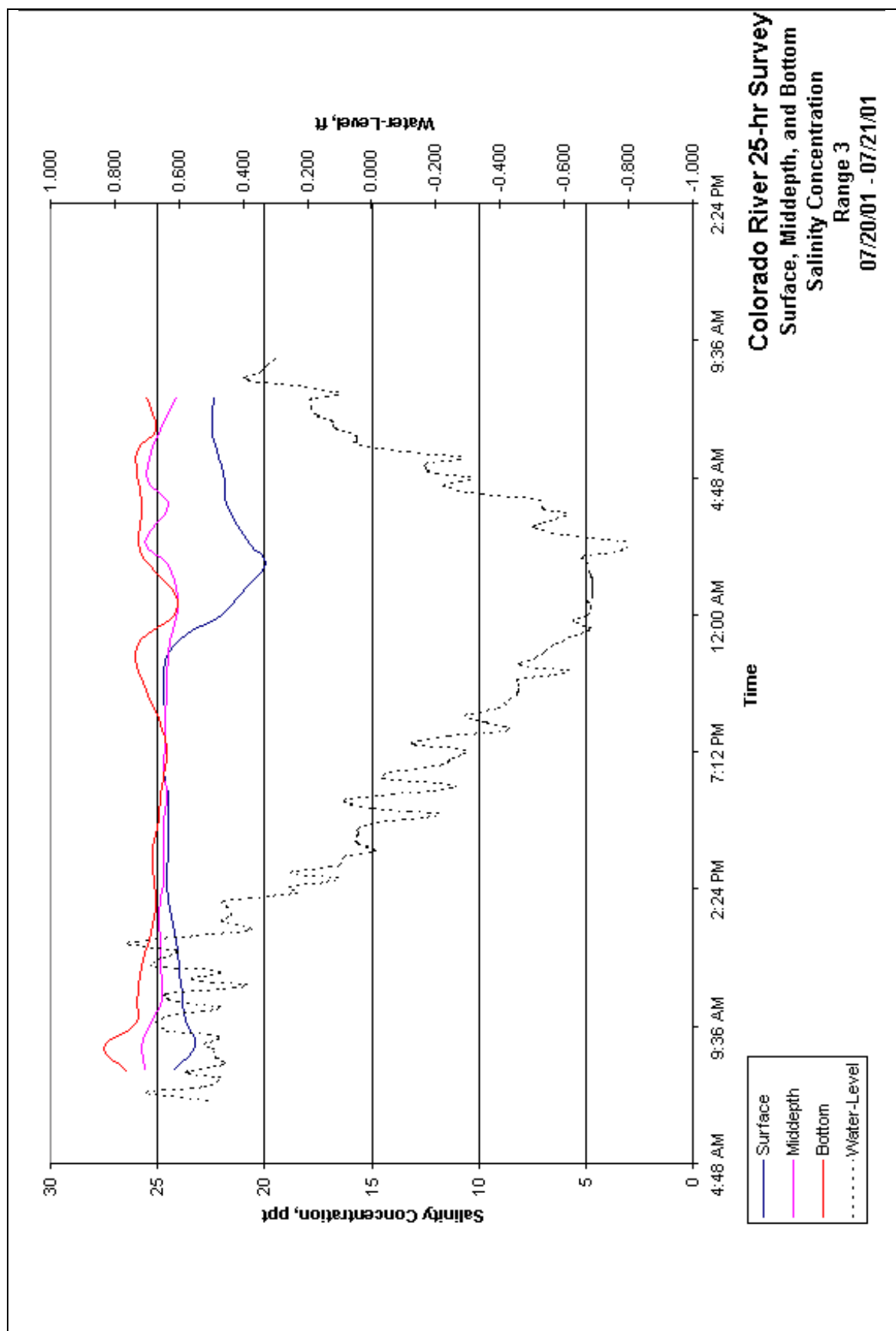


Figure 33. Range 3 salinity concentration variations with depth during a tidal cycle

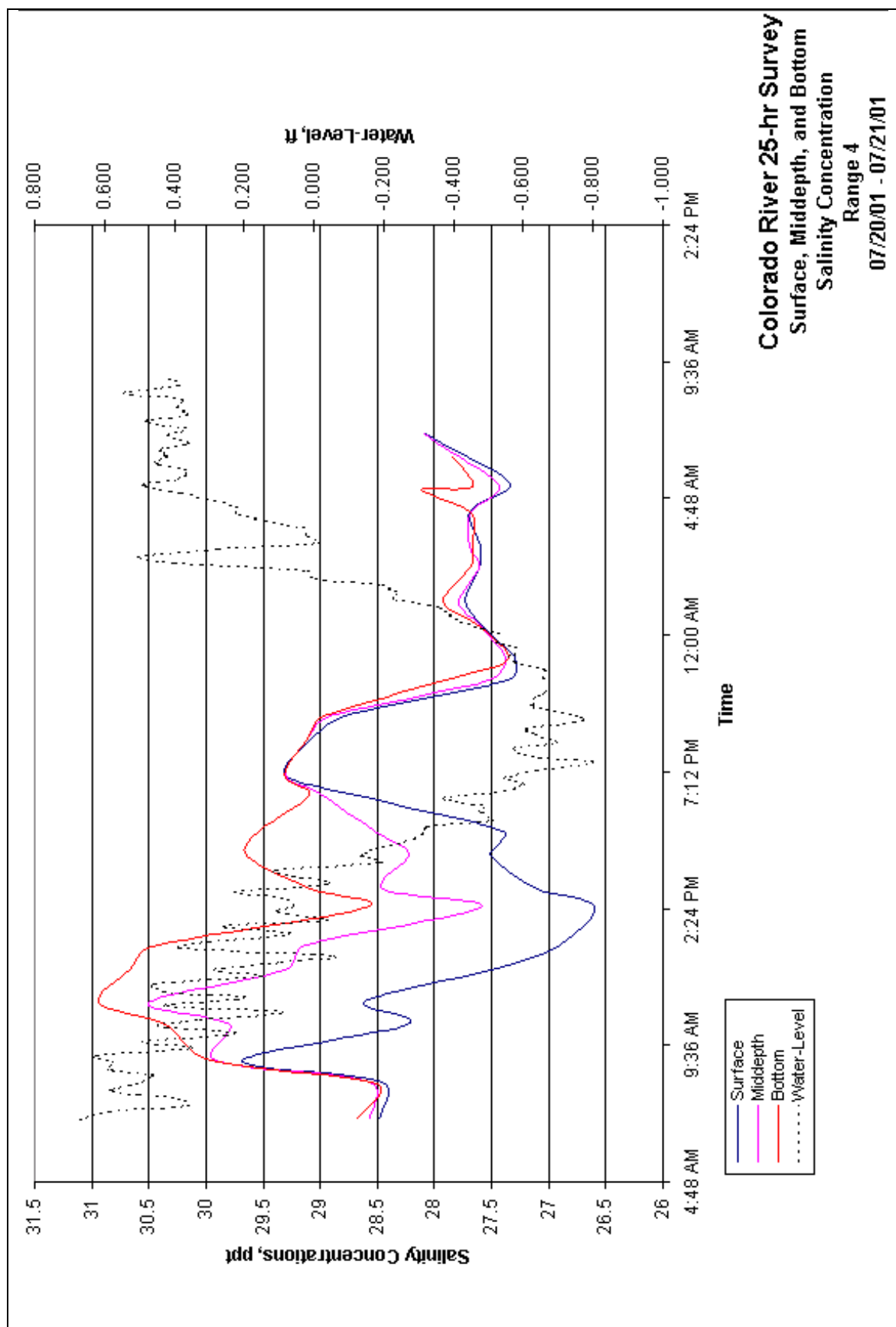


Figure 34. Range 4 salinity concentration variations with depth during a tidal cycle

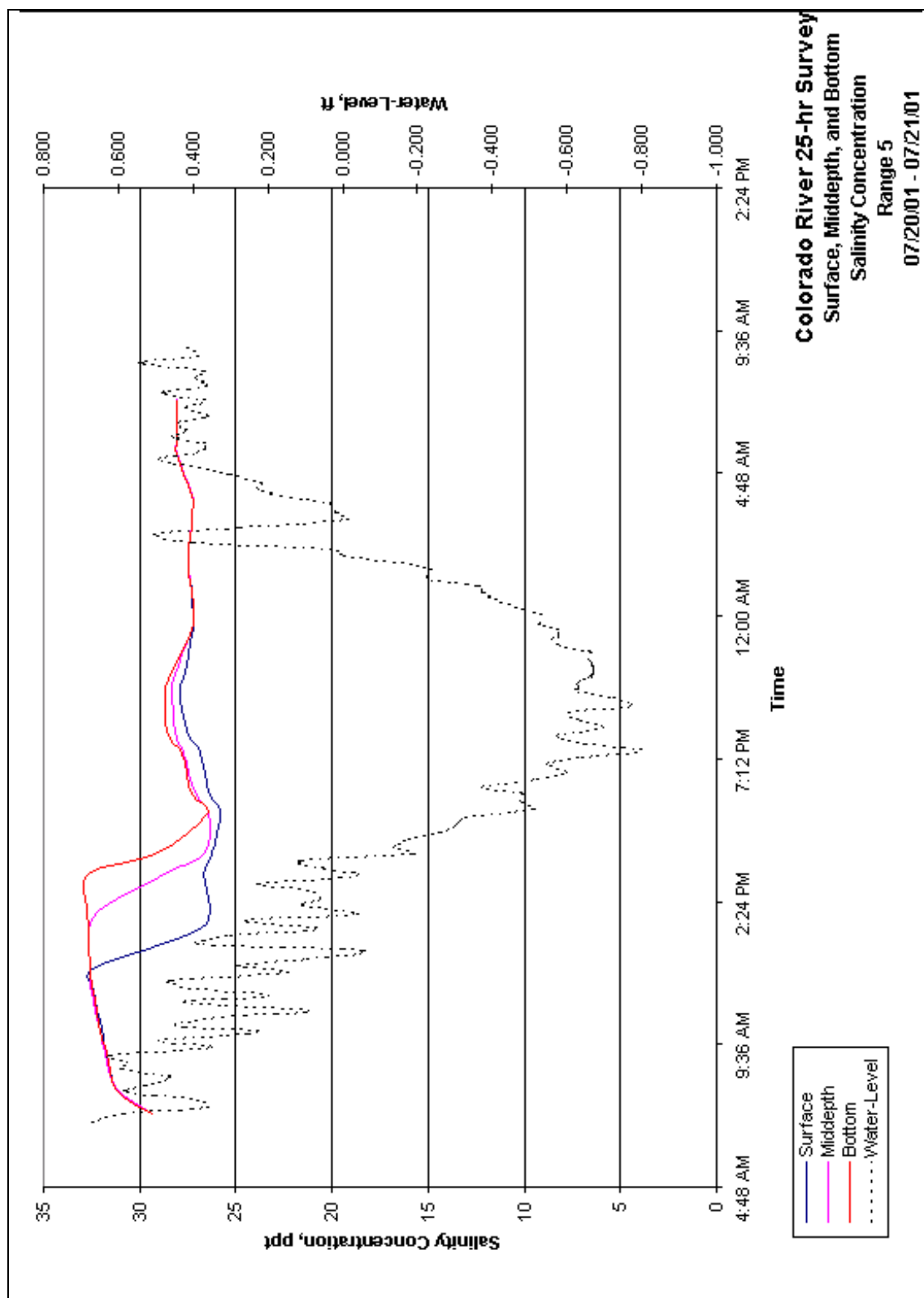


Figure 35. Range 5 salinity concentration variations with depth during a tidal cycle

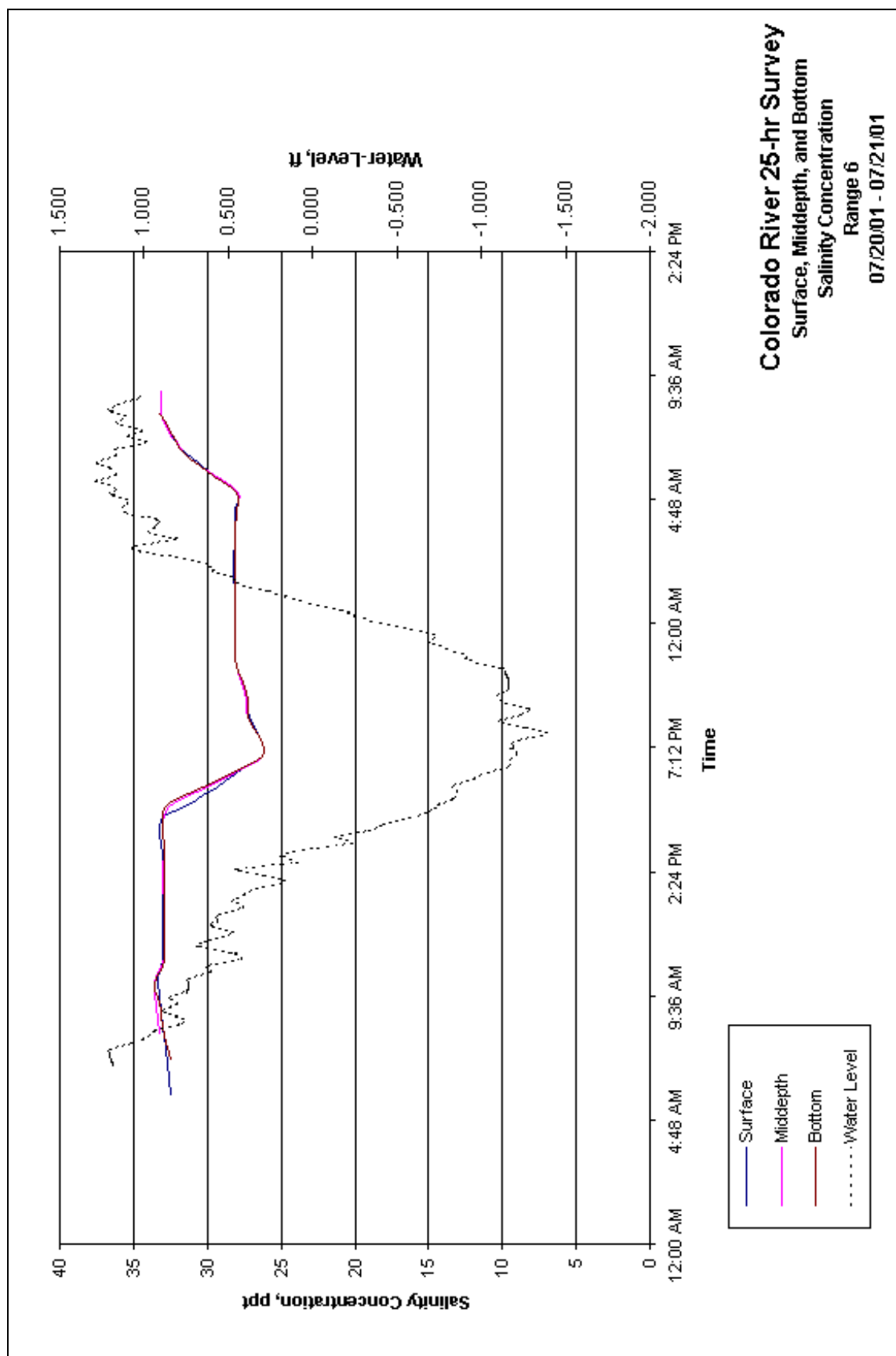


Figure 36. Range 6 salinity concentration variations with depth during a tidal cycle

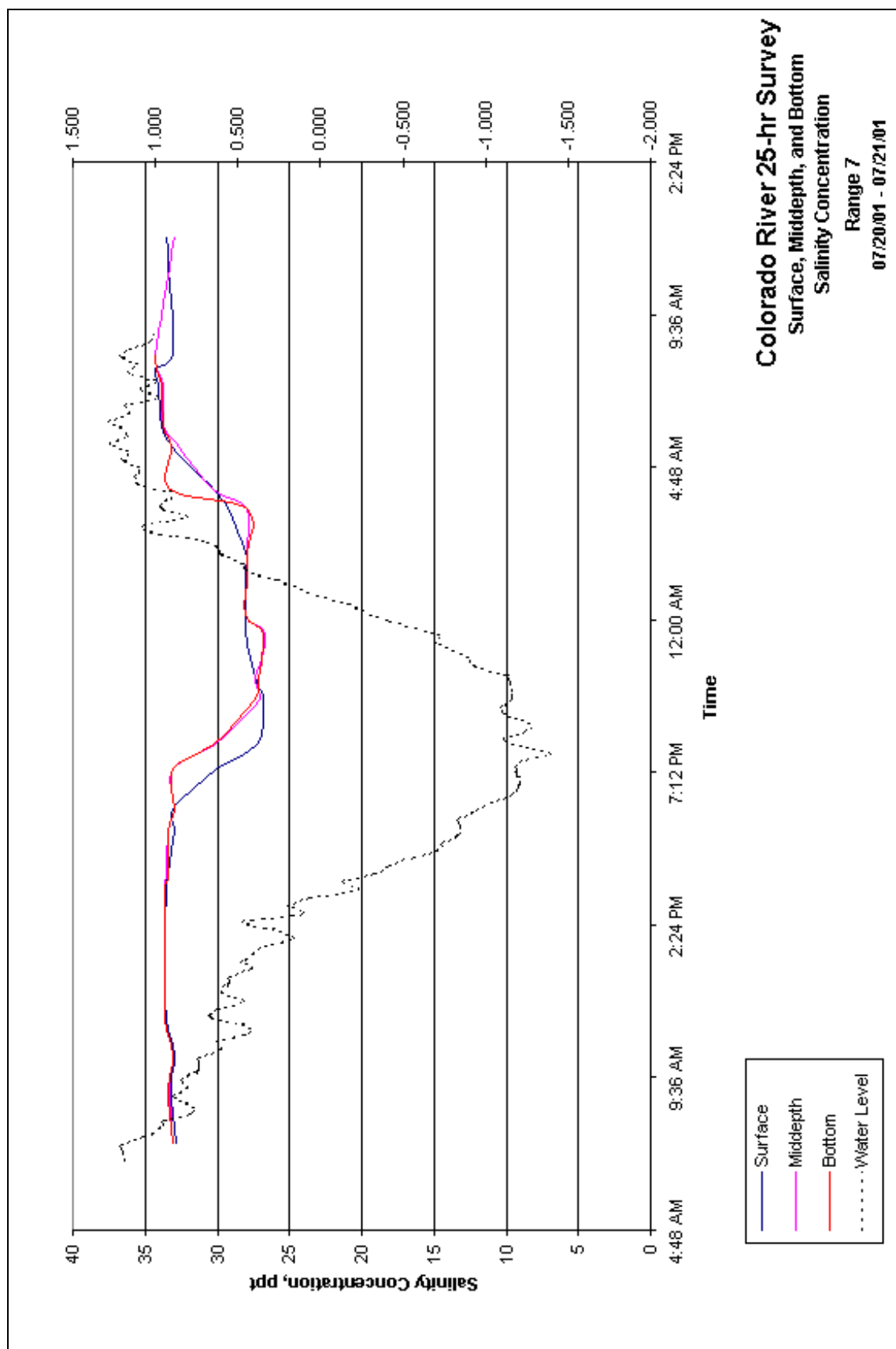


Figure 37. Range 7 salinity concentration variations with depth during a tidal cycle

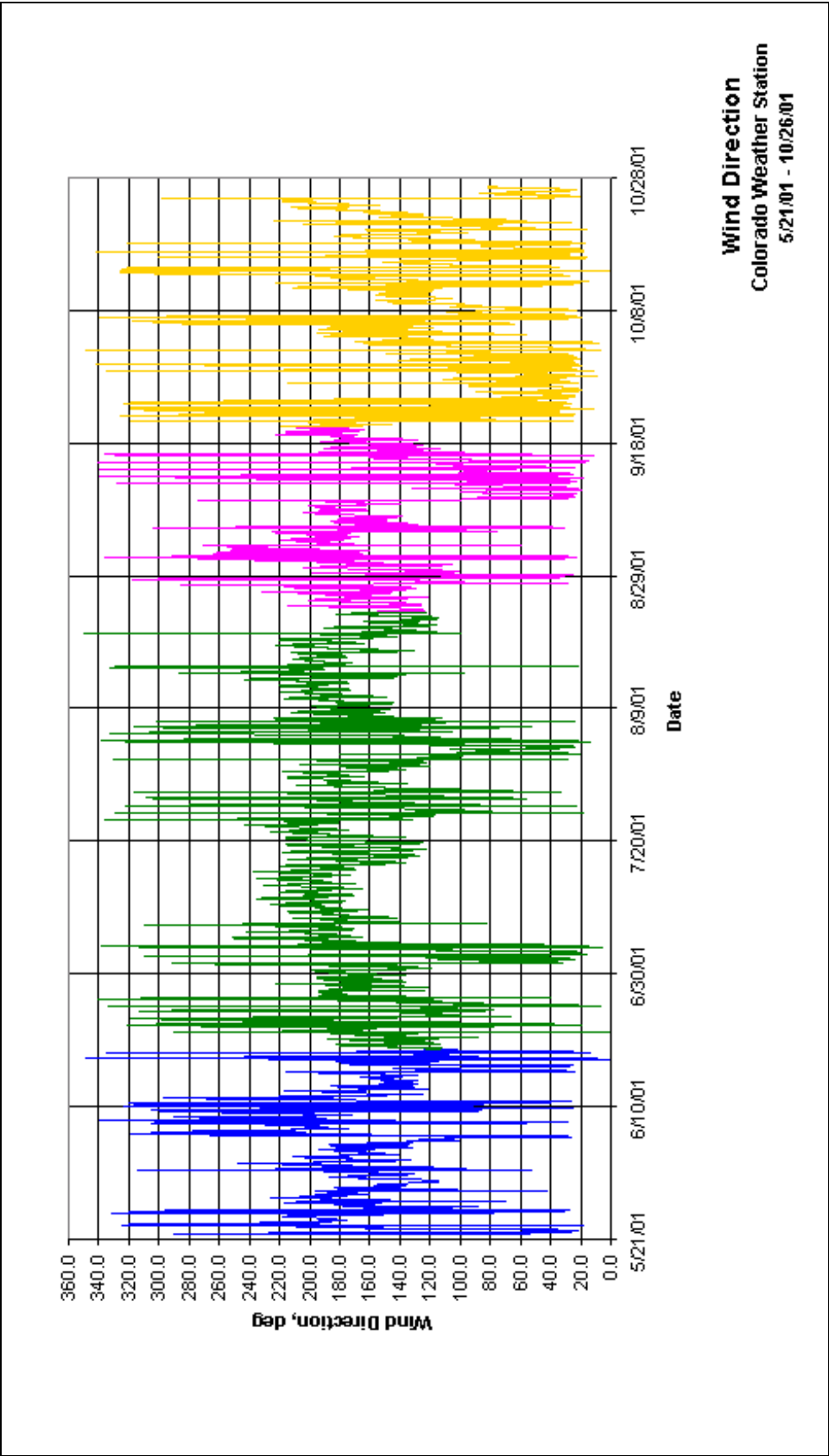


Figure 38. Time-history of wind direction during the period 5/21/01 – 9/20/01

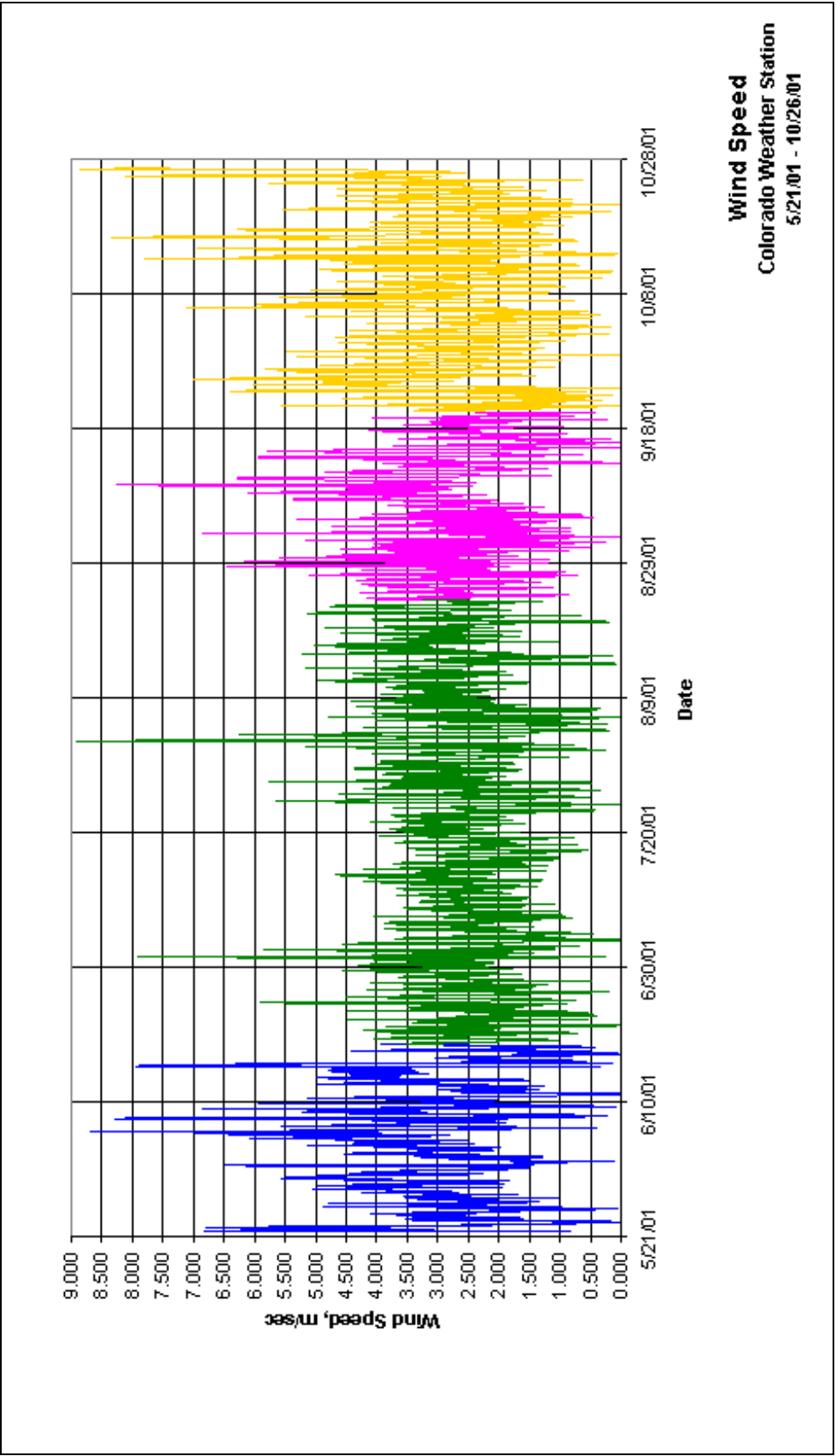


Figure 39. Time-history of wind speed during the period 5/21/01 – 9/20/01

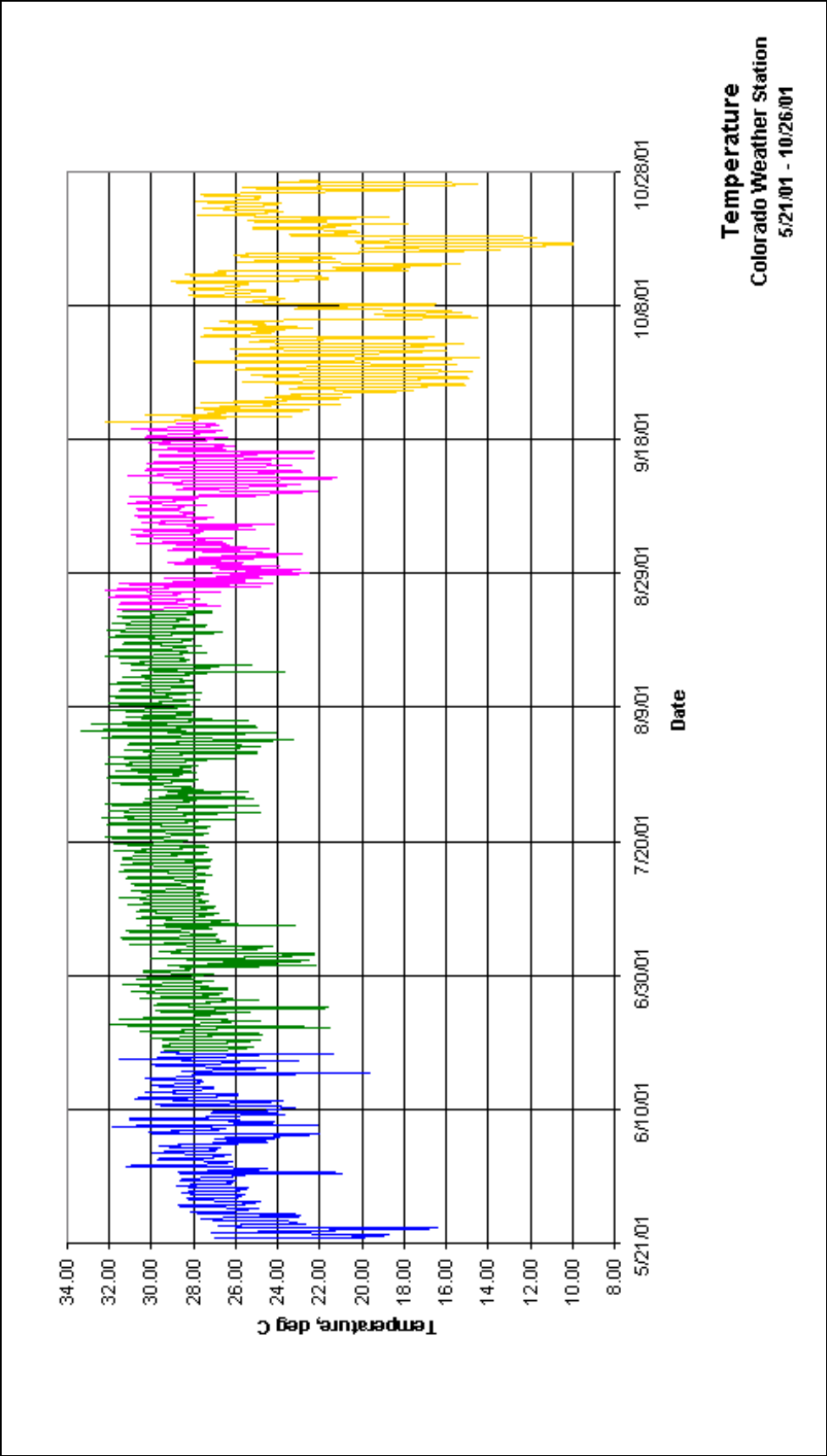


Figure 40. Time-history of temperature during the period 5/21/01 – 9/20/01

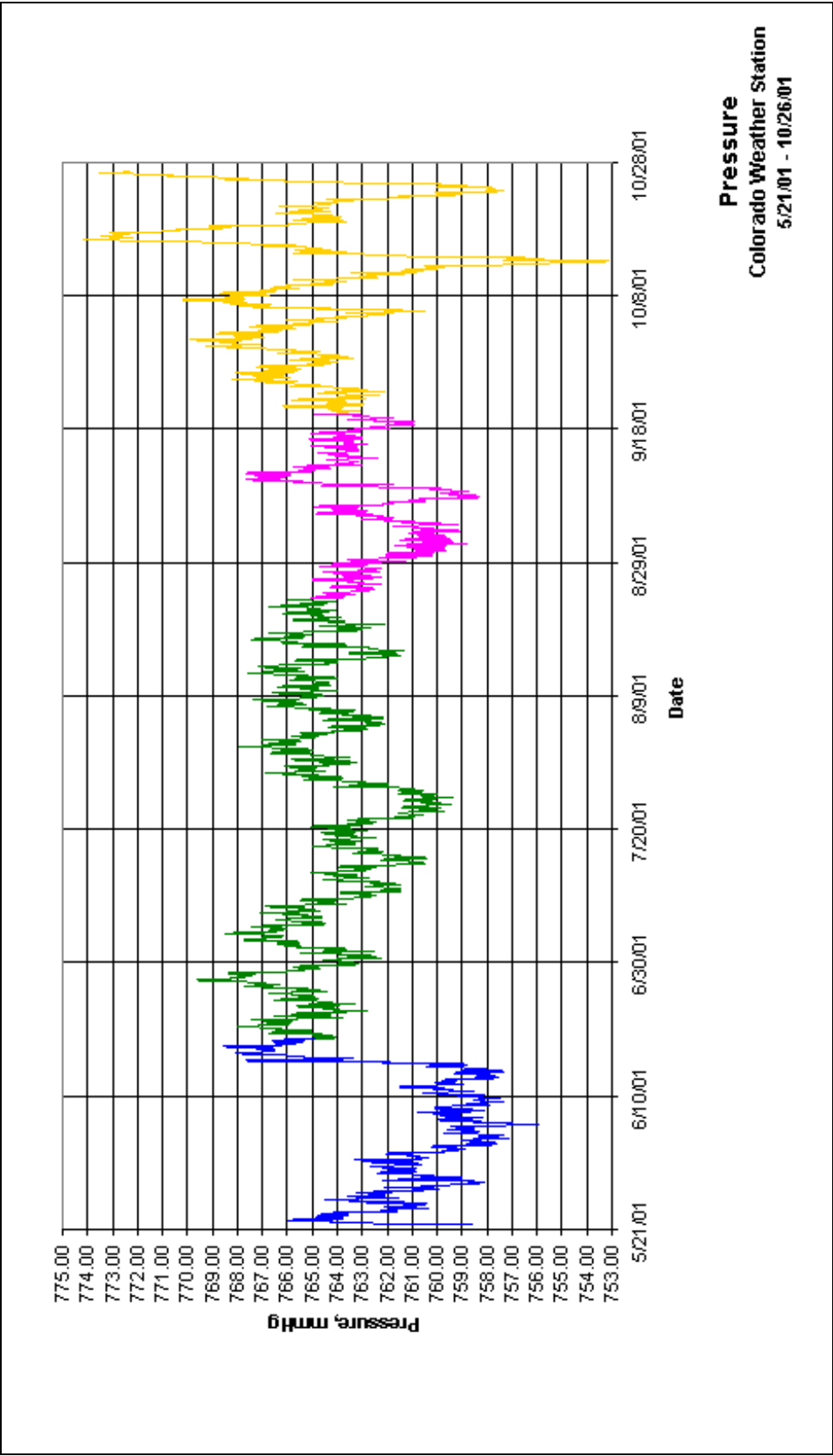


Figure 41. Time-history of atmospheric pressure during the period 5/21/01 – 9/20/01

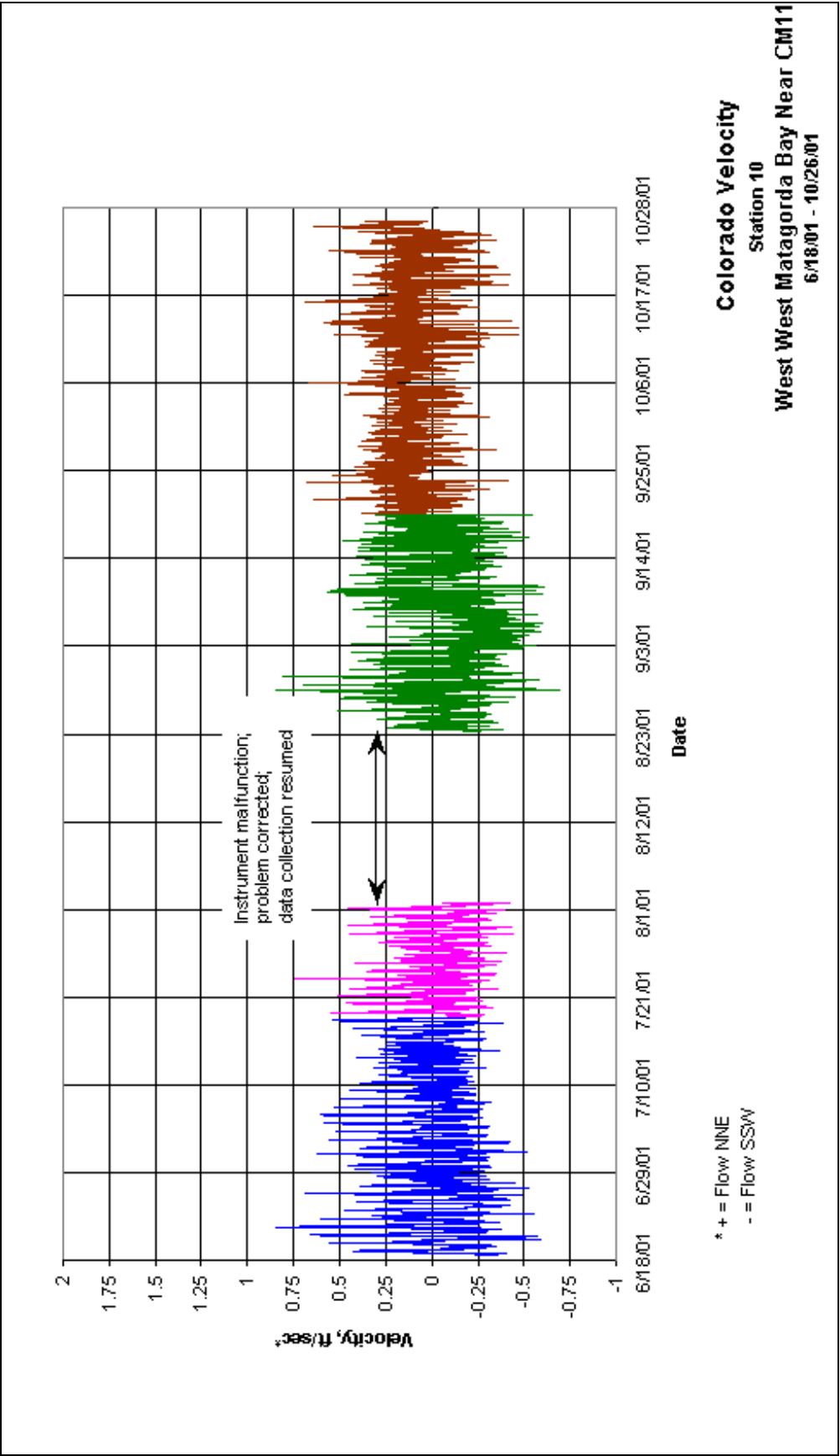


Figure 42. Time-history of velocity for Station 10 during the period 6/18/01 – 10/26/01

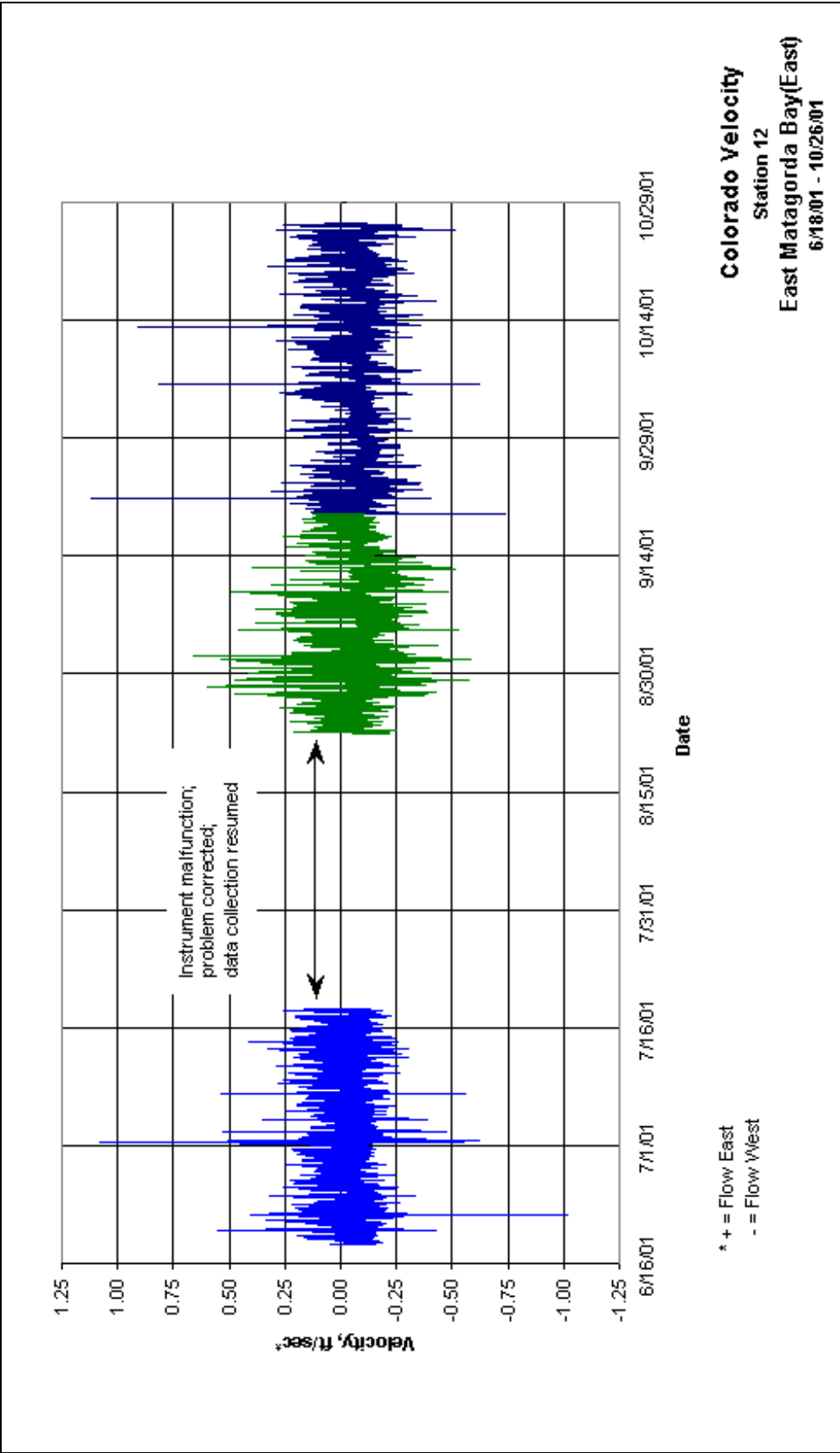


Figure 43. Time-history of velocity for Station 12 during the period 6/18/01 – 10/26/01

